NASA Contractor Report 198443

Probabilistic Fiber Composite Micromechanics

Thomas A. Stock
Cleveland State University
Cleveland, Ohio

January 1996

Prepared for
Lewis Research Center
Under Grant NAG3–550

National Aeronautics and
Space Administration

PROBABILISTIC FIBER COMPOSITE MICROMECHANICS

THOMAS A. STOCK

Bachelor of Science in Civil Engineering

Northwestern University

June, 1983

Submitted in partial fulfillment of requirements for the degree

MASTER OF SCIENCE IN CIVIL ENGINEERING

at the

CLEVELAND STATE UNIVERSITY

March, 1987

This thesis has been approved

for the Department of Civil Engineering

and the College of Graduate Studies by

Paul X Bellini 3/26/87

Prof. Paul X. Bellini, Thesis Committee Chairman

CCChamis 3-24-87

Dr. C C. Chamis, Adjunct Associate Professor

John H Hemann 3/24/87

Dr. John H. Hemann, Department Chairman

ACKNOWLEDGEMENTS

This thesis is the result of work performed at NASA- Lewis Research Center under grant NAG 3-550.

I wish to express my gratitude to Dr. Christos Chamis, from the Structures Division at Lewis, for his insight, enthusiasm, patience, and wit, all of which contributed to my learning, of which this thesis is a small part. His example is an inspiration to me, in school, work, and life. Dr. Bellini, my advisor, deserves thanks for patiently reading the many drafts, and supplying perspective and criticism to aid in clarifying my ideas. He has been a teacher and a friend.

ABSTRACT

Probabilistic composite micromechanics methods are developed that simulate expected uncertainties in unidirectional fiber composite properties. These methods are in the form of computational procedures using Monte Carlo simulation. The variables in which uncertainties are accounted for include constituent and void volume ratios, constituent elastic properties and strengths, and fiber misalignment. A graphite/epoxy unidirectional composite (ply) is studied to demonstrate fiber composite material property variations induced by random changes expected at the material micro level. Regression results are presented to show the relative correlation between predictor and response variables in the study. These computational procedures make possible a formal description of anticipated random processes at the intraply level, and the related effects of these on composite properties.

TABLE OF CONTENTS

CHAPTER	PAGE
I. INTRODUCTION	1
A. Background	1
B. Purpose	6
C. Formulation of the Model	7
D. Method of Investigation	9
1. Brief Description of ICAN	9
2. Summary of Variables	10
3. Monte Carlo Methods	13
E. Brief Summary of Results	15
II. METHODS OF CALCULATION	17
A. Overall Plan	17
1. Input Structure for ICAN	17
2. Constituent Property Variations	18
3. Repeated Runs	20
4. Data Collection	20
B. Generation of Pseudo Random Numbers	23
1. Uniform Distribution	23
2. Normal Distribution	25
3. Gamma Distribution	26
4. Weibull Distribution	28
C. Property Distribution Assumptions	31

D. Use of ICAN 47

1. Composite Micromechanics 47

2. Laminate Theory 48

3. Strength Theories 49

E. Review of Applicable Statistical Concepts 51

1. Sample Means 51

2. Sample Standard Deviation 51

3. Confidence Interval Estimates 51

4. Multiple Linear Regression 53

III. RESULTS 57

A. Property Histograms and Distributions 57

B. Fiber Strength Effect 73

C. Matrix Strength Effect 76

D. Fiber Orientation Effect 80

E. Fiber Stiffness Effect 80

F. Regression Models 101

IV. DISCUSSION 130

A. Overview 130

B. Histograms and Distributions 131

C. Confidence Curves 133

D. Examination of Regression Models 134

V. CONCLUSIONS 136

REFERENCES 138

APPENDIX A- SOURCE PROGRAM LISTINGS 140

APPENDIX B- ICAN PROGRAM DETAILS 154

1. Composite Micromechanics 155

2. Laminate Theory 157

3. Strength Theories 171

LIST OF TABLES

TABLE	TITLE	PAGE
I	INPUT DATA FOR SAMPLING	58
II	CASE 1 RESULTS	59
III	LONGITUDINAL MODULUS (EC11), SIMPLE	104
IV	TRANSVERSE MODULUS (EC22), SIMPLE	105
V	SHEAR MODULUS (EC12), SIMPLE	106
VI	POISSON'S RATIO, MAJOR (NUC12), SIMPLE	107
VII	POISSON'S RATIO, MINOR (NUC21), SIMPLE	108
VIII	LONG. THERM. EXPANSION (CTE11), SIMPLE	109
IX	TRANS. THERM. EXPANSION (CTE22), SIMPLE	110
X	LONG. TENSILE STRENGTH (SCXXT), SIMPLE	111
XI	LONG. COMPRESSIVE STRENGTH (SCXXC), SIMPLE	112
XII	TRANSVERSE TENSILE STRENGTH (SCYYT), SIMPLE	113
XIII	TRANSVERSE COMPRESSIVE STRENGTH (SCYYC), SIMPLE	114
XIV	IN PLANE SHEAR STRENGTH (SCXYS), SIMPLE	115
XV	LONGITUDINAL MODULUS (EC11), INTERACTION	118
XVI	TRANSVERSE MODULUS (EC22), INTERACTION	119
XVII	SHEAR MODULUS (EC12), INTERACTION	120
XVIII	LONGITUDINAL THERMAL EXPANSION	121

XIX TRANSVERSE THERMAL EXPANSION 122

XX POISSON RATIO, MAJOR (NUC12), INTERACTION 123

XXI POISSON RATIO, MINOR (NUC21), INTERACTION 124

XXII LONGITUDINAL TENSILE STRENGTH (SCXXT), INTERACTION 125

XXIII LONG. COMPRESSIVE STRENGTH (SCXXC), INTERACTION 126

XXIV TRANSVERSE TENSILE STRENGTH (SCYYT), INTERACTION 127

XXV TRANSVERSE COMPRESSIVE STRENGTH (SCYYC), INTERACTION 128

XXVI IN PLANE SHEAR STRENGTH (SCXYS), INTERACTION 129

LIST OF FIGURES

FIGURE	TITLE	PAGE
1	Photomicrograph of Graphite/Epoxy cross section showing variation in fiber content.	5
2	Conventional Model	8
3	Substructure Model	8
4	Coordinate Systems	11
5	Order of ICAN input data cards	11
6	Command Input	19
7	Constituent Variation Input	19
8	Flow Chart of Probabilistic Integrated Composites Analyzer	22
9	Uniform Distribution: general form	29
10	Normal Distribution	29
11	Gamma Distribution density functions	30
12	Weibull Distribution function	30
13	Normal Distribution Simulation	32
14	Gamma Distribution Simulation	33
15	Gamma Distribution Simulation	34
16	Gamma Distribution Simulation	35
17	Gamma Distribution Simulation	36

18	Weibull Distribution Simulation Matrix Shear Strength	37
19	Weibull Distribution Simulation Matrix Shear Strength	38
20	Weibull Distribution Simulation Matrix Tensile Strength	39
21	Weibull Distribution Simulation Matrix Tensile Strength	40
22	Weibull Distribution Simulation Matrix Tensile Strength	41
23	Weibull Distribution Simulation Matrix Compressive Strength	42
24	Weibull Distribution Simulation Matrix Compressive Strength	43
25	Weibull Distribution Simulation Fiber Tensile and Compressive Strength	44
26	Weibull Distribution Simulation Fiber Tensile and Compressive Strength	45
27	Weibull Distribution Simulation Fiber Tensile and Compressive Strength	46
28	Typical Stress-Strain behavior of unidirectional fiber composites	50
29	In-plane fracture modes of unidirectional (ply) fiber composites	50
30	Sampling results for Longitudinal Elastic Modulus	60
31	Sampling results for Transverse Elastic Modulus	61
32	Sampling results for In plane Shear Modulus	62
33	Sampling results for Poisson Ratio (major)	63
34	Sampling results for Poisson Ratio (minor)	64
35	Sampling results for Longitudinal Thermal Expansion	65

36	Sampling results for Transverse Thermal Expansion	66
37	Sampling results for Thermal Expansion Coupling	67
38	Sampling results for Longitudinal Tensile Strength	68
39	Sampling results for Longitudinal Compressive Strength	69
40	Sampling results for Transverse Tensile Strength	70
41	Sampling results for Transverse Compressive Strength	71
42	Sampling results for In- plane Shear Strength	72
43	Longitudinal Tensile Strength, for various shape parameters of fiber strength	74
44	Longitudinal Compressive Strength, for various shape parameters of fiber strength	75
45	Transverse Tensile Strength, for various shape parameters of matrix strength	77
46	Transverse Compressive Strength, for various shape parameters of matrix strength	78
47	In-plane Shear Strength, for various shape parameters of matrix strength	79
48	Longitudinal Elastic Modulus, for various shape parameters of fiber orientation	81
49	Transverse Elastic Modulus, for various shape parameters of fiber orientation	82
50	In-plane Shear Modulus, for various shape parameters of fiber orientation	83
51	Longitudinal Tensile Strength, for various shape parameters of fiber orientation	84
52	Longitudinal Compressive Strength, for various shape parameters of fiber orientation	85
53	Transverse Tensile Strength, for various shape parameters of fiber orientation	86

54	Transverse Compressive Strength, for various shape parameters of fiber orientation	87
55	In-plane Shear Strength, for various shape parameters of fiber orientation	88
56	Poisson's Ratio (major); for various shape parameters of fiber orientation	89
57	Poisson's Ratio (minor); for various shape parameters of fiber orientation	90
58	Longitudinal Elastic Modulus; for various shape parameters of fiber modulus	91
59	Transverse Elastic Modulus; for various shape parameters of fiber modulus	92
60	In Plane Shear Modulus; for various shape parameters of fiber modulus	93
61	Poisson's Ratio (major); for various shape parameters of fiber modulus	94
62	Poisson's Ratio (minor); for various shape parameters of fiber modulus	95
63	Longitudinal Tensile Strength; for various shape parameters of fiber modulus	96
64	Longitudinal Compressive Strength; for various shape parameters of fiber modulus	97
65	Transverse Tensile Strength; for various shape parameters of fiber modulus	98
66	Transverse Compressive Strength; for various shape parameters of fiber modulus	99
67	In Plane Shear Strength; for various shape parameters of fiber modulus	100

B.1 Components of Stress acting on elemental unit cube 174

B.2 Rotation of coordinates from 1-2 to x-y. 174

B.3 Bending geometry in the x-z plane 175

B.4 Shearing force deformations on straight cross section 175

B.5 Stress and Moment resultants 176

B.6 Laminate index notation convention 176

CHAPTER I

INTRODUCTION

A. Background

The diverse requirements of recent engineering applications have motivated designers to explore specialized structural and material systems. Ceramic materials, for example, have several attractive structural properties, such as their high stiffness/weight ratios, and low variation of stiffness and strength over wide ranges of environmental conditions. A significant disadvantage inherent to brittle structural materials is their vulnerability to failure due to cracks propagating from flaws. The increased probability of a flaw occurring in a material as the volume increases leads to bulk strengths which are a fraction of the theoretical strength of the material. The size effect on material strength (Ref. 1) can be explained by the "weakest link" concept. Griffith (Ref. 2) reasoned that very small solids, for example wires or fibers, might be expected to be stronger than large ones, due to the additional restriction on the size of the flaws. In the limit, a single line of molecules must possess the theoretical molecular tensile strength of a material. A consequence of

the size effect on strength was the development of fiber composite materials which consist of thin, strong fibers bound together by a ductile matrix. The advantages of fine, strong fibers can explain the current trend toward increased use of fiber composite materials in demanding aerospace applications.

Properties of a composite laminate depend on the properties of the constituent materials, their distribution, and orientation. Laminates are composed of layers of unidirectionally reinforced plies (laminae). The lamina is typically considered the basic unit of material in a composite structural analysis, which requires knowledge of the material properties of each individual lamina and its geometric orientation. The branch of composite mechanics that predicts ply material properties based on the properties, concentration, and orientation of its constituents is known as composite micromechanics, and frequently incorporates the traditional Mechanics of Materials assumptions. The desired laminate is created by stacking of plies in specific directions. The integration of ply properties to yield laminate properties is called laminate theory. Laminate variables such as ply orientation and stacking sequence can be tailored to yield a laminate with the desired material properties. Thus, the laminated composite is a suitable material for component design.

Analysis of fiber composite structures is currently performed using a variety of computer codes. From the original codes based on classical micromechanics and laminate theory, recent codes (Ref. 3,4) have been developed which incorporate the current state of the art. Complete

mechanical, thermal, and hygral properties are calculated, and can be used to compute response. Advanced failure criteria are used to calculate composite strengths. Environmental effects are also quantified. The usefulness of these codes has been demonstrated by comparison with experimental and finite element results (Ref. 5,6).

The analytical capability of many codes is limited by the deterministic nature of the computations. Specifically, fixed values for constituent material properties, fabrication process variables (i.e. constituent volume ratios) and internal geometry must be used as input. However, random variations in these parameters are not only expected, but easily observed experimentally. (See Fig. 1)

The analysis of composite structures requires reliable predictive models for material properties and strengths. However, the prediction efforts have been complicated by inherent scatter in experimental data. Since uncertainties in the constituent properties, fabrication variables, and internal geometry would lead to uncertainties in the measured composite properties, the question arises:

> How much of the "statistical" scatter of experimentally observed composite properties can be explained by reasonable statistical distribution of input parameters in composite micromechanics and laminate theory predictive models?

The increasing use of probabilistic methods in structural mechanics has been shown to provide a more realistic depiction of structural response due to load variations. (Ref. 7) The recognition that material parameters are characterized by a spectra of values (that is, are

statistical in nature) rather than by a unique set of values, points to probabilistic methods as a logical analysis approach.

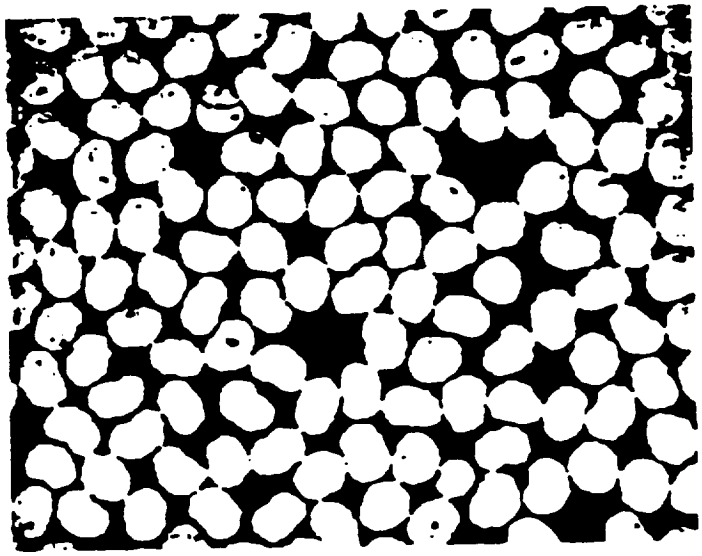

Fig. 1- Photomicrograph of Graphite/Epoxy cross section showing variation in fiber content. (Ref. 19)

B. Purpose

The aim of this thesis is to develop a computational capability to simulate the probabilistic variations in the mechanical behavior of unidirectional fiber composites. The Monte Carlo method is used to simulate a variety of random processes, to quantify fiber composite material variations induced by random changes in composite fiber alignment, constituent properties, and fabrication process variables. This random process description is an attempt to more accurately predict the behavior of manufactured materials, which inherently include these random variations. The characterization of fiber reinforced composites through simulation of local nonuniformities provides an economical alternative to experimentation to measure material properties.

C. Formulation of the Model

The model commonly used in characterizing fiber composites is based on the calculation of properties of the basic unit of an orthotropic ply. The layup geometry is then used in laminate equations to calculate composite properites (See Figs. 2a, 2b). In this work, however, the basic unit is taken as the sub-ply, which consists of only one fiber-matrix level in the material. Micromechanics theory is used to calculate the properties of the assumed orthotropic sub-ply, each with randomly distributed fabrication variables and material properties. Distributed fiber directions, due to possible misalignment within the ply, are then used in the laminate equations to calculate ply properties. This substructuring of the composite ply represents a novel attempt at characterization of fiber composite material properties based on probabilistically distributed constituent properties, individual fiber misalignment, and fabrication process variables (See Figs. 3a,3b).

This formulation is particularly well suited to the probabilistic description of fiber composite material properties. Since the micromechanics and laminate equations can be used to calculate ply properties at any number of points in a ply, a tractable finite element structural analysis based only on simple distributional assumptions for physical parameter variations can be performed. This model supplies a rational procedure for composite material property assessment, because it treats the material as the result of a series of random processes which occur at the intraply level.

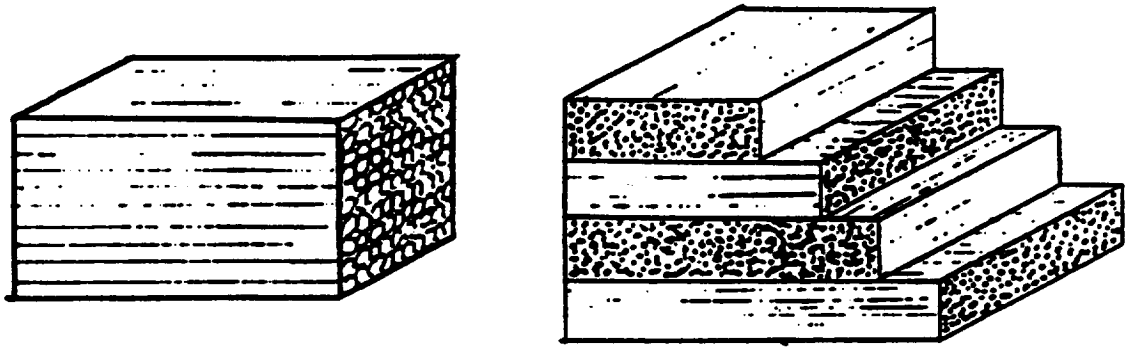

(a) orthotropic ply (b) laminate

Fig. 2- Conventional Model

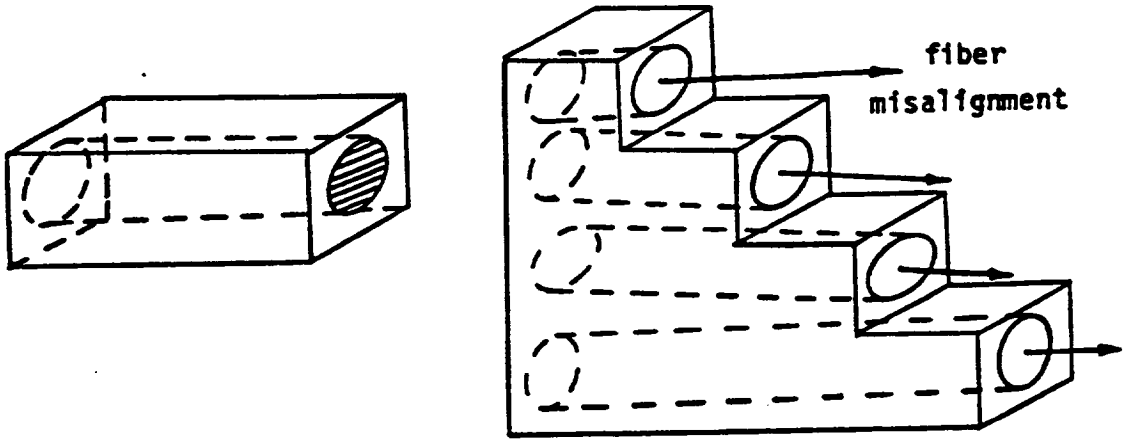

(a) subply (b) ply

Fig. 3- Substructure Model

D. Method of Investigation

1. Brief Description of ICAN

The Integrated Composite Analyzer (ICAN) is a computer program for comprehensive linear analysis of multilevel fiber composite structures. The program contains the essential features required to effectively design structural components made from fiber composites. It now represents the culmination of research conducted since the early 1970's, at the National Aeronautics and Space Administration (NASA) Lewis Research Center (LeRC), to develop and code reliable composite mechanics theories. This user friendly, publicly available code incorporates theories for

1. conventional laminate analysis
2. intraply and interply hybrid composites
3. hygral, thermal, mechanical properties and response
4. ply stress-strain influence coefficients
5. microstresses and microstress influence coefficients
6. stress concentration factors around a circular hole
7. predictions of delamination locations around a circular hole
8. Poisson's ratio mismatch details near a straight free edge
9. free edge interlaminar stresses
10. laminate failure stresses
11. normal and transverse shear stresses
12. explicit specification of matrix-rich interply layers
13. finite element material cards for NASTRAN, MARC

A detailed description of ICAN can be found in Reference (3). The ICAN code and documentation are available through COSMIC, the Computer Software Management and Information Center, Suite 112, Barrow Hall, Athens GA, 30602.

2. Summary of Variables

The variables studied in this work can be separated into two categories. The independent variables to be simulated using random sampling consist of the following (see Fig. 4a for fiber coordinate system):

Geometry:	
fiber orientation angle	(THETA)
Fabrication variables:	
fiber volume ratio	(FVR)
void volume ratio	(VVR)
Fiber properties	
longitudinal elastic modulus	(EFP1)
transverse elastic modulus	(EFP2)
shear modulus, 1-2 plane	(GFP12)
shear modulus, 2-3 plane	(GFP23)
fiber tensile strength	(SFPT)
fiber compressive strength	(SFPC)
Matrix properties	
elastic modulus	(EMP)
matrix tensile strength	(SMPT)
matrix compressive strength	(SMPC)
matrix shear strength	(SMPS)

The dependent variables to be calculated using ICAN consist of the following ply properties, measured about the material axes (see Fig. 4b):

normal modulus in 1-1 direction	(EC11)
normal modulus in 2-2 direction	(EC22)
shear modulus in 1-2 plane	(EC12)
Poisson's ratio for strains in 2 direction induced by stresses in 1 direction	(NUC12)
Poisson's ratio for strains in 1 direction induced by stresses in 2 direction	(NUC21)
Coefficients of thermal expansion	
in 1-1 direction	(CTE11)
in 2-2 direction	(CTE22)
coupling coefficient	(CTE12)

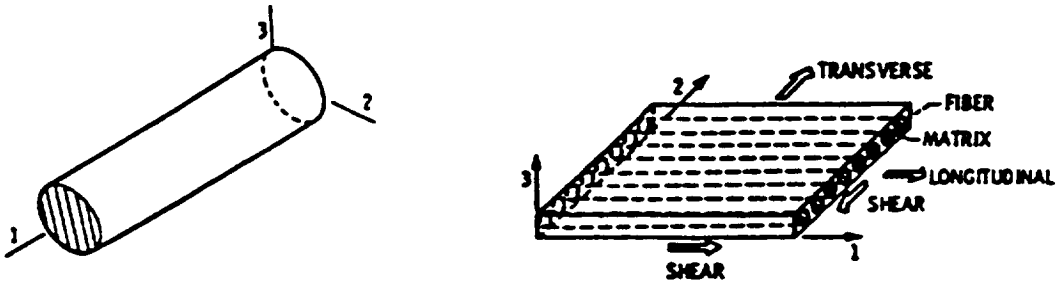

(a) fiber (b) material

Fig. 4- Coordinate Systems

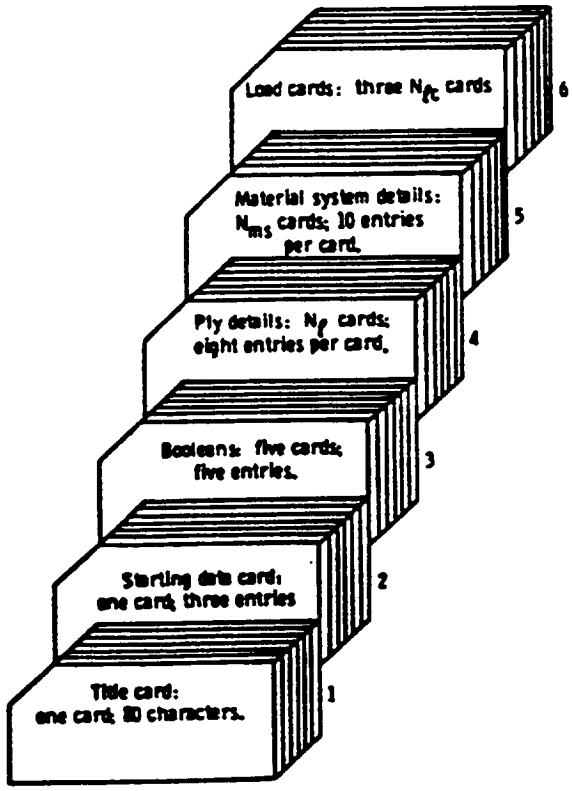

Fig. 5- Order of ICAN input data cards

Ply strengths in material directions

longitudinal tensile	(SCXXT)
longitudinal compressive	(SCXXC)
transverse tensile	(SCYYT)
transverse compressive	(SCYYC)
in-plane shear	(SCXYS)

The descriptions above should be consulted periodically for the definitions of variables that henceforth will be referred to symbolically.

3.Monte Carlo Methods

Complicated stochastic processes can be simulated by a variety of numerical methods generally referred to as Monte Carlo methods (Ref. 8). The term refers to that branch of experimental mathematics concerned with experiments on random numbers. Since the advent of high speed computers, they have found extensive use in most fields of science and engineering, in analyzing many physical processes of a statistical nature, or where direct experimentation is not feasible. In general, they can be economically used to achieve a level of precision between 90 and 95 percent.

A Monte Carlo experiment refers to the procedure of randomly assigning a value to an independent random variable in a chosen model, and observing the dependent variable at the conclusion of the process being modeled. A Monte Carlo procedure is composed of n such independent experiments. When n is sufficiently large, the observations will yield, by virtue of the laws of large numbers, a statistically meaningful description of the physical problem.

The form of Monte Carlo used in this study is as follows:

1. Define the system model by assuming
   a. model regression function
   b. method of error incorporation
   c. probability distributions of all errors (for all independent variables)
   d. any equations used to model the phenomena of interest
2. Use the computer and random sampling techniques to select values of the independent variables.
3. Calculate dependent (output) variables using the prescribed

equations.

4. Estimate regression parameters for the assumed model.

5. Replicate the experiment, each time with a new set of input values.

6 Use appropriate statistical methods to calculate properties of the distribution of parameter estimates.

E. Brief Summary of Results

A ply made from the AS-Graphite /IM6S epoxy composite system is studied. The monte carlo scheme is used to generate a number of response results, which are analyzed in graphical and numerical form, to supply a random process description of composite ply elastic constants, thermal expansion coefficients, and strengths. Histogram and distribution plots of results for assumed narrow and wide variations in input properties are compared with a deterministic base case for an aligned ply. The figures demonstrate the range of values that response variables assume for the example data under consideration.

Confidence intervals are calculated for response variables in subsequent samples, which are normalized with respect to an appropriate independent variable, to yield plots of normalized response as a function of fiber volume ratio, for various values of distribution parameters for the related independent variable. These plots demonstrate the sensitivity of ply properties to randomly selected uncertainties in constituent and fabrication variables.

Several multiple linear regression models were calculated for response variables. The relative correlation of predictor (independent) variables with response is studied for all output properties considered. Varying levels of significance were achieved in the regression equations, due to the differences in complexity of response variables. Elastic constants can be described adequately with simple regressor functions, and generally explain between 80 and 99 percent of the observed response variations about a mean. The regression models

studied for strength, although achieving better reliability with higher order regressor functions, demonstrate such low significance as to be practically useless for predictive purposes. This is not an unexpected result, because of the complex nature of strength behavior in composite materials.

CHAPTER II

METHODS OF CALCULATION

A. Overall plan

1. Input structure for ICAN

The input data for a typical execution of the available ICAN program consists of (see Fig 5)

1. header card
2. control cards
3. ply data cards
4. material system cards
5. load cards

For repeated use of the ICAN program, input data files must be created and used one at a time. Each successive run of the master program (of which ICAN is made a subroutine) writes the input file from user-supplied parameters and calls ICAN. The ply data cards contain randomly generated fiber orientation angle values. The material system cards contain randomly generated values for fiber and void volume ratios.

2. Constituent Property Variations

Each successive execution of ICAN uses a distinct set of material properties for fiber and matrix. The random number generation is performed with user-supplied parameters which are stored in a separate file. The options of using either generated properties or using the values contained in the resident data bank are available. Any subset of the parameters described may be generated or held constant with proper specification of the Booleans which control the input to the ICAN program. (see Figs. 6,7)

```
FIBER STRENGTH VARIES; CONSTANT FIBER VOLUME RATIO OF 0.30;TAPE 003131
  STDATA      15       1      15       T
     T     50      T      F      T      T
     F          000.0   10.0  0.300  0.200   3.00      5
     F
     F
     T                          70.00   70.00      .0              .000
     PLY                                AS-1IMHS   0.0      .57     .03
  MATCRDAS-1IMHS
   PLOAD    10.        0.0      0.0      0.0
   PLOAD     0.0       0.0      0.0
   PLOAD     0.0       0.0
  OPTION       0
```

Fig. 6- Command Input

```
EFP1      T    0.3100E 08    0.3000E 07
EFP2      T    0.2000E 07    0.2000E 06
GFP12     T    0.2000E 07    0.2000E 06
GFP23     T    0.1000E 07    0.1000E 06
SFPT      T    0.4000E 06    0.1000E 02
SFPC      T    0.4000E 06    0.1000E 02
EMP       T    0.5000E 06    0.5000E 05
SMPT      T    0.1500E 05    0.1000E 02
SMPC      T    0.3500E 05    0.1000E 02
SMPS      F    0.1300E 05    0.1000E 02
```

Fig. 7- Constituent Variation Input. Example for AS-1 Graphite fiber and IMHS Epoxy matrix, with wide variations of stiffnesses and strengths.

3. Repeated runs

The user must specify the number of ICAN runs desired in a given sample. In this study, fifty (50) runs were used throughout, to take advantage of the simplification in statistics by using suitably large samples. From elementary statistics, it is known that any process that is the result of the combined interaction of several probabilities can be assumed to approximate a normal distribution. For phenomena that are assumed to approximate a normal distribution, the simplest forms for calculating statistics apply to suitably large samples (usually greater than thirty). The sample size of fifty was chosen to supply a practicably large amount of data, within the restrictions imposed on computation time.

The data generated by repeated execution of the ICAN routines is stored in a sequential access dataset, where the 50 output files are separated by end of file markers. This arrangement allows a single Fortran unit to be used for output throughout. A simple flowchart of the data generation routines is shown in Fig. 8(a).

4. Data collection

The ICAN output files are searched to locate the specific material properties and strengths of interest in this study. The flowchart of data collection routines is shown in Fig. 8(b). After obtaining the sample of ICAN output, the investigator may choose to scrutinize parameters or calculate statistics aside from those chosen in this study. This is likely, in light of the large quantity of data available and the need for limiting the scope of this particular study to

representative properties. The user would have to supply additional code or adapt existing code to suit his purposes in this case. The coded modifications to ICAN used in this study are included in Appendix A.

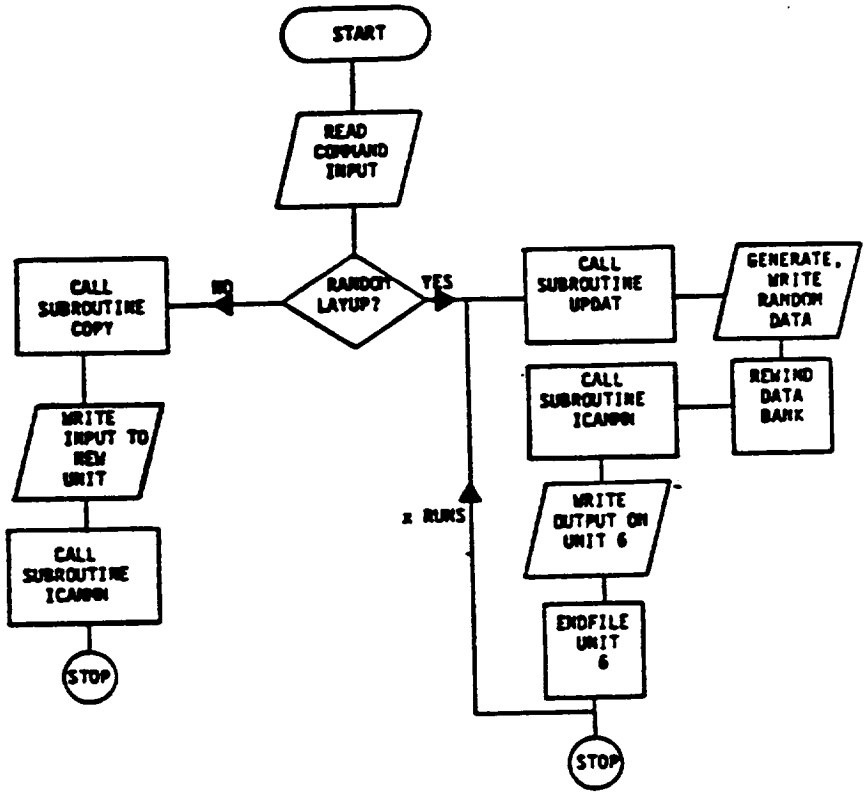

(a) data generation program

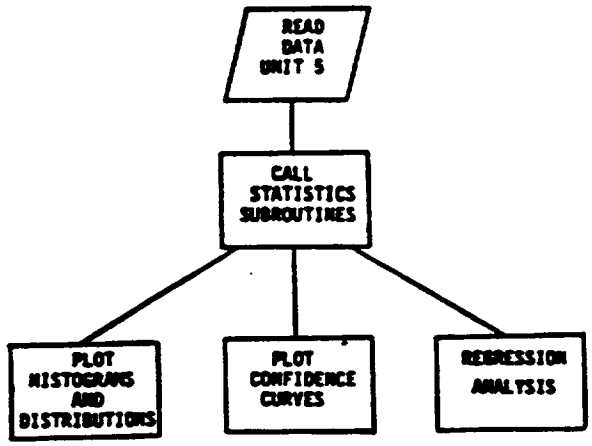

(b) analysis procedures

Fig. 8- Flow chart of Probabilistic Integrated Composites Analyzer

B. Generation of Pseudo Random Numbers

An integral part of any monte carlo simulation is the use of random numbers having a specified distribution which is assumed to characterize the process under study. Indeed, many statistics textbooks carry tables of random numbers as appendices. Simulations using large samples require many repeated calculations, each with different "random" numbers. Since filling of a computer memory with a large table of random numbers is wasteful, algorithms have been developed (Ref. 9) to generate streams of random numbers whenever needed in the process of calculations. The numbers used are usually obtained using some form of a recursion relation, hence the sequence is termed pseudo-random.

1. Uniform Distribution

The starting point for many random number schemes is the uniform random number generator, which simulates a sample from the uniform distribution. A continuous random variable has a uniform distribution over an interval a to b (b > a) if it is equally likely to take on any value in this interval. The probability density function is thus constant over (a,b) and has the form

$$f(x) = \frac{1}{b - a} \qquad a \leq x \leq b$$

$$= 0 \qquad \text{elsewhere}$$

The probability distribution function is, on integrating

$$F(x) = 0 \qquad x < a$$

$$= \frac{x - a}{b - a} \qquad a \leq x \leq b$$

$$= 1 \qquad x > b$$

The uniform distribution is shown in density and distribution form in Figs. 9a and 9b.

Lehmer (Ref. 10) proposed the congruential method of generating pseudo random numbers conforming to the uniform distribution. The recurrence relation takes the form:

$$x_i = (ax_{i-1} + b) \quad \text{modulo } m$$

where the notation signifies that x_i is the remainder when $(ax_{i-1} + b)$ is divided by m. The multiplier a, increment b, and modulus m are integers. The starting value x_0 must be assumed, and is known as the "seed" of the generator. Generators for which $b = 0$ are known as multiplicative. They are called mixed when b is nonzero. Because selection of the multiplier a and modulus m strongly influence the generator, most generators in use are of the multiplicative form. A discussion of the choice of parameters, maximum period, and degree of correlation of this generator is available (Ref. 11).

For a given uniform random number u on the interval (0,1) a random number x having a desired distribution $F(x)$ is often obtained by solving the equation $u = F(x)$ for x (Ref. 12). Since the process requires the determination of the inverse distribution function $F^{-1}(x)$, its use depends on the ease of deriving the expression or some approximation. The following sections describe the distributions used, and methods for generating random numbers on those distributions.

2. Normal (Gaussian) Distribution

The most common distribution is the familiar normal distribution, with the "bell shaped" density function, given by

$$f(x;\mu,\sigma^2) = \frac{1}{\sqrt{2\pi\sigma^2}} \exp\left[- \frac{(x-\mu)^2}{2\sigma^2} \right]$$

$$-\infty < x < \infty, \ \mu < \infty, \text{ and } \ \sigma > 0$$

with mean μ and standard deviation σ. The distribution function is written

$$F(x) = \frac{1}{\sqrt{2\pi\sigma^2}} \int_{-\infty}^{x} \exp\left[- \frac{(u-\mu)^2}{2\sigma^2} \right] du$$

which cannot be expressed in closed form analytically but can be numerically evaluated at any value of x.

The Box-Muller or "Polar" method (Ref. 13) is most commonly used for generating random deviates from a mean to approximate the normal distribution. If x_1 and x_2 are independent uniform random variables, then

$$y_1 = \sigma(-2 \ln x_1)^{0.5} \cos 2\pi x_2 + \mu$$
$$y_2 = \sigma(-2 \ln x_1)^{0.5} \sin 2\pi x_2 + \mu$$

are independent random variables with the standard normal distribution having mean μ and standard deviation σ.

3. Gamma Distribution

The gamma distribution is a two-parameter distribution which is flexible in fitting a variety of random processes. It is a one sided distribution in that physical quantities that are limited to values in the positive range are frequently modeled by it. Its density function is given by

$$f(x) = \frac{\lambda^k}{\Gamma(k)} e^{-\lambda x} x^{k-1}$$

where $x, \lambda, k > 0$, and k is an integer.

The parameters λ and k may be interpreted as scale and shape parameters, respectively. $\Gamma(k)$ is the well known gamma function,

$$\Gamma(k) = \int_0^\infty u^{k-1} e^{-u} du,$$

which is widely tabulated. The gamma distribution function is given by

$$F(x) = \frac{\lambda^k}{\Gamma(k)} \int_0^x u^{k-1} e^{-\lambda u} du$$

$$= \frac{\Gamma(k,\lambda x)}{\Gamma(k)} \qquad x \geq 0$$

$$= 0 \qquad \text{elsewhere}$$

where $\Gamma(k,u)$ is the incomplete gamma function

$$\Gamma(k,u) = \int_0^u x^{k-1} e^{-x} dx$$

which is also widely tabulated. For integer values of k,

$$\Gamma(k) = (k-1)!$$

and the gamma distribution is known as the Erlangian distribution after A. K. Erlang, who introduced it in the theory of queues and Markov processes.

Gamma variates are generated using the sequence

$$u_1, u_2, u_3, \ldots \ldots u_k$$

satisfying the uniform distribution on the interval (0,1).

The recursion relation is

$$y_i = -\frac{1}{\lambda} \ln u_i,$$

$$x = \sum_{i=1}^{k} y_i = -\frac{1}{\lambda} \ln \prod_{i=1}^{k} u_i$$

where x is a gamma variate having parameters λ and k (Ref. 14).

4. Weibull Distribution

The Weibull distribution (Ref. 15) is most popular when modeling problems of reliability, material strength, and fatigue. The Weibull density function is given by

$$f(x;\alpha,\beta) = \alpha\beta x^{\beta-1}\exp(-\alpha x^{\beta})$$

$$0 \leq x < \infty, \quad \alpha > 0, \ \beta > 1$$

where α and β are the shape and scale parameters, respectively. The cumulative distribution function

$$y = F(x) = 1 - \exp[-(x/\beta)^{\alpha}]$$

leads immediately to the inverse relationship

$$F^{-1}(y) = x = -\beta[\ \ln(1-y)\ ]^{1/\alpha}$$

as the desired Weibull random generator when y is a uniform random variable.

Figures 9-12 show the above distributions in analytical form.

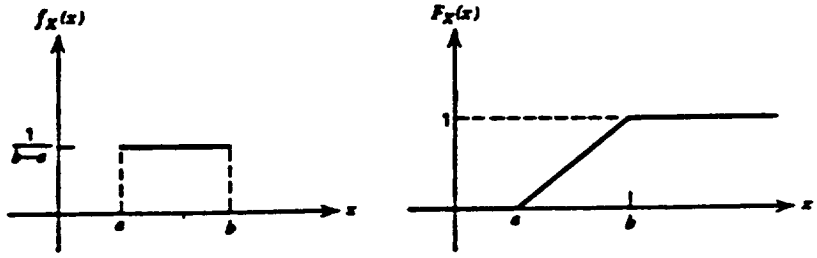

(a) density (b) distribution

Fig. 9- Uniform Distribution: general form.

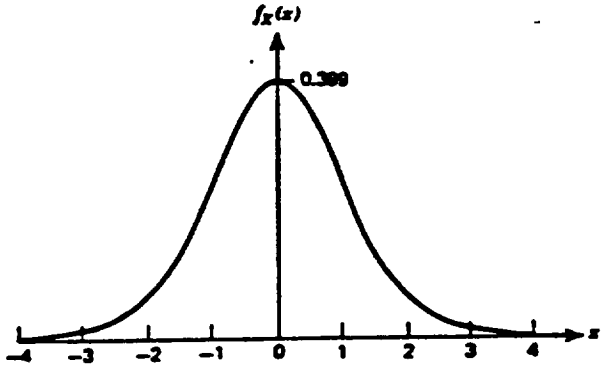

(a) density

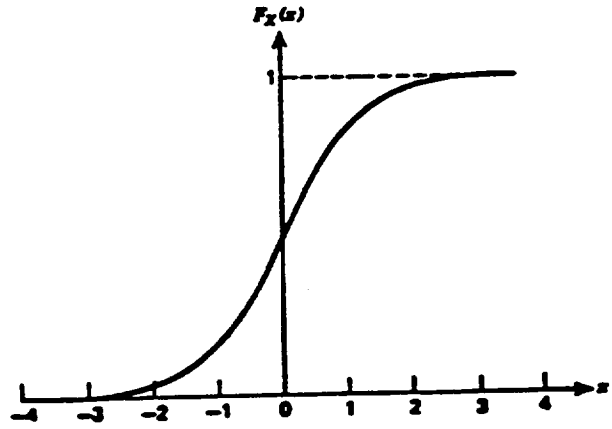

(b) distribution

Fig. 10- Normal Distribution

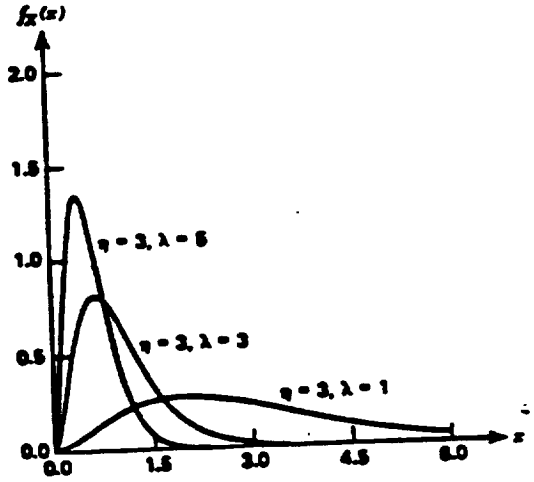

Fig. 11- Gamma Distribution density functions.

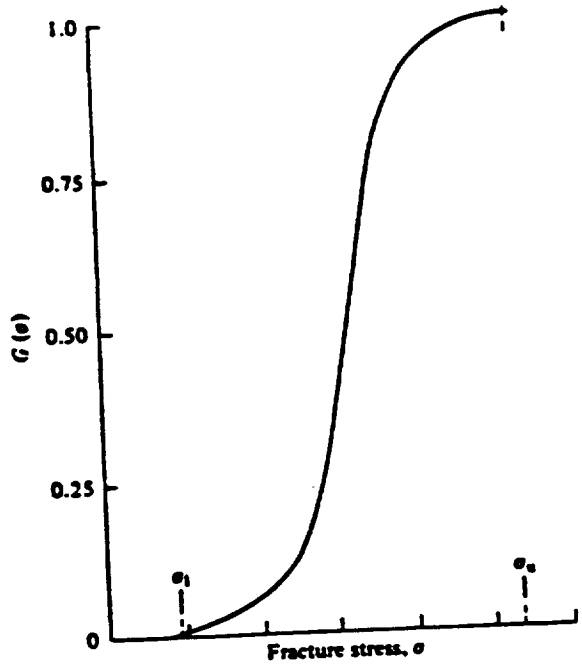

Fig. 12- Weibull Distribution function.

C. Distribution Assumptions

The variables chosen for variation are those for which reasonable assumptions can be made to describe their distribution. The fiber geometric configuration with respect to ply axes is assumed to follow a normal distribution with mean of zero (degrees) and some small standard deviation, to be specified. The fiber volume ratio is assumed to be normally distributed about some mean between 0.3 and 0.7. The void volume ratio, which is ideally small, is assumed to follow a gamma distribution skewed toward zero. (Note that in the gamma distribution used, a value of zero has a probability of zero. This model is chosen because the state of most present manufacturing technology precludes the fabrication of a fiber composite completely free of void.)

The properties of individual fibers and matrix are varied. The normal and shear moduli are assumed to follow the normal distribution, and the strengths are assumed to be Weibull distributed.

Figs. 13-27 show the results of random number generation in each distribution studied. The density (or histogram) and cumulative distribution plots are shown. Several weibull and gamma distribution simulations are shown, to demonstrate the effects of assumed parameter variations on the distribution sampling.

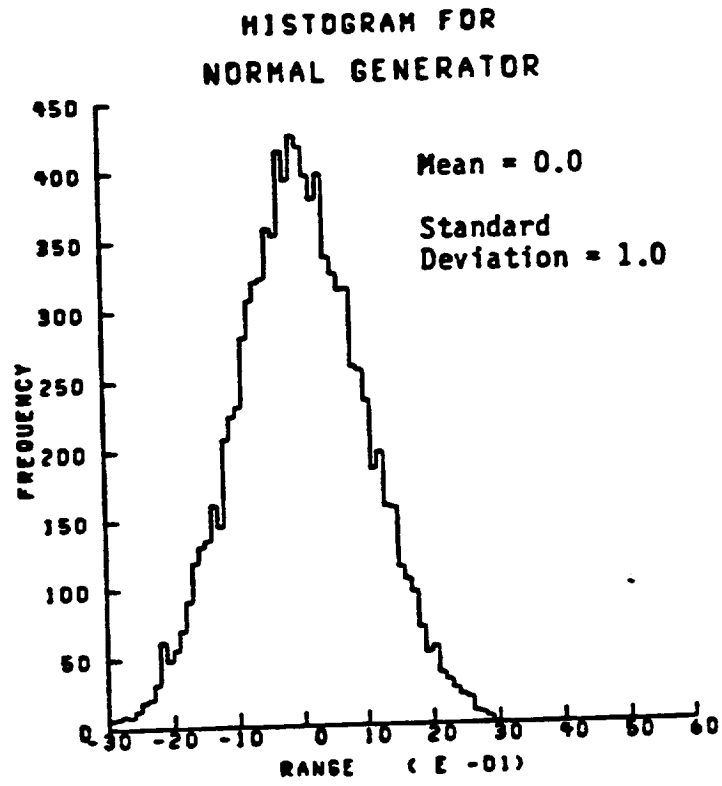

(a) histogram

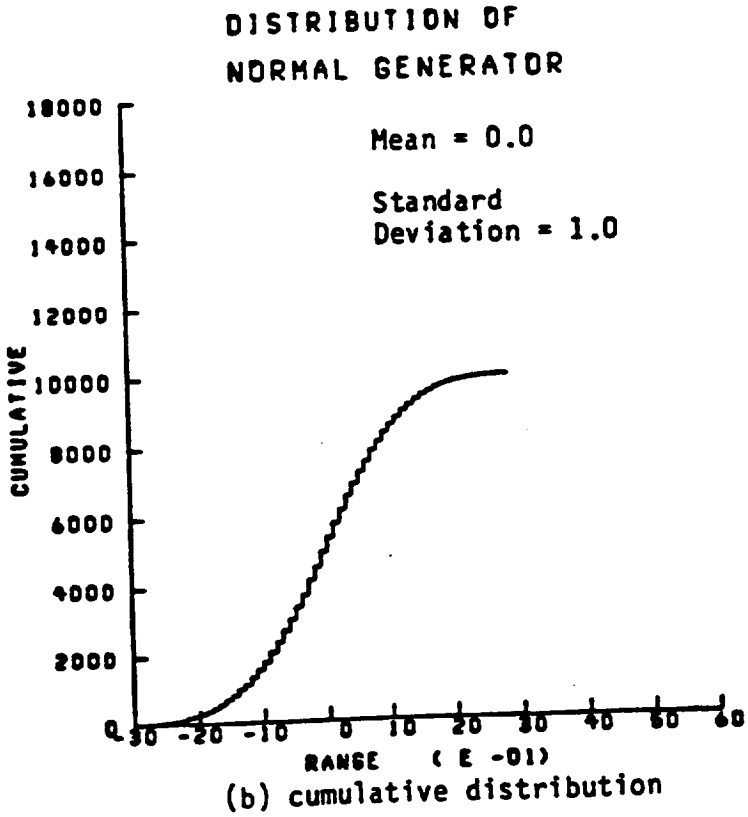

(b) cumulative distribution

Fig. 13- Normal Distribution Simulation with mean of 0.0 and standard deviation of 1.0.

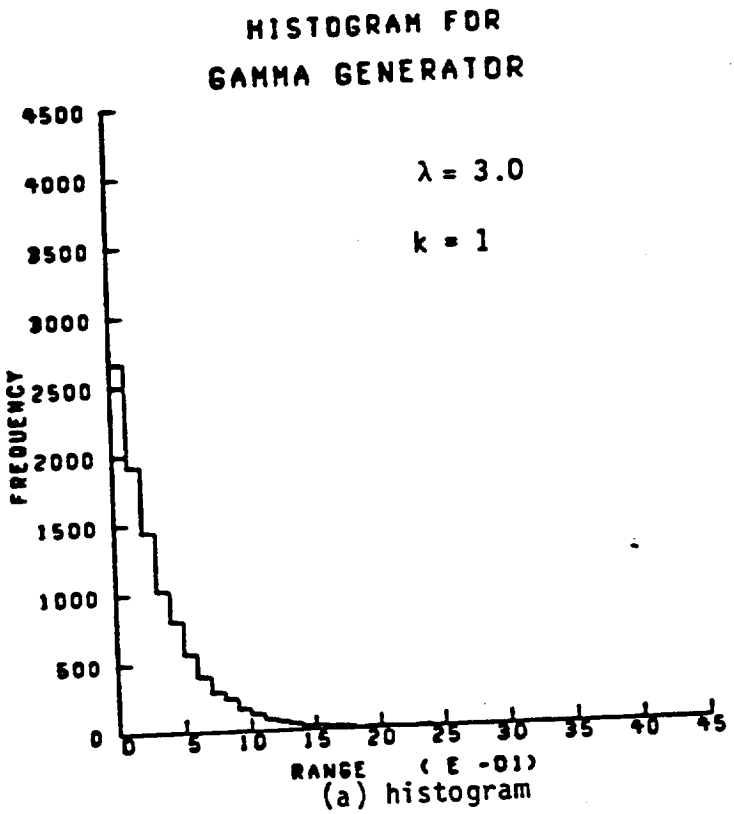

(a) histogram

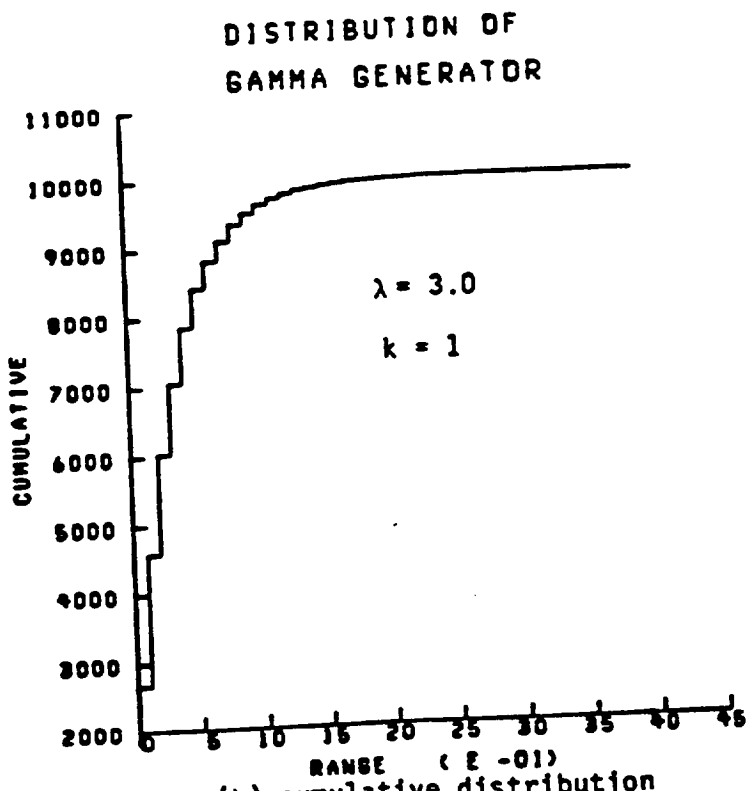

(b) cumulative distribution

Fig. 14- Gamma Distribution Simulation

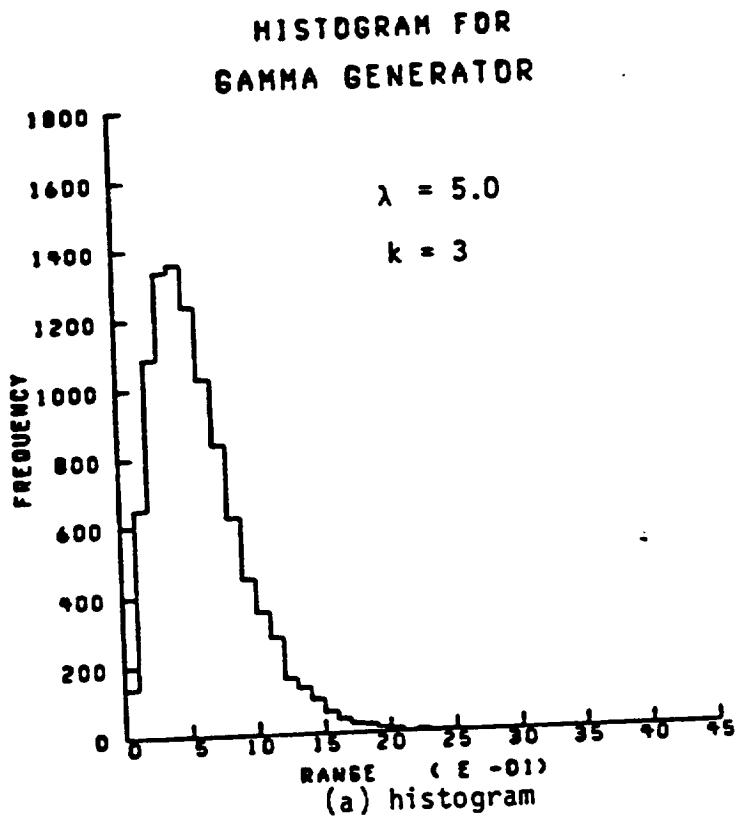

(a) histogram

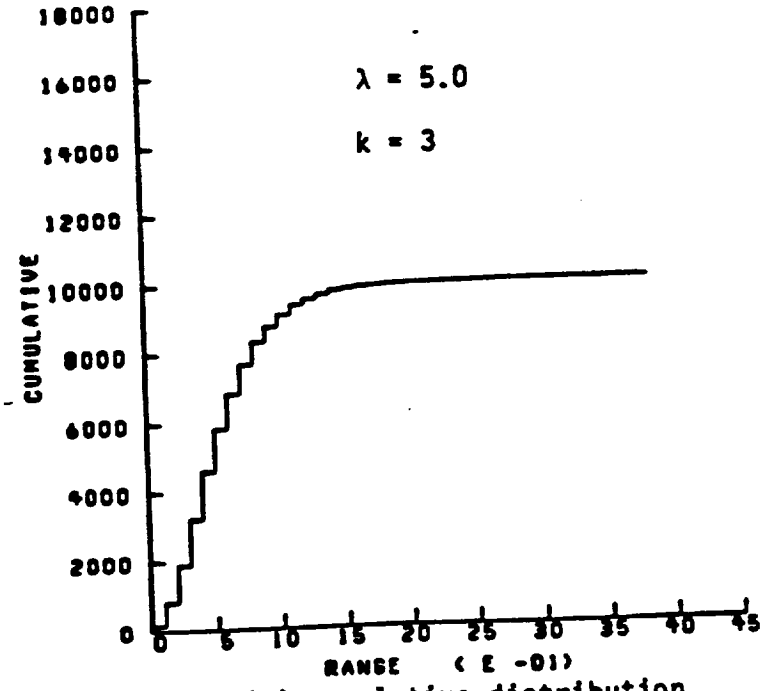

(b) cumulative distribution

Fig. 15- Gamma Distribution Simulation

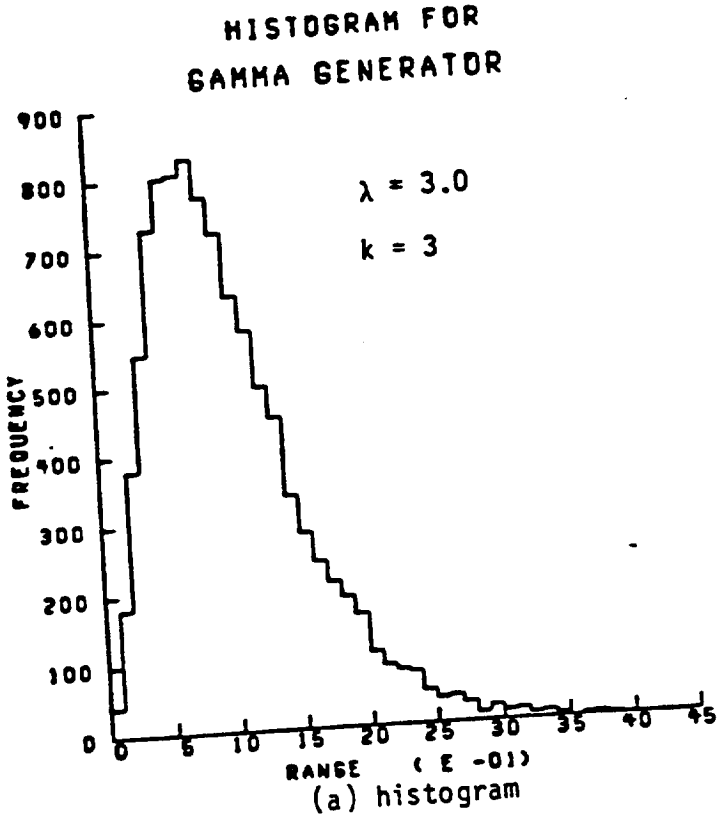

(a) histogram

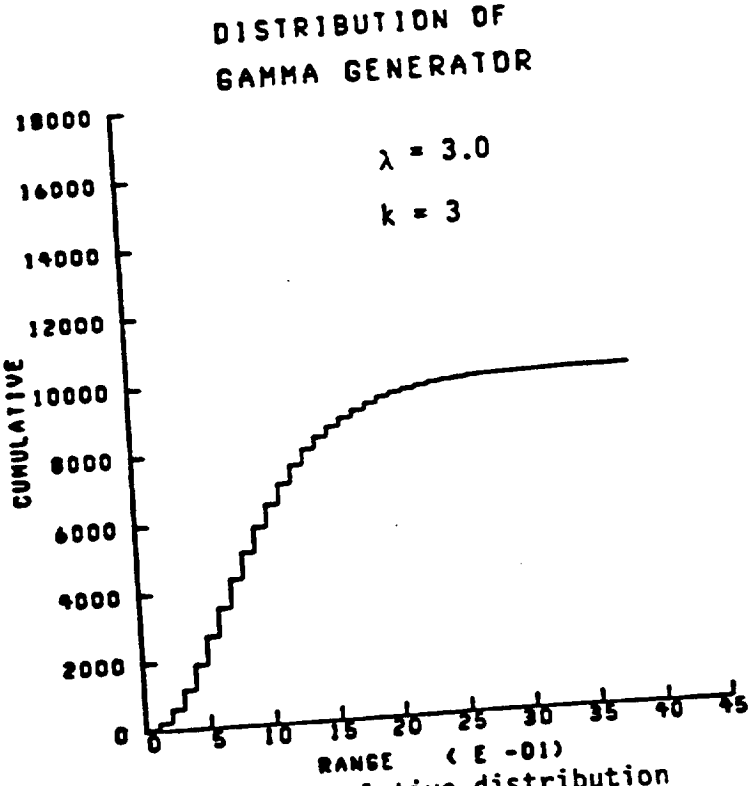

(b) cumulative distribution

Fig. 16- Gamma Distribution Simulation

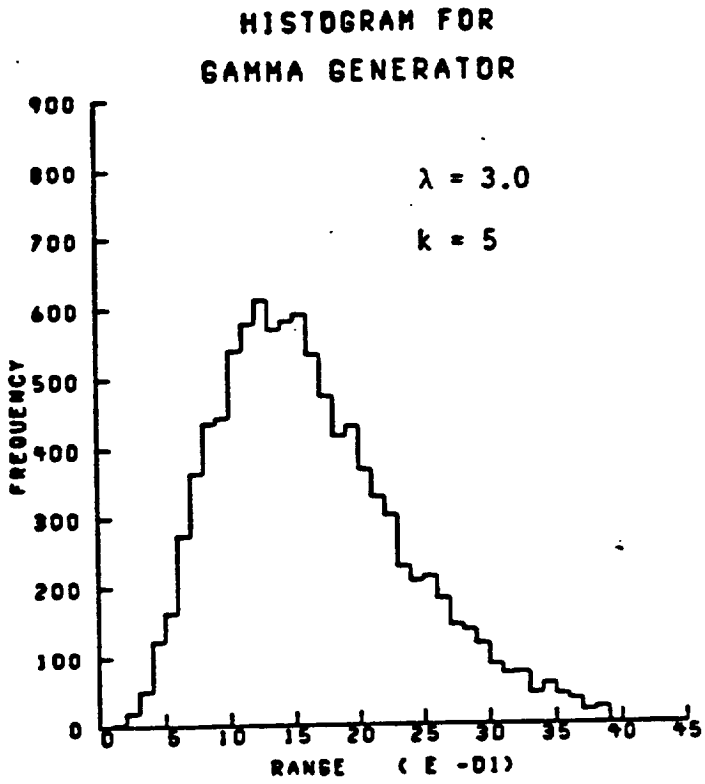

(a) histogram

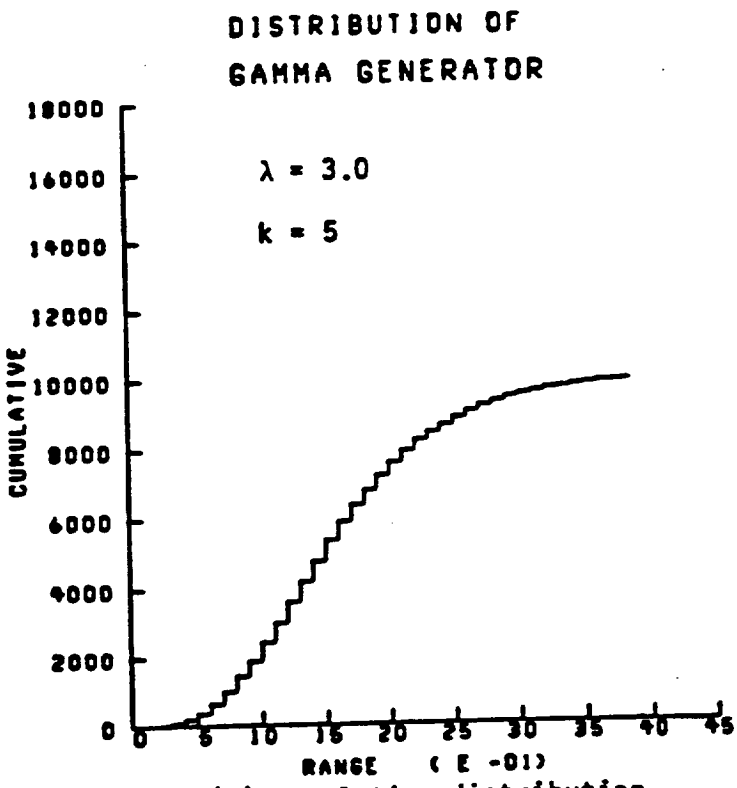

(b) cumulative distribution

Fig. 17- Gamma Distribution Simulation

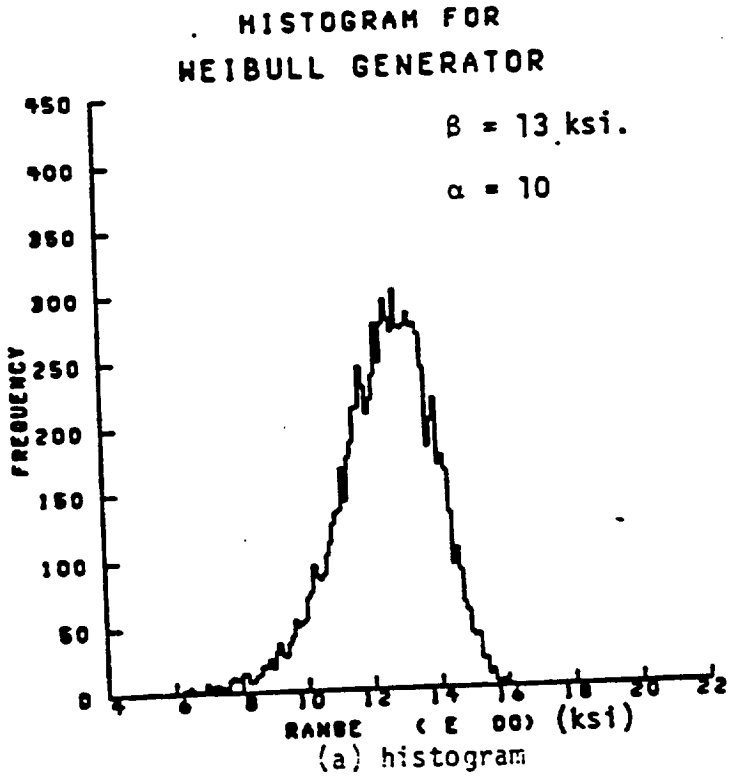

(a) histogram

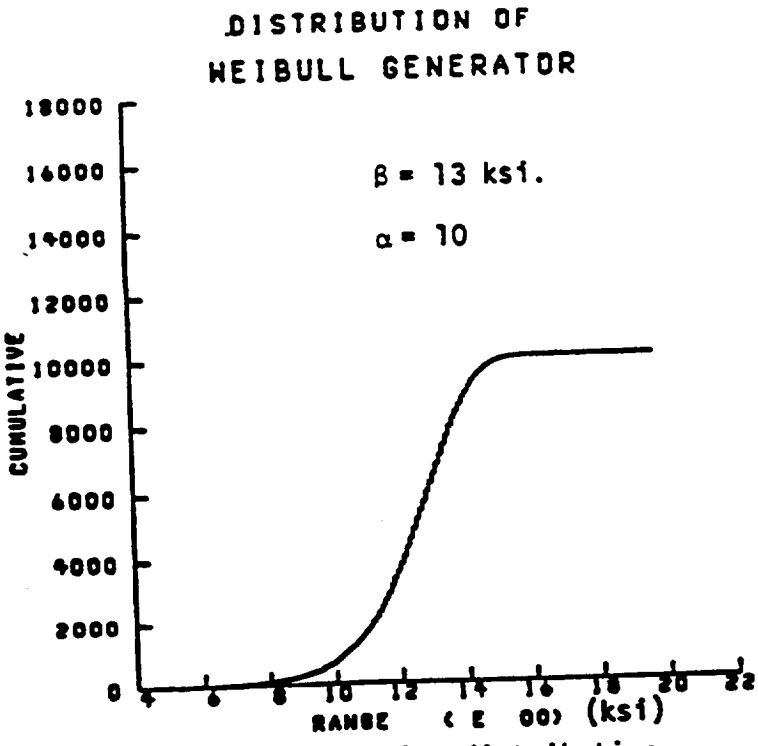

(b) cumulative distribution

Fig. 18- Weibull Distribution Simulation Matrix Shear Strength

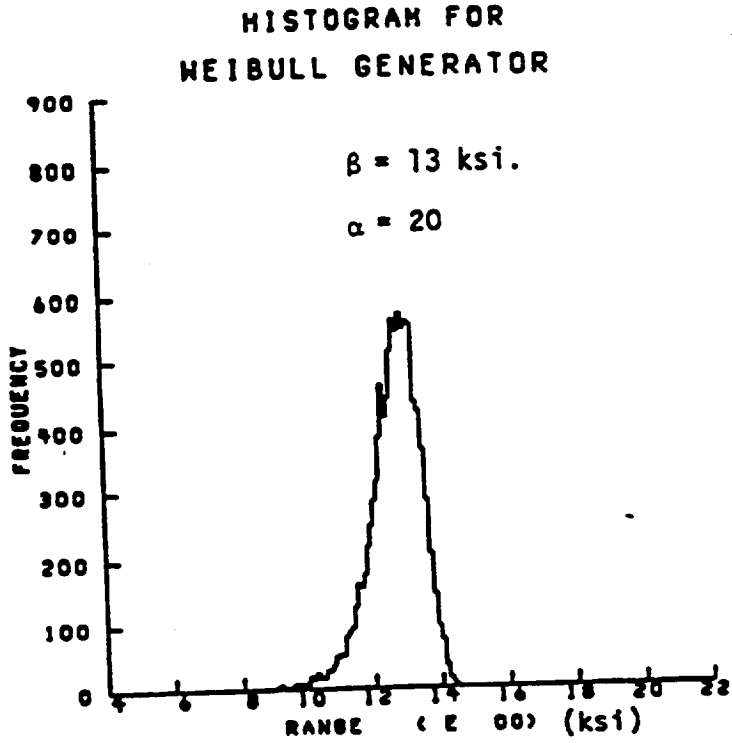

(a) histogram

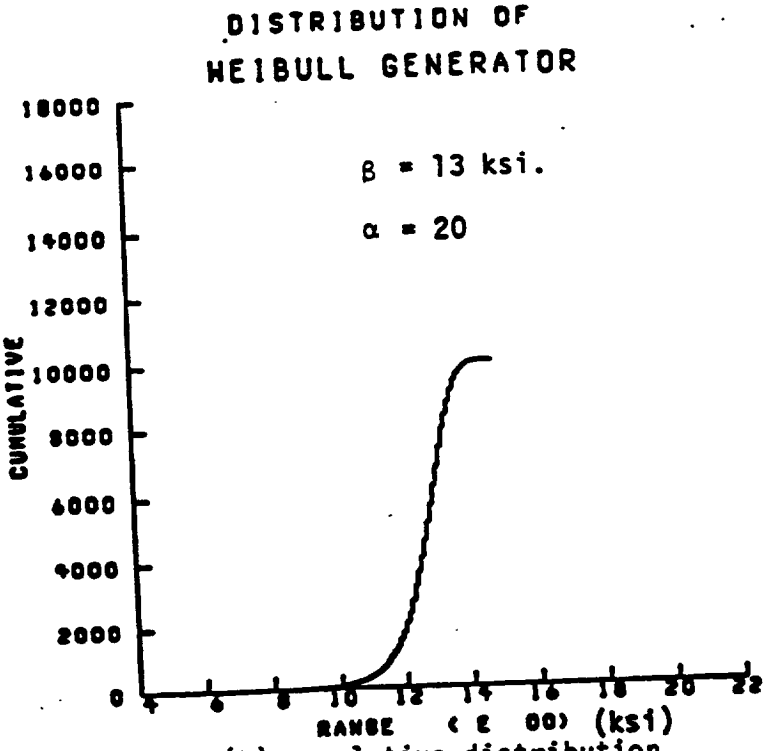

(b) cumulative distribution

Fig. 19- Weibull Distribution Simulation
Matrix Shear Strength

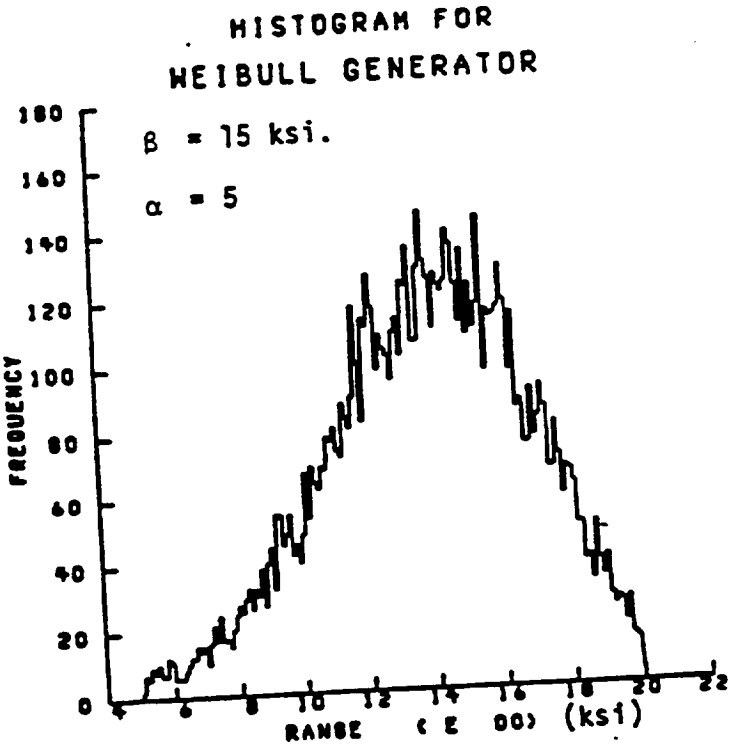

(a) histogram

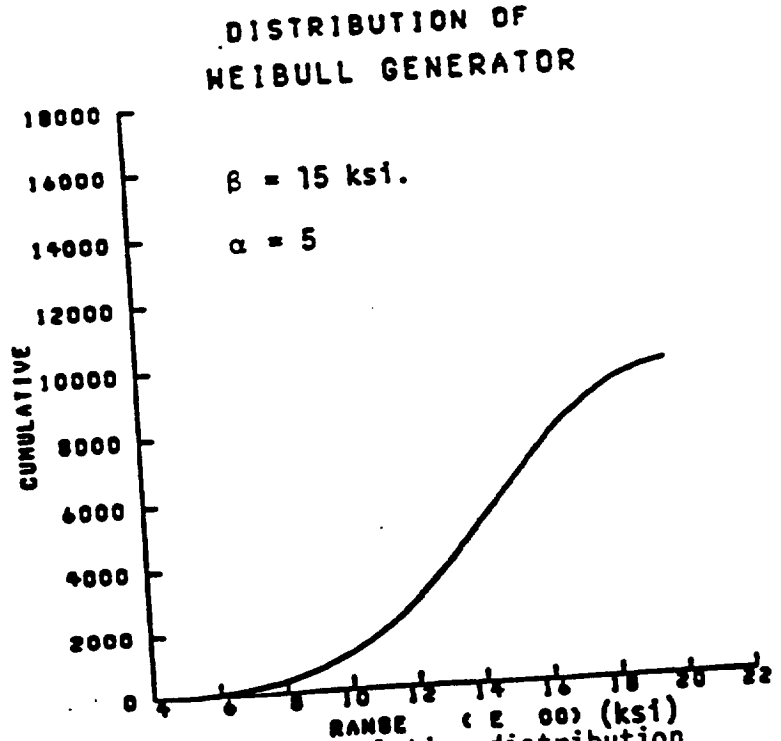

(b) cumulative distribution

Fig. 20- Weibull Distribution Simulation
Matrix Tensile Strength

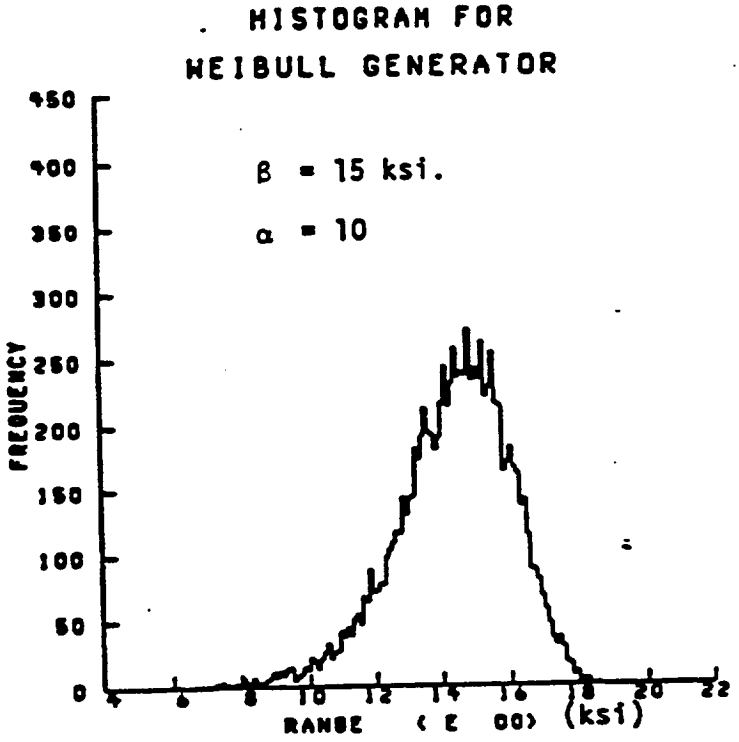

(a) histogram

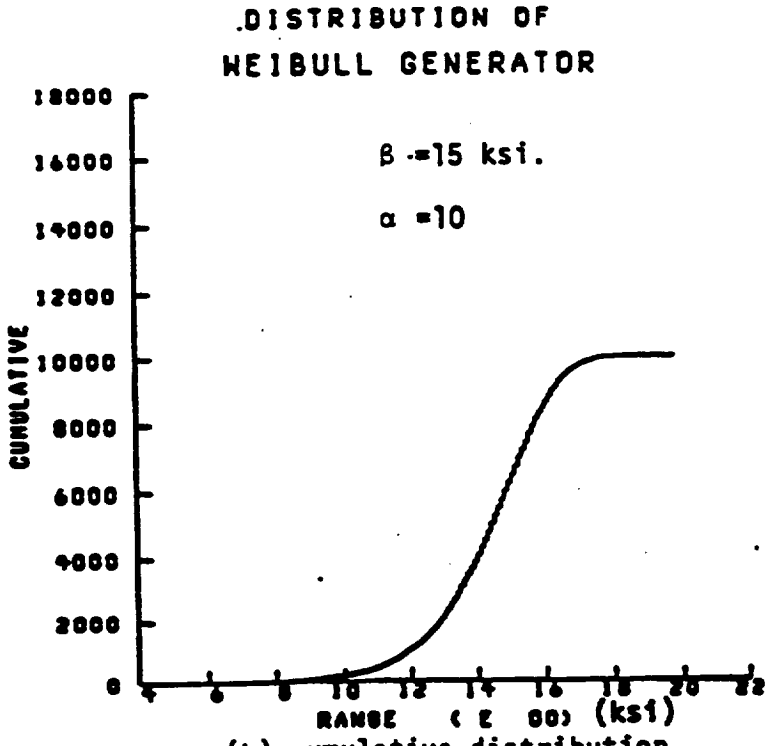

(b) cumulative distribution

Fig. 21- Weibull Distribution Simulation Matrix Tensile Strength

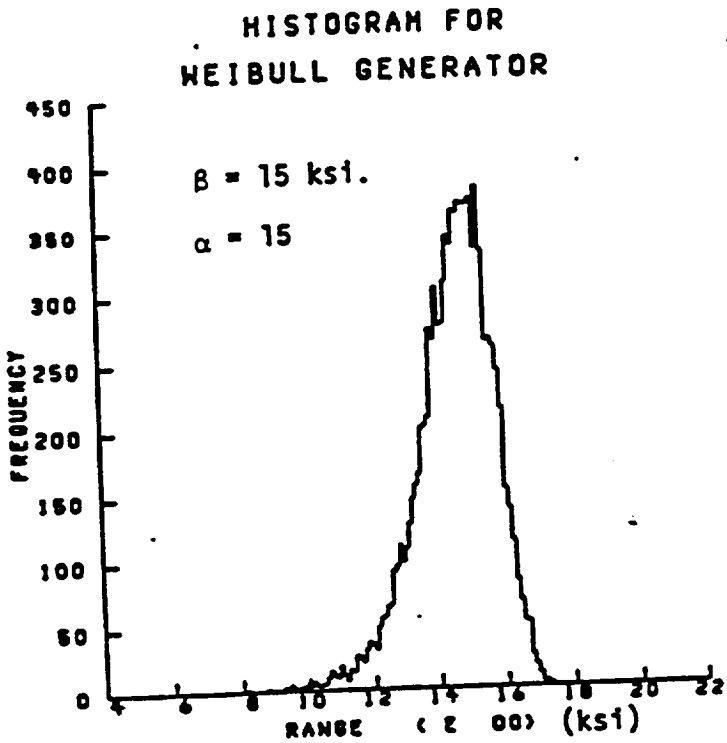

(a) histogram

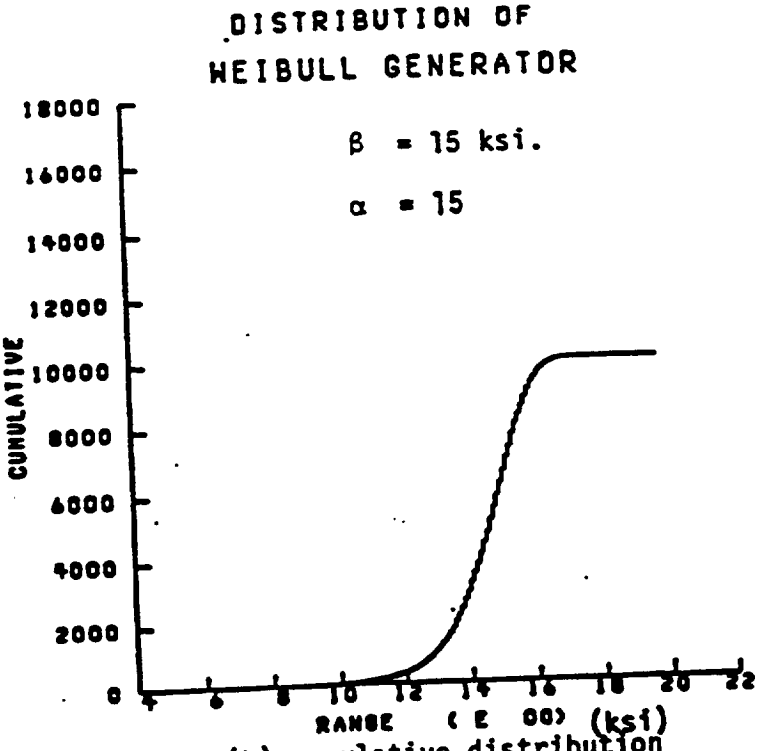

(b) cumulative distribution

Fig. 22- Weibull Distribution Simulation
Matrix Tensile Strength

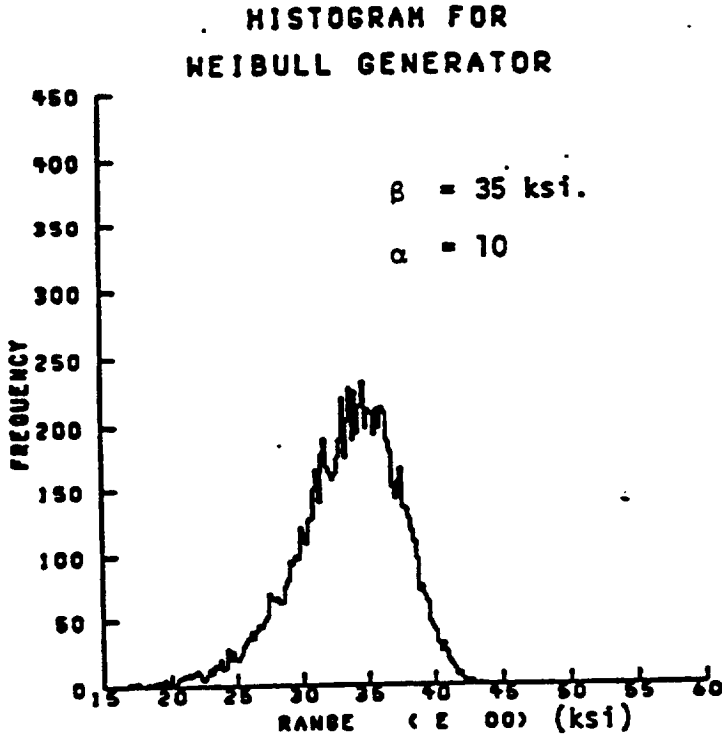

(a) histogram

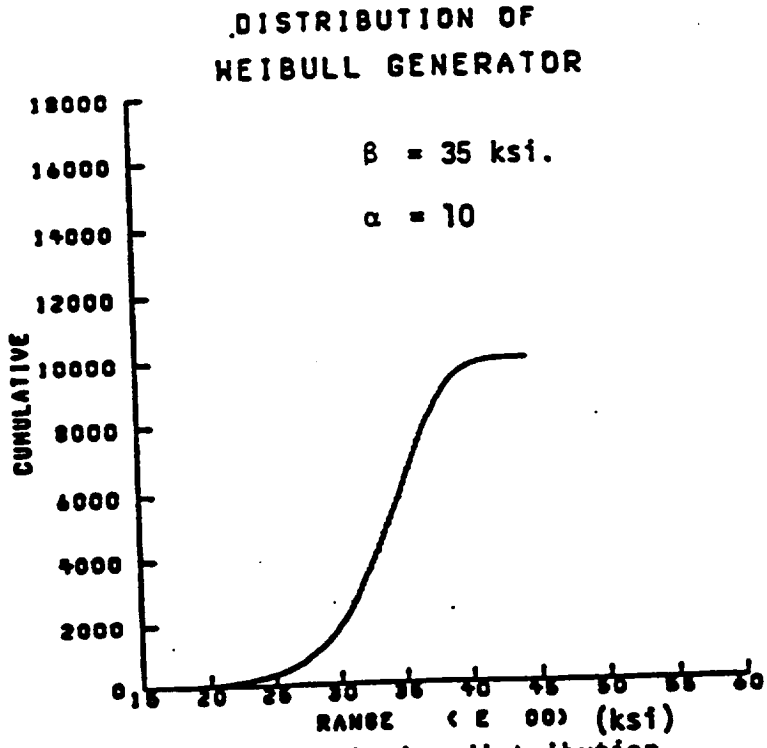

(b) cumulative distribution

Fig. 23- Weibull Distribution Simulation Matrix Compressive Strength

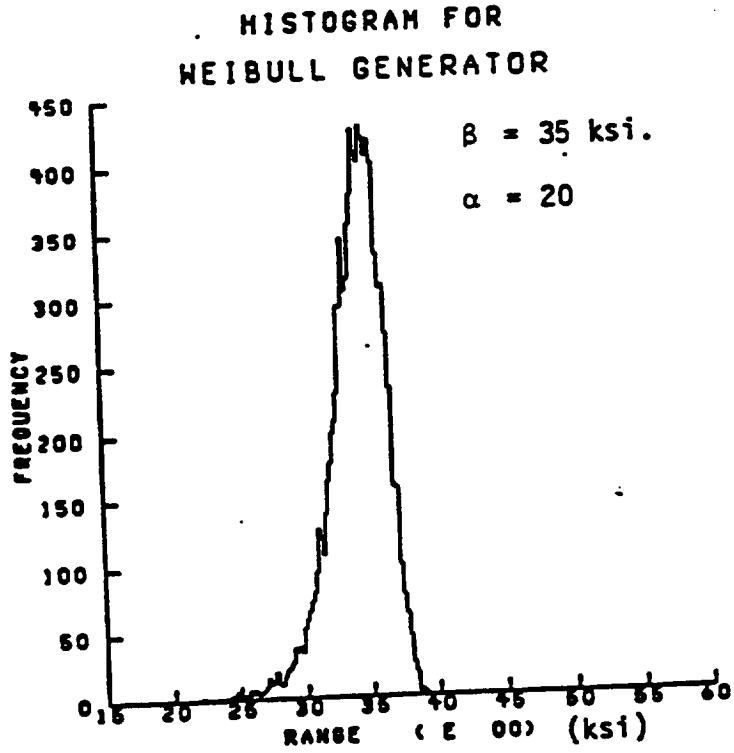

(a) histogram

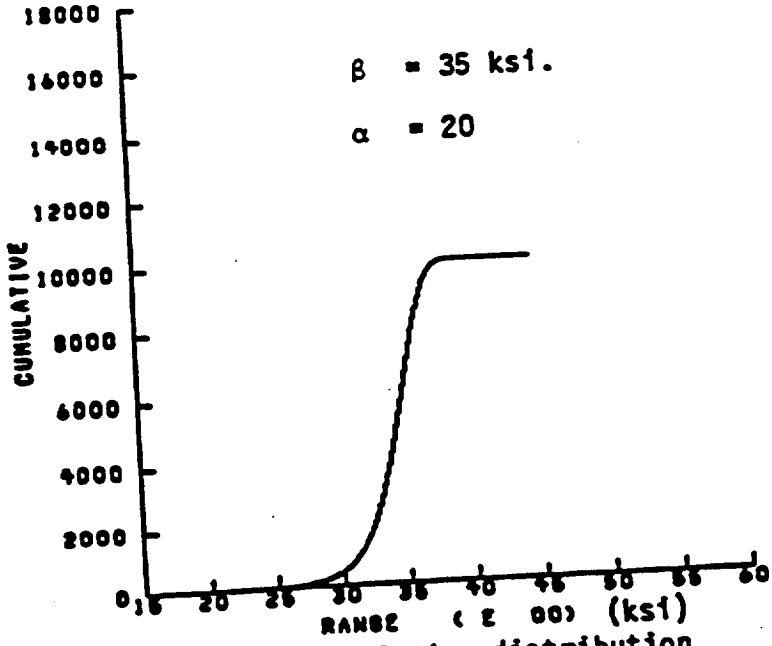

(b) cumulative distribution

Fig. 24- Weibull Distribution Simulation Matrix Compressive Strength

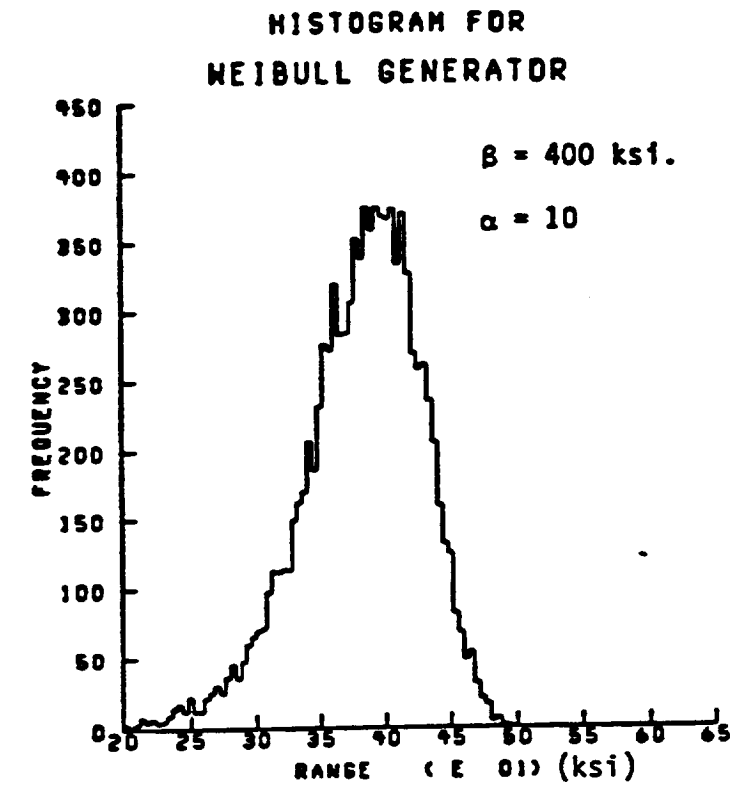

(a) histogram

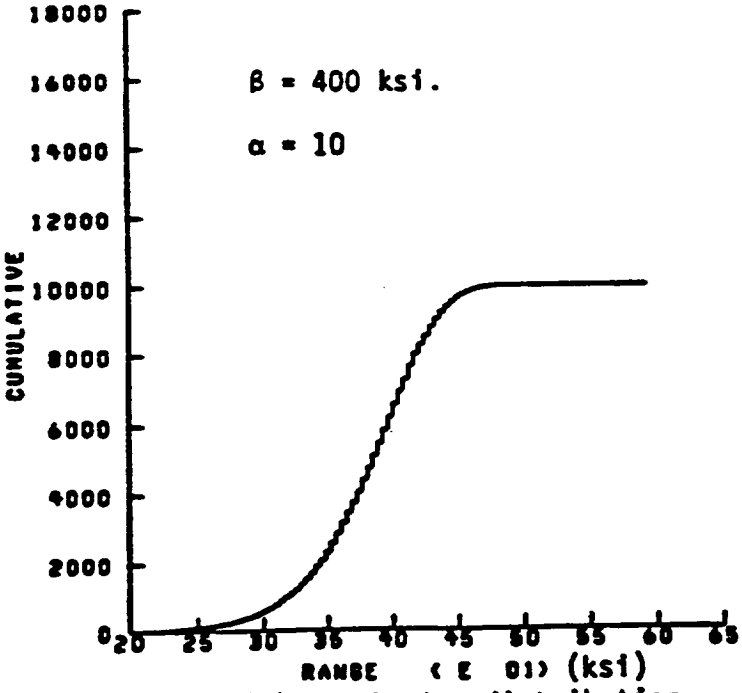

(b) cumulative distribution

Fig. 25- Weibull Distribution Simulation
Fiber Tensile and Compressive Strength

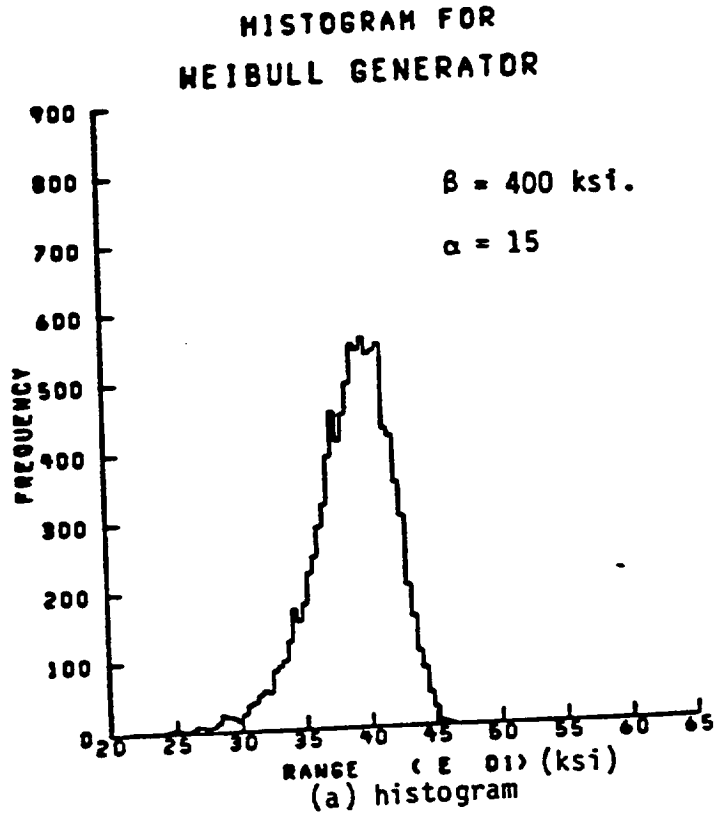

(a) histogram

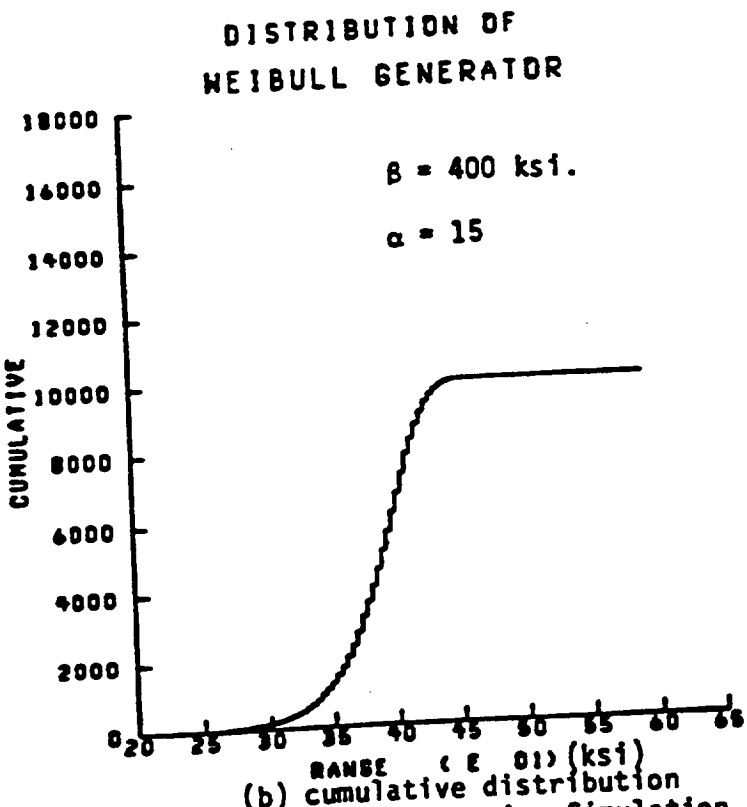

(b) cumulative distribution

Fig. 26- Weibull Distribution Simulation
Fiber Tensile and Compressive Strength

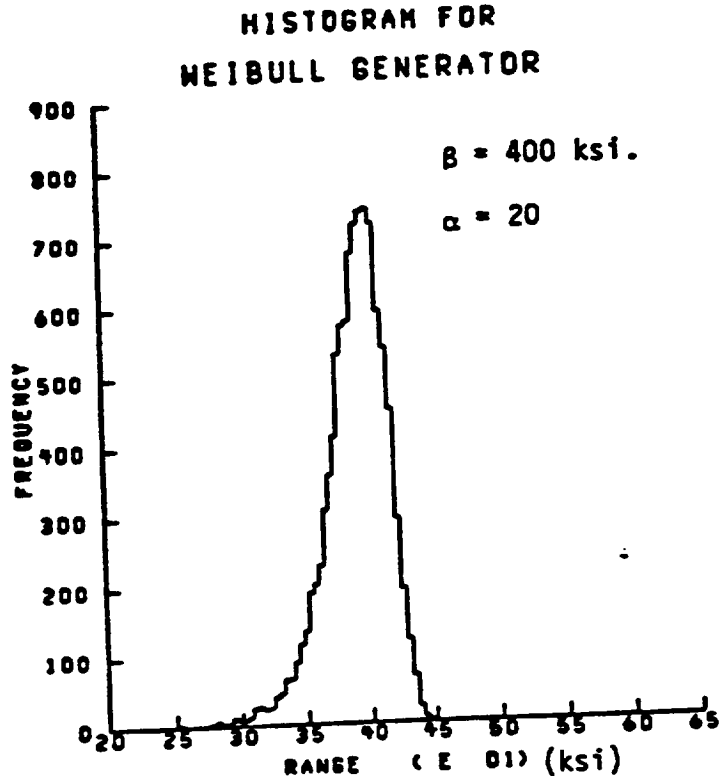

(a) histogram

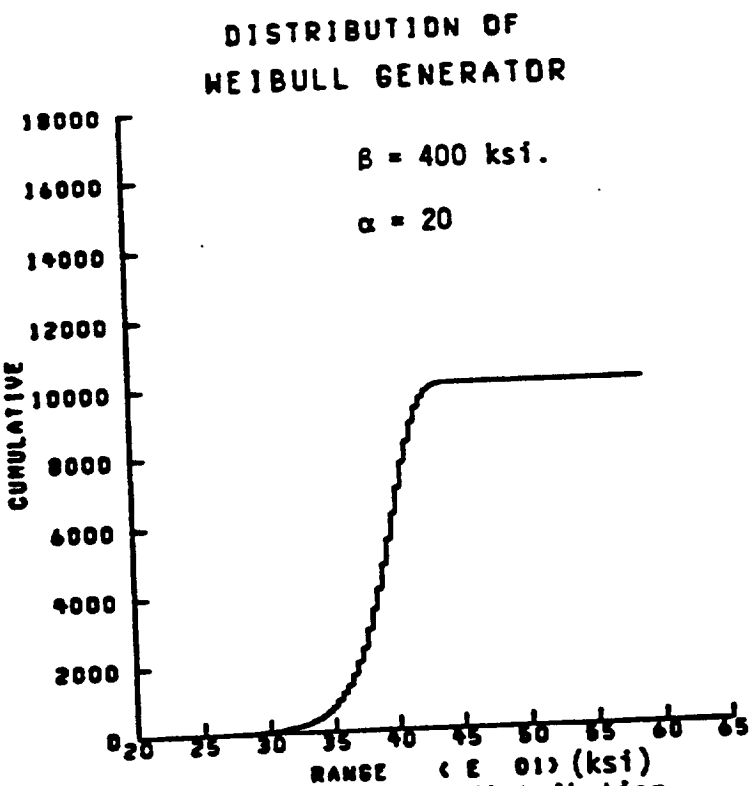

(b) cumulative distribution

Fig. 27- Weibull Distribution Simulation
Fiber Tensile and Compressive Strength

D. Use of ICAN

This section describes the essential theories and assumptions incorporated in the ICAN program. The symbolic notation conventions, formulations, and definitions are included in Appendix B.

1. Composite Micromechanics

The branch of composite mechanics which relates ply properties to constituent properties is known as composite micromechanics. The inputs consist not only of constituent material properties (fiber and matrix), but geometric configuration and fabrication process. Output includes ply hygral, thermal, and mechanical properties. The assumptions for equation development are: (Ref. 16)

1. The Mechanics of Materials are used to derive the equations, allowing each property to be individually identified.
2. The ply resists in-plane loads according to the schematic shown in Fig. 4(b).
3. The ply and its constituents behave in a linear elastic manner to fracture (see Fig. 28).
4. The ply is transversely isotropic in the 2-3 plane.
5. The matrix is isotropic.
6. Complete bond exists at the fiber-matrix interface.

The direction conventions and terminology used in the equations are:

1. Properties measured along fiber direction are called longitudinal.
2. Properties measured transverse to fiber direction are called transverse.
3. In-plane shear is also known as intralaminar shear.
4. All ply properties are defined with respect to ply material axes (1,2,3) for description and analysis.

2. Laminate Theory

Classical laminate theory supplies a convenient procedure to predict the response of a laminate to external load. The theory uses anisotropic elasticity to obtain the stress-strain relationship for the basic lamina. The stress-strain relations of individual laminae are transformed to coincide with a global set of reference axes. The stress-stain law of the laminate in terms of the properties and distribution of individual laminae are calculated using a summation. Resultant forces and moments are defined by integrating the stresses through the thickness of the laminate. The plate constitutive equation is inverted, giving midplane strains and plate curvatures in terms of applied forces and moments. These strains and curvatures are substituted into the lamina stress-strain equation to obtain lamina stresses in the global system. The stresses obtained are then transformed into the principal material system of the lamina in question and compared with ultimate stresses obtained using failure criteria.

3. Strength Theories

The strength theories in ICAN make use of several assumptions. First, it is assumed that there are five characteristic values of strength of a unidirectional composite:

1. longitudinal tensile strength
2. longitudinal compressive strength (3 separate criteria)
   a. rule of mixtures
   b. fiber microbuckling
   c. delamination
3. transverse tensile strength
4. transverse compressive strength
5. in-plane or intralaminar shear strength

The fracture modes usually associated with these strengths are shown schematically in Fig. 29.

Once ply strengths are calculated (in the ply coordinate systems), geometric transformations are used to calculate composite failure loads. The process used is briefly described below.

1. Calculate loads (in composite system) required to induce load equal to ply strengths (in ply systems) for each mode.
2. Calculate minimum of failure loads for each ply.
3. Calculate minimum of failure loads of all plies, and use this load as the failure strength of the composite for a particular failure mode.

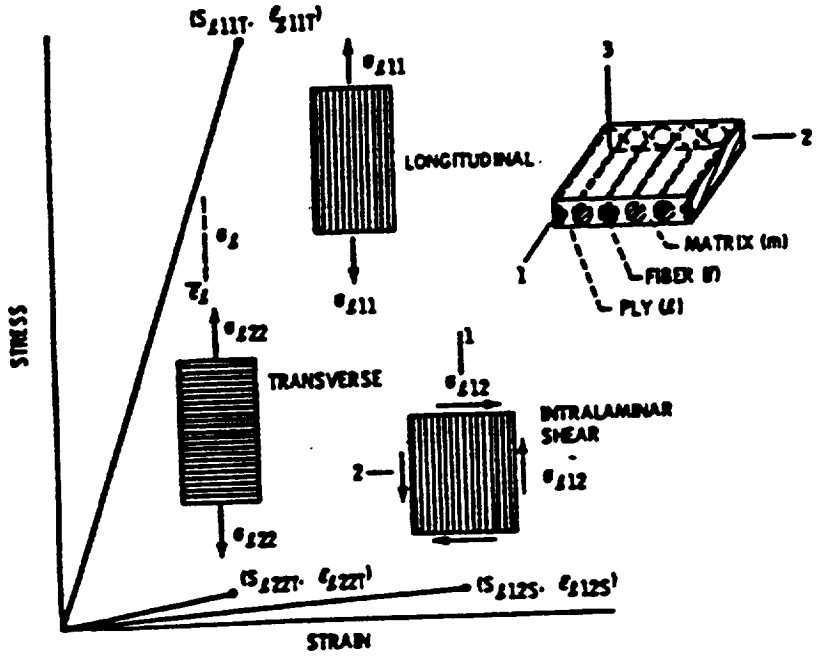

Fig. 28- Typical Stress-Strain behavior of unidirectional fiber composites.

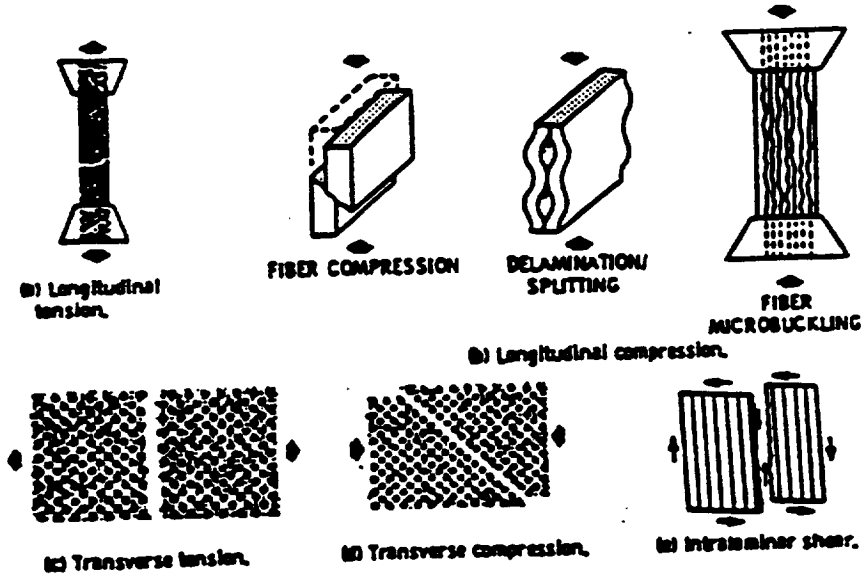

Fig. 29- In-plane fracture modes of unidirectional (ply) fiber composites.

E. Review of Applicable Statistical Concepts

Composite properties are calculated for large samples using a specific set of distributions of input properties. In this context, small sampling theory does not apply, because the samples used are sufficiently large.

1. Sample Means

Calculation of the mean sample values proceeds by defining

$$\text{mean} = \bar{x} = \frac{\sum_{i=1}^{n} x_i}{n}$$

where n = sample size

x_i = sample data values

The population mean is unknown, so the sample mean is assumed to be the best estimator of the population mean.

2. Sample Standard Deviation

An estimate of the population standard deviation is calculated using the statistically efficient estimator

$$\sigma = \left[\frac{n}{n-1} \sum_{i=1}^{n} (x_i - \bar{x})^2 \right]^{1/2} \quad , n \geq 30$$

3. Confidence Interval Estimates

An important problem in the area of statistical inference is the estimation of population parameters (such as mean, variance, etc.) from sample statistics. Parameters $\bar{x}$ and σ are the mean and standard

deviation of the sampling distribution of a statistic S. The sampling distribution of S is assumed as approximately normal (which is true for many statistical distributions if $n \geq 30$). Confidence interval estimates are constructed for the statistic S. Thus, intervals are identified for which it can be asserted with a reasonable degree of certainty that they contain the parameter considered. Obviously, the degree of certainty (or confidence level) will vary with the size of the interval chosen. Values of confidence coefficients, z_c, are associated with confidence levels. For example, an actual sample statistic S is expected to be found lying in the interval $(\bar{x} - z_c\sigma)$ to $(\bar{x} + z_c\sigma)$ (where σ is the unknown population standard deviation) some percent of the time. Let the z_c value in this example be 1. Assuming a normal sampling distribution, (with $z_c = 1$) the normal distribution area function specifies that S falls between $(\bar{x} - \sigma)$ and $(\bar{x} + \sigma)$ about 68.27% of the time. Similarly, the confidence of $\bar{x}$ lying in the interval $(S - \sigma)$ to $(S + \sigma)$ is about 68.27%. The endpoints of the intervals are known as confidence limits. Various confidence coefficients z_c, corresponding to frequently used confidence levels, have been tabulated.

In this work, the confidence interval for means is given in terms of the sample statistics by

$$\bar{x} \pm z_c \frac{\sigma}{\sqrt{n}}$$

where z_c is the confidence coefficient, which takes on values of 1.645, 1.960, and 2.580 for the 90, 95, and 99% confidence levels,

respectively.

4. Regression

The term "regression" as used in the area of statistics refers to the process of formulating a mathematical model to explain randomly observed phenomena. Some functional form for the way each variable enters the model must be assumed. Comparison of the degree of fit of different assumed models ideally leads to a better model. The basic regression strategy used here consists of:

1. Assume a multiple linear regression model. The normal equations for such a model are:

$$\{Y\} = [X]\{\beta\} + \{\epsilon\}$$

where

$\{Y\}$ = vector of dependent variable values

$[X]$ = matrix of functions of independent variable

$\{\beta\}$ = regression "true" values

$\{\epsilon\}$ = errors

The normal equations can be solved as follows:

$$[X]^T\{Y\} = [X]^T[X]\{\beta\} + [X]^T\{\epsilon\}$$

$$\{b\} = [X^TX]^{-1}[X]^T\{Y\}$$

where

$\{b\}$ = parameter estimates

2. Use a standard statistical package (Ref. 17) to estimate regression parameters.

3. Calculate properties of regression parameter distributions to assess model precision.

In the event that $[X^TX]$ is singular, implying that some of the normal equations are linearly dependent, $[X^TX]^{-1}$ does not exist. The model should be expressed in terms of fewer parameters, or should include assumed restrictions on the parameters.

The square of the multiple correlation coefficient, R^2, is usually calculated for each regression model, and supplies a convenient measure of the degree of fit between data values $\{Y\}$ and values $\{\hat{Y}\}$ predicted by the regression equation. It is defined by

$$R^2 = \frac{\text{Sum of Squares due to regression model}}{\text{Total Sum of squares about mean } Y}$$

$$= \frac{\Sigma \ (\hat{Y}_i - \bar{Y})^2}{\Sigma \ (Y_i - \bar{Y})^2}$$

Frequently, it is necessary to determine if inclusion of particular terms in a regression model is worthwhile. To this end, the extra portion of the regression sum of squares which arises due to the terms under consideration is calculated. The mean square (defined as the sum of squares divided by the corresponding degrees of freedom) derived from this extra sum of squares can be compared with s^2, the estimate of σ^2, to see if it appears significantly large. If it does, the terms under

consideration should be included. The statistic is frequently compared to the appropriate percentage point of the F- distribution, which is tabulated.

Supopose the extra sum of squares due to a parameter, given that a number of other parameters are already in the model, is calculated. Symbolically,

$$SS(b_i | b_0, b_1, \ldots, b_{i-1}, b_{i+1}, \ldots, b_k) \quad i = 1,2,\ldots,k$$

represents a one degree of freedom (1 df) sum of squares which measures the portion of the regression sum of squares due to the coefficient b_i. This is a measure of the value of adding a β_i term to the model which previously did not include β_i. The corresponding mean square, equal to the SS (since it has one df) can be compared by an F- test to s^2. This is known as a partial F- test for the single parameter β_i, which is a special case of the F- test described earlier.

The stepwise regression procedure (Ref. 18) is a structured way to insert variables in order of correlation until the regression equation is satisfactory. The partial correlation coefficient measures the relative importance of terms not yet in the model, to choose the next candidate for entry. The analagous statistic, F- to enter (or F- to remove) is usually evaluated for each predictor at every stage as though it were the last term to enter the model, to determine if terms retained at a previous step have become superfluous, because of some linear dependence with terms now in the model. The largest F- statistic calculated at each step is compared with the appropriate percentage point of the F- distribution, and the predictor variable is entered (or

removed) based on the significance of this F- test. Testing of the least useful predictor is performed at every step. The R^2 statistic is calculated, to provide a measure of the value of the regression at each step. This stepwise linear regression scheme is used in this work because of its computational economy, and because it allows the analyst to assess the relative influence (or correlation) between individual predictor variables of a selected model and response for a particular data sample. Other schemes are available (Ref. 18), such as backward elimination. The stepwise procedure is recommended for its direct nature in testing the model with only significant predictor terms.

CHAPTER III

RESULTS

A. Property Histograms and Distributions

In this work, fiber and matrix properties are allowed to assume a range of values to assess the sensitivity of the composite ply properties to constituent perturbations. Graphite fiber and epoxy matrix are used as the constituents. Initially, two separate samples of output data are generated and studied to demonstrate the effects of input parameter changes on composite material properties. These two cases are compared with a deterministic base case with no random input property generation. The data for all three cases is given in Table I.

The results of cases 2 and 3 are shown in histogram and cumulative distribution form in Figs. 30 - 42. The results of the deterministic case 1 are summarized in Table II, and can be easily compared with the histograms and distributions.

TABLE I- INPUT DATA FOR SAMPLING

INPUT	CASE 1	CASE 2	CASE3
THETA(degrees)	0.0	-	-
μ	-	0.0	0.0
σ	-	5.0	10.0
FVR	0.50	-	-
μ	-	0.5	0.5
σ	-	0.1	0.2
VVR	0.01	-	-
λ	-	3.0	3.0
k	-	3	5
EFP1(ksi)	31000	-	-
μ	-	31000	31000
σ	-	1500	3000
EFP2(ksi)	2000	-	-
μ	-	2000	2000
σ	-	100	200
GFP12(ksi)	2000	-	-
μ	-	2000	2000
σ	-	100	200
GFP23(ksi)	1000	-	-
μ	-	1000	1000
σ	-	50	100
SFPT(ksi)	400	-	-
β	-	400	400
α	-	20	10
SFPC(ksi)	400	-	-
β	-	400	400
α	-	20	10
EMP(ksi)	500	-	-
μ	-	500	500
σ	-	25	50
SMPT(ksi)	15	-	-
β	-	15	15
α	-	20	10
SMPC(ksi)	35	-	-
β	-	35	35
α	-	20	10
SMPS(ksi)	13	-	-
β	-	13	13
α	-	20	10

TABLE II- CASE 1 RESULTS

PROPERTY	VALUE
EC11	15750 ksi
EC22	1065 ksi
EC12	516 ksi
NUC12	0.275
NUC21	0.018
CTE11	0.775×10^{-8}
CTE22	0.181×10^{-4}
CTE12	0.000
SCXXT	203 ksi
SCXXC	165 ksi
SCYYT	11.74 ksi
SCYYC	27.41 ksi
SCXYS	10.01 ksi

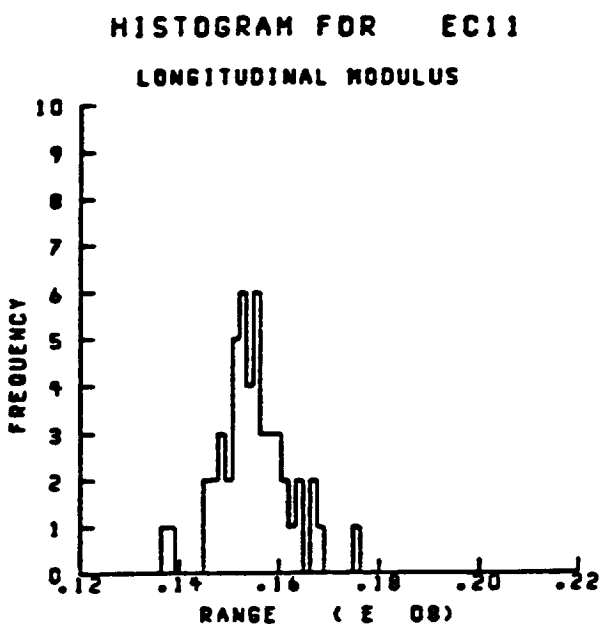

(a) case 2 histogram

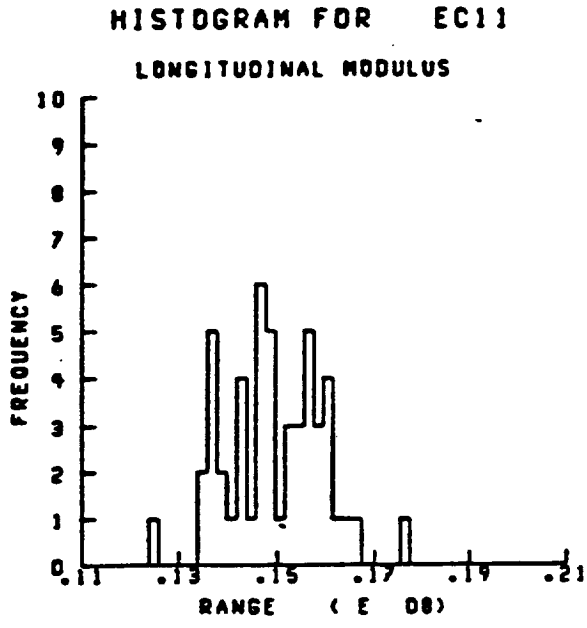

(b) case 3 histogram

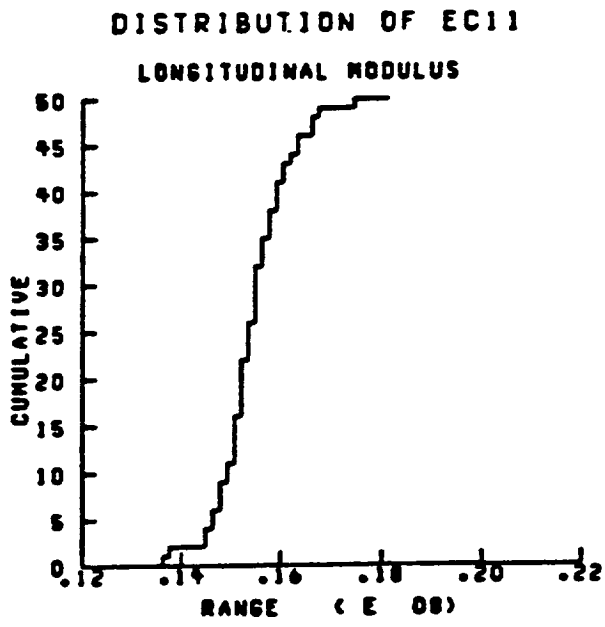

(c) case 2 distribution

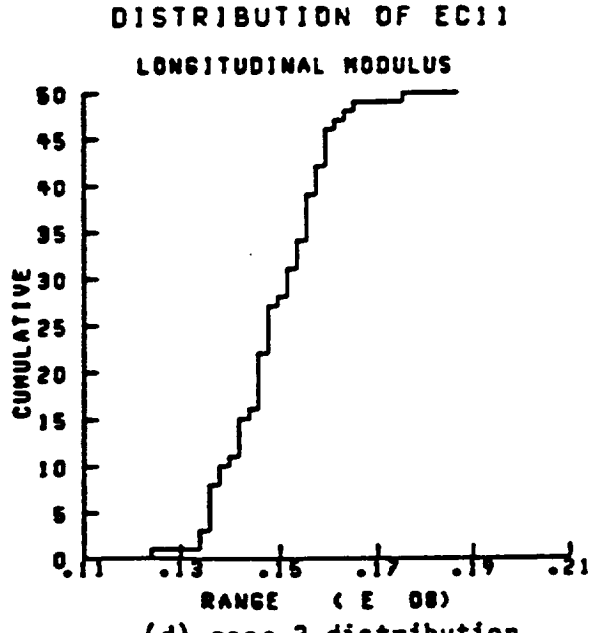

(d) case 3 distribution

Fig. 30- Sampling results for Longitudinal Elastic Modulus

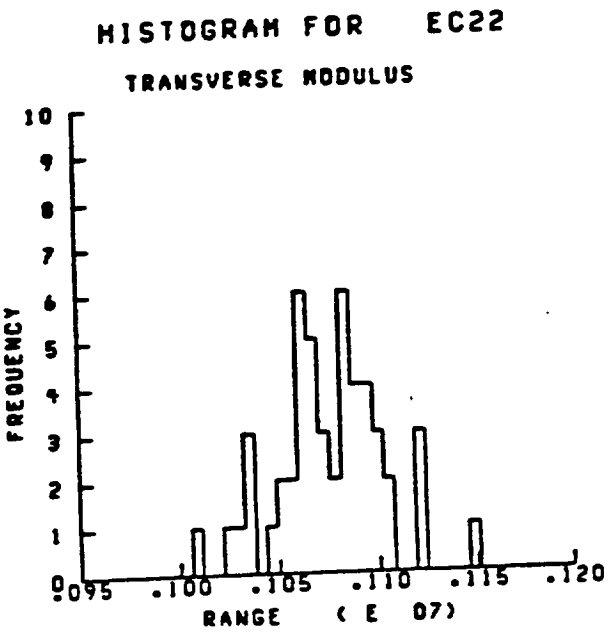

(a) case 2 histogram

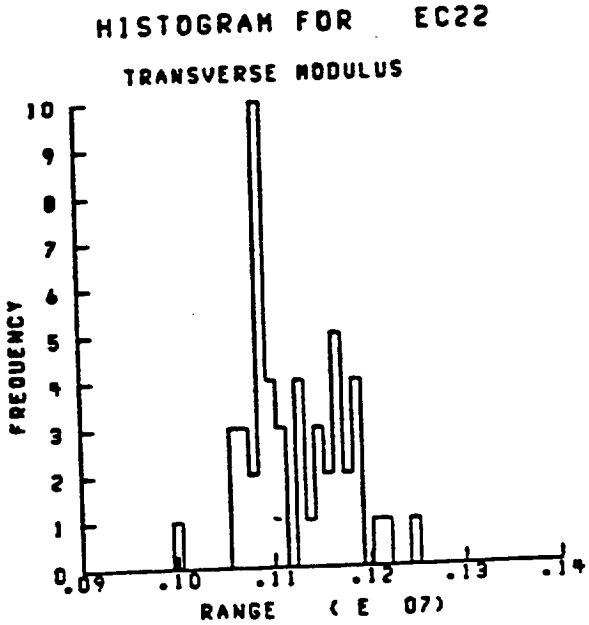

(b) case 3 histogram

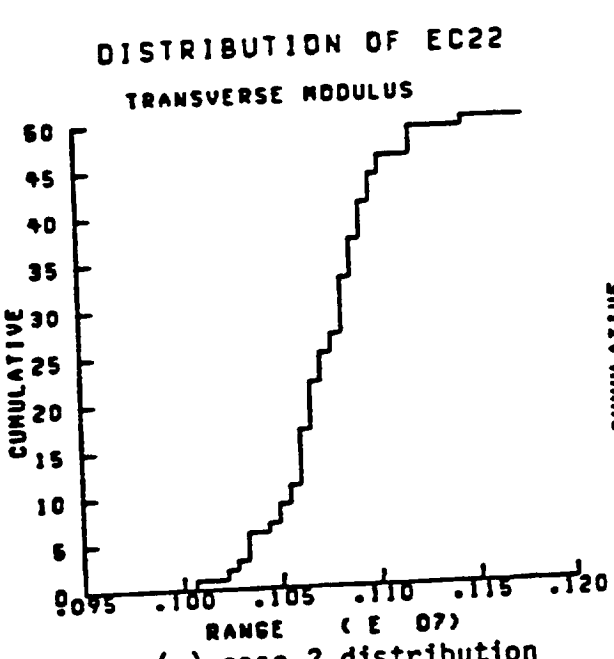

(c) case 2 distribution

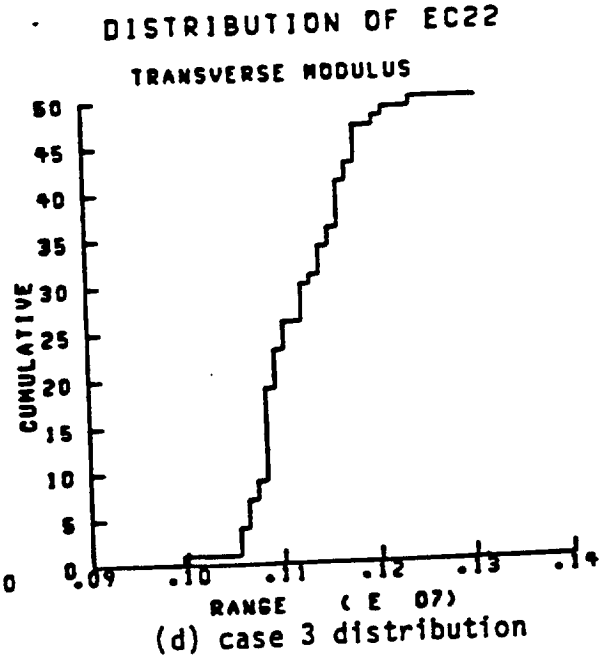

(d) case 3 distribution

Fig. 31- Sampling results for Transverse Elastic Modulus

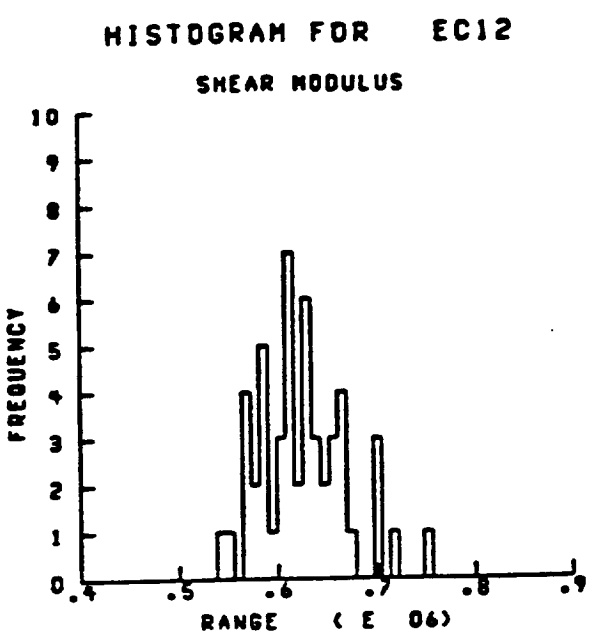

(a) case 2 histogram

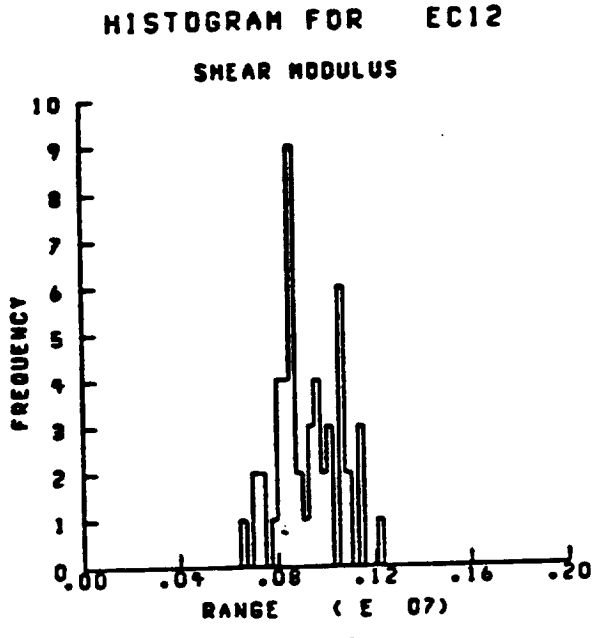

(b) case 3 histogram

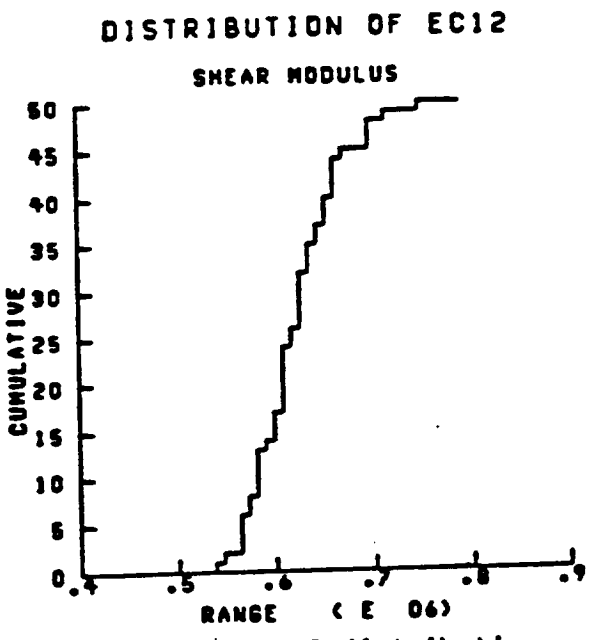

(c) case 2 distribution

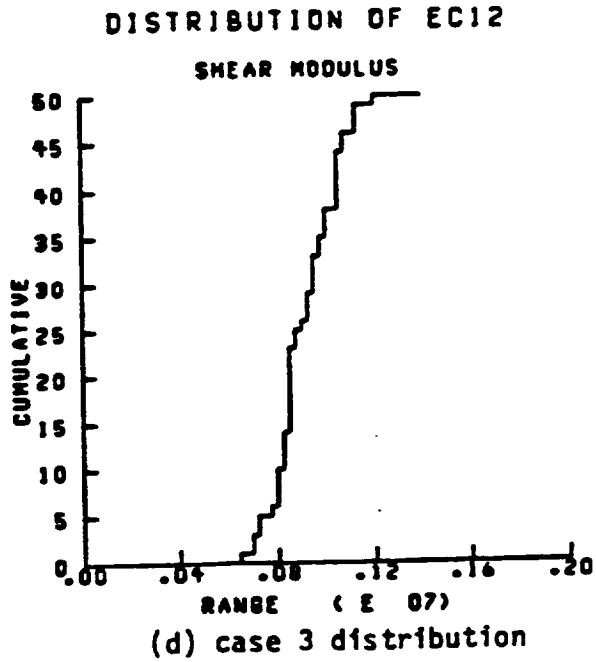

(d) case 3 distribution

Fig. 32- Sampling results for In-plane Shear Modulus

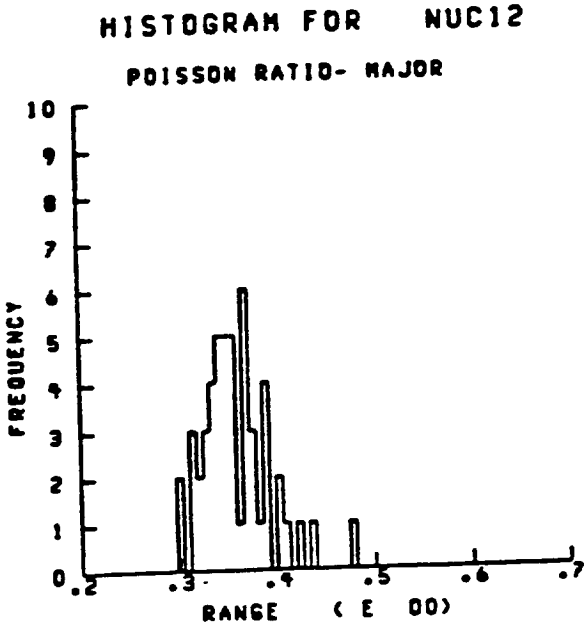

(a) case 2 histogram

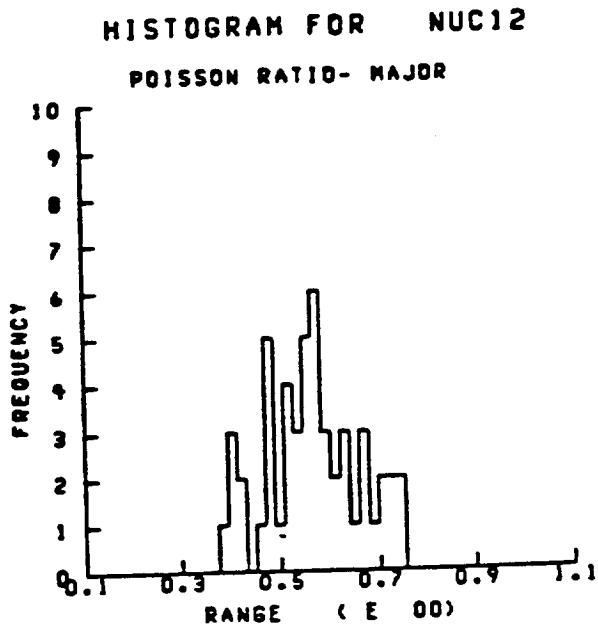

(b) case 3 histogram

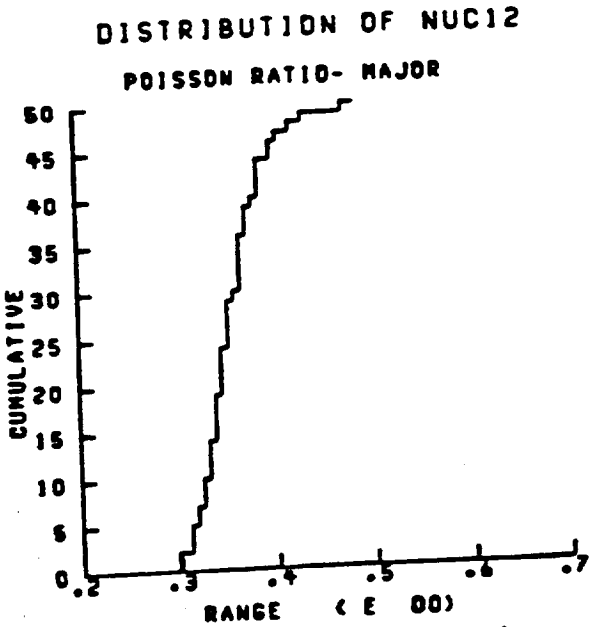

(c) case 2 distribution

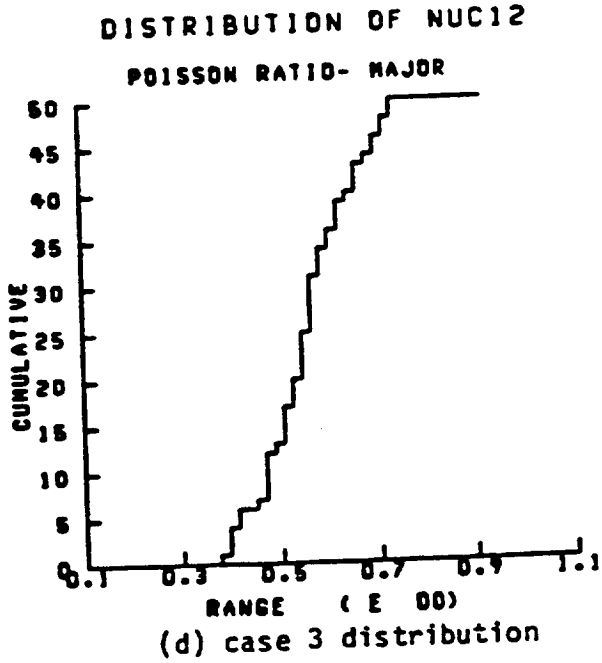

(d) case 3 distribution

Fig. 33- Sampling results for Poisson Ratio (major)

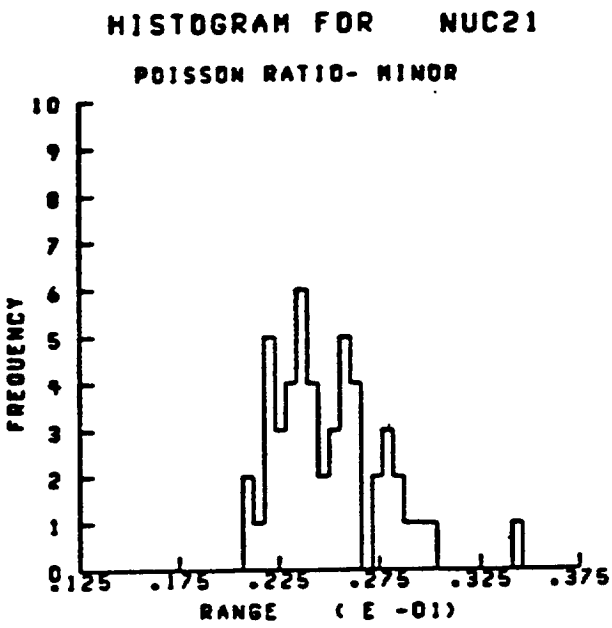

(a) case 2 histogram

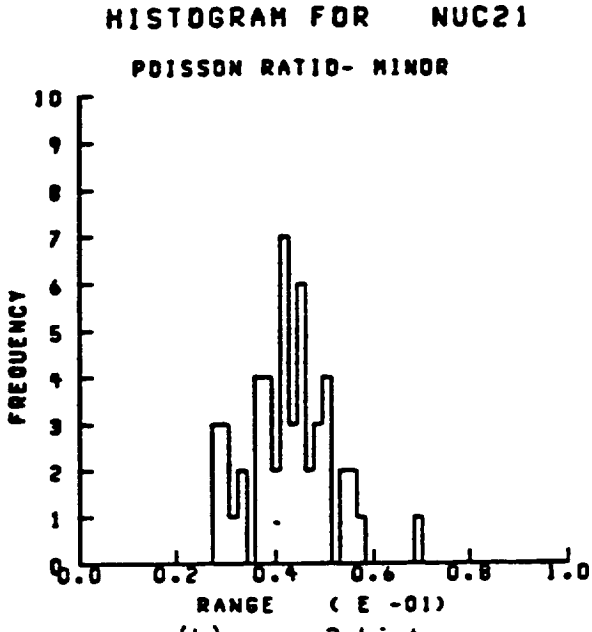

(b) case 3 histogram

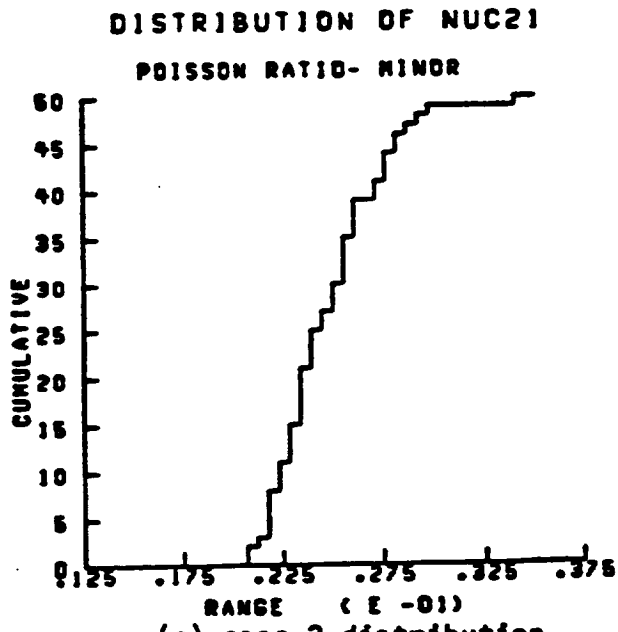

(c) case 2 distribution

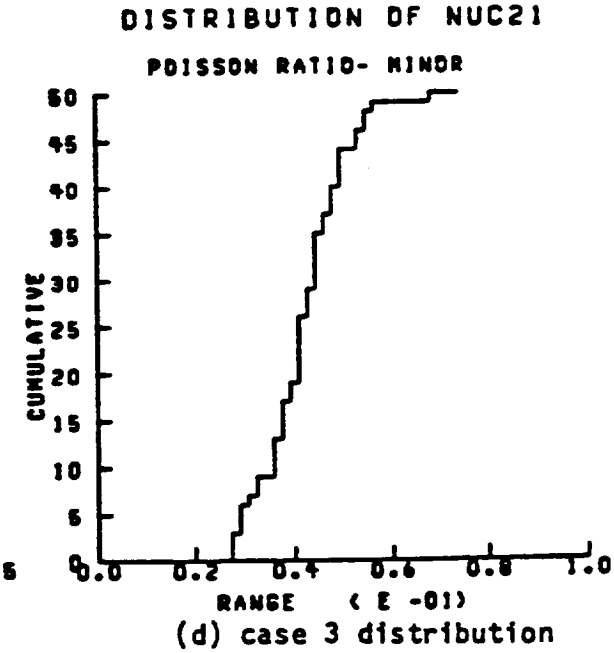

(d) case 3 distribution

Fig. 34- Sampling results for Poisson Ratio (minor)

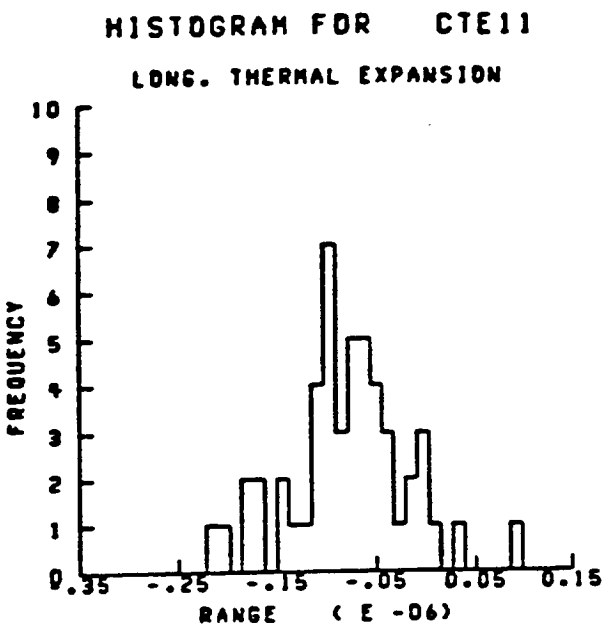

(a) case 2 histogram

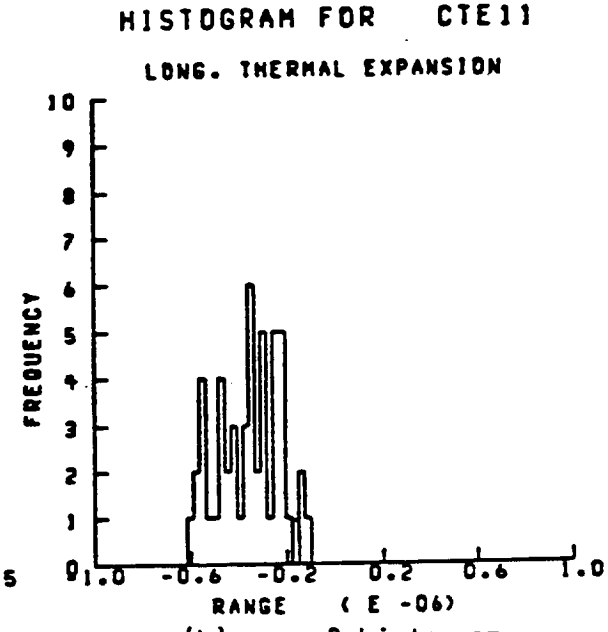

(b) case 3 histogram

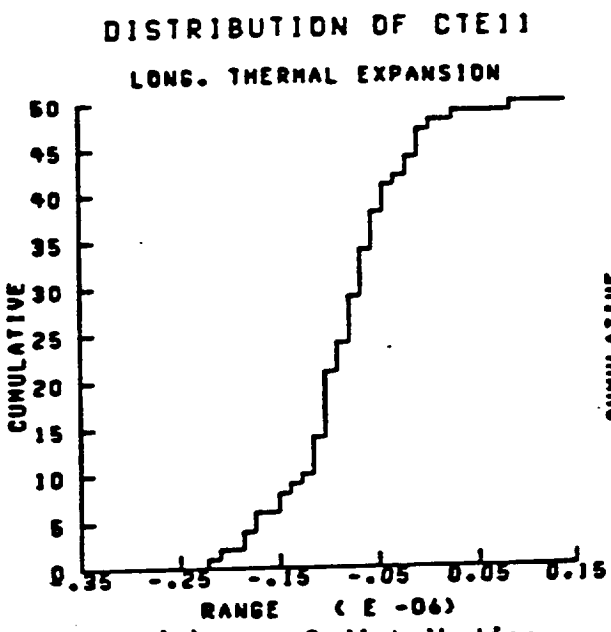

(c) case 2 distribution

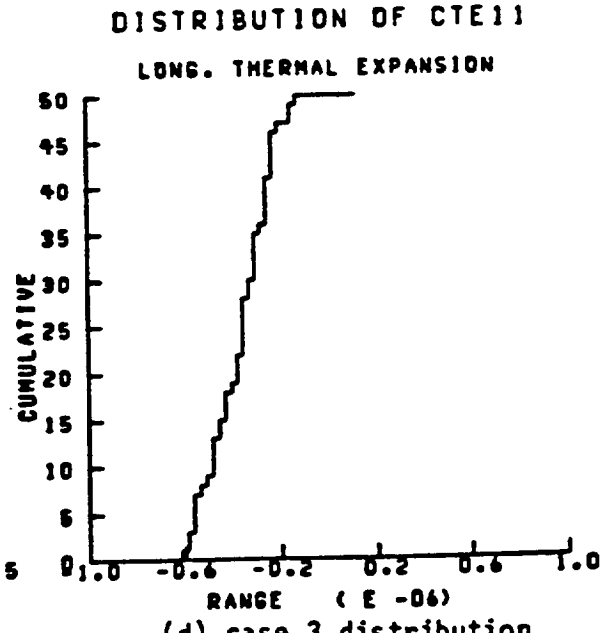

(d) case 3 distribution

Fig. 35- Sampling results for Longitudinal Thermal Expansion

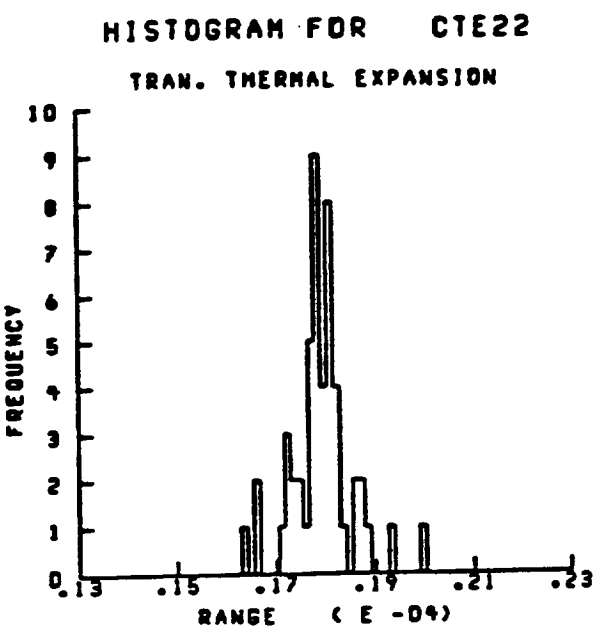

(a) case 2 histogram

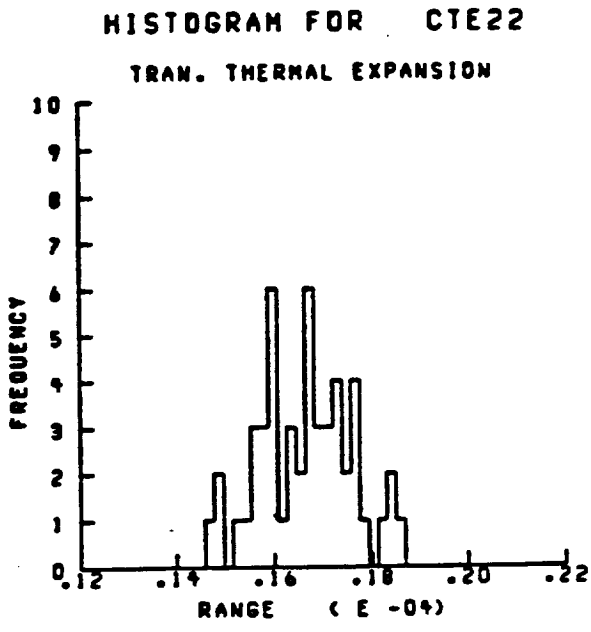

(b) case 3 histogram

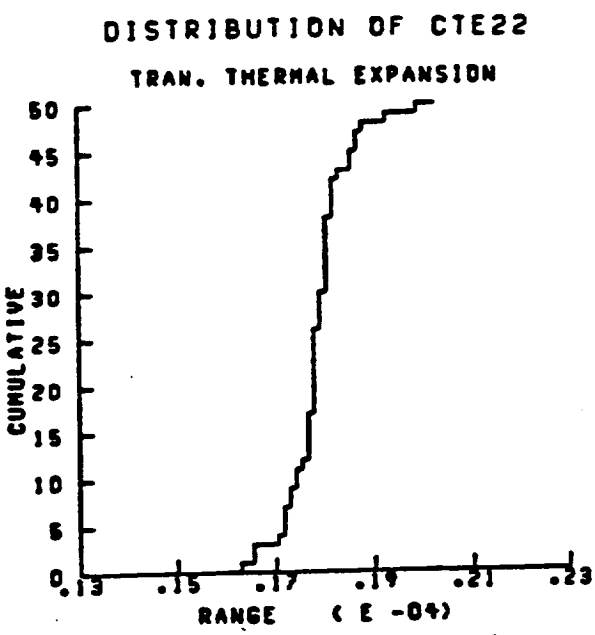

(c) case 2 distribution

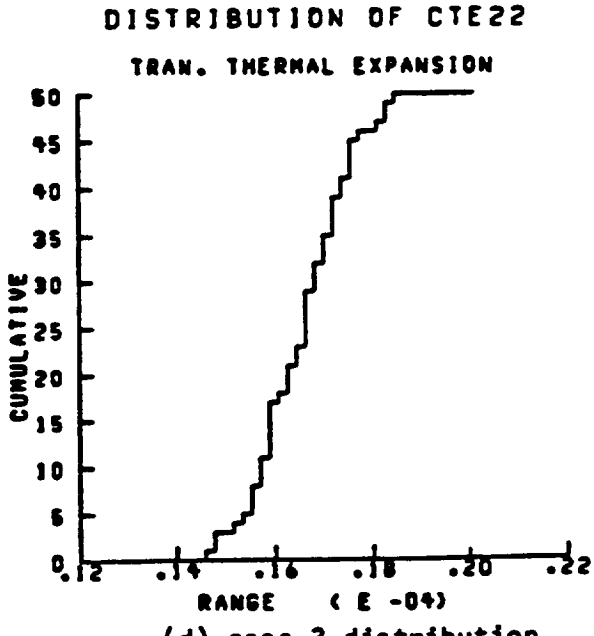

(d) case 3 distribution

Fig. 36- Sampling results for Transverse Thermal Expansion

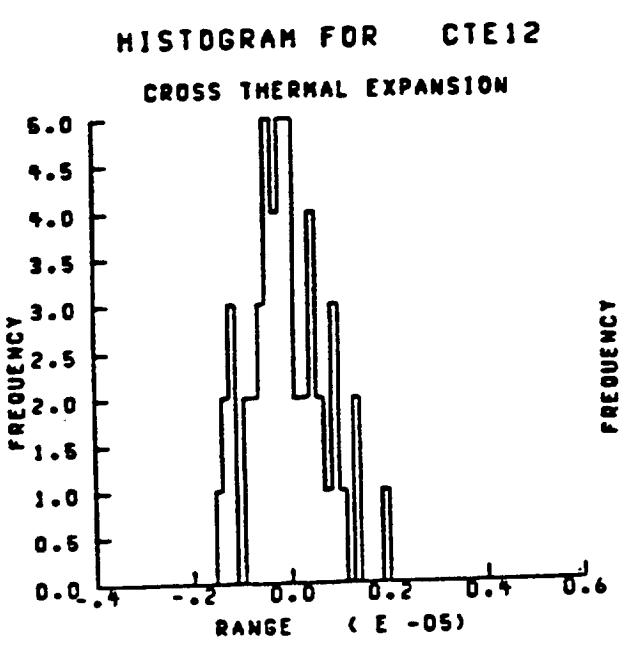

(a) case 2 histogram

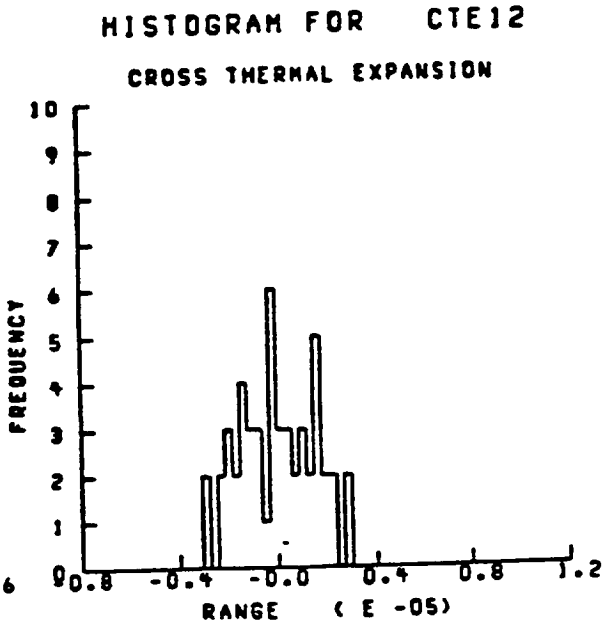

(b) case 3 histogram

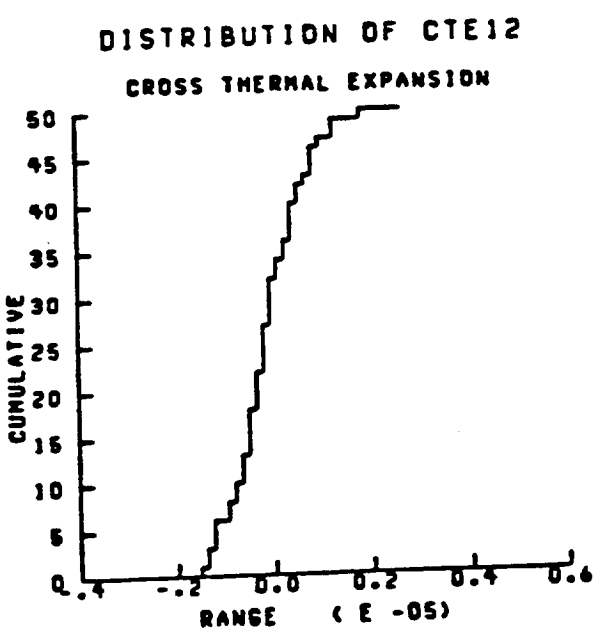

(c) case 2 distribution

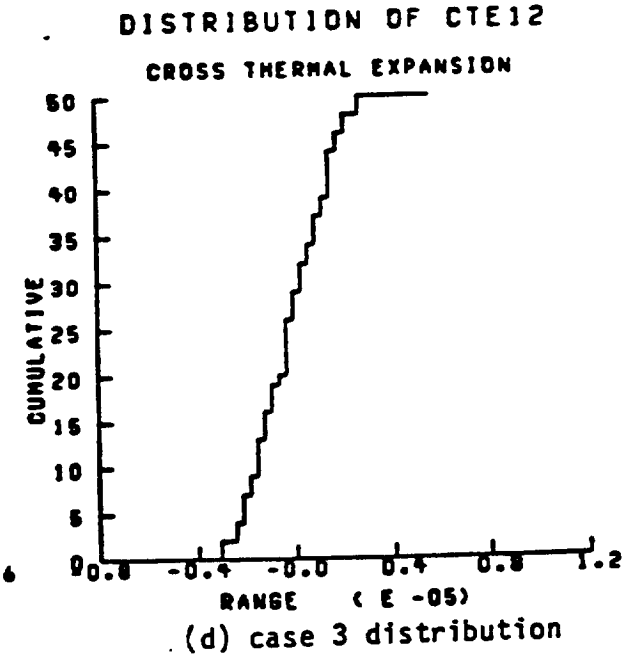

(d) case 3 distribution

Fig. 37- Sampling results for Thermal Expansion Coupling

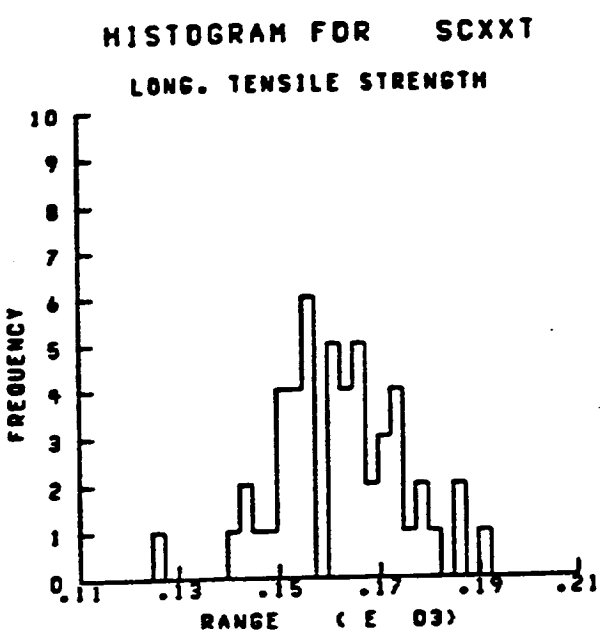

(a) case 2 histogram

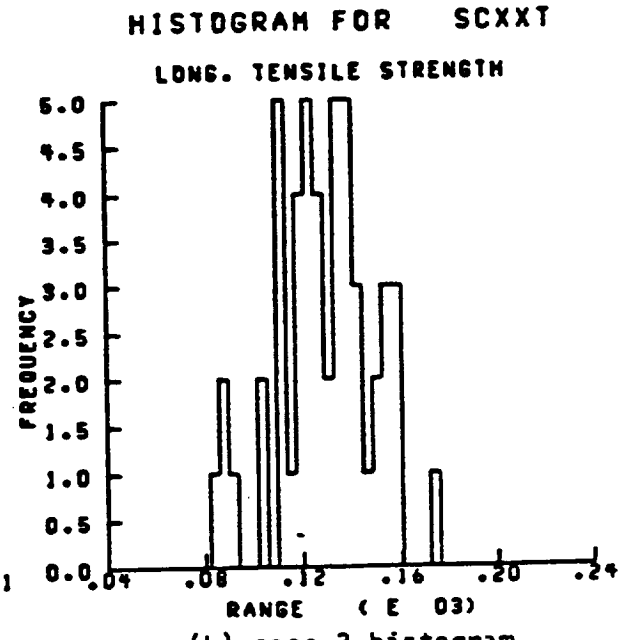

(b) case 3 histogram

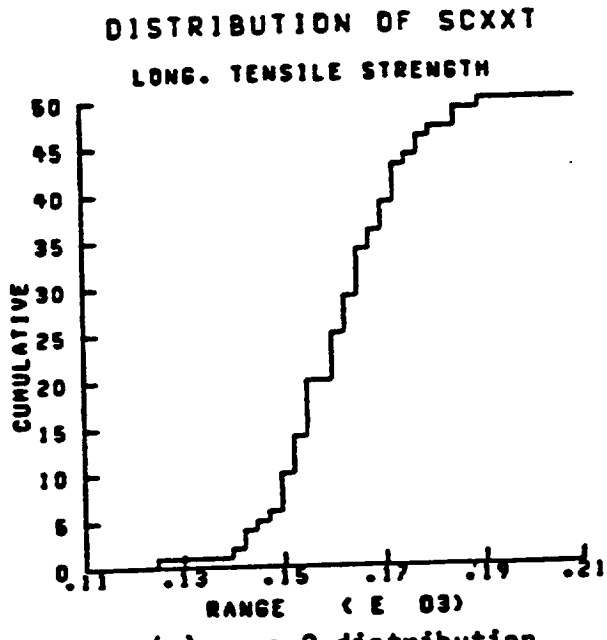

(c) case 2 distribution

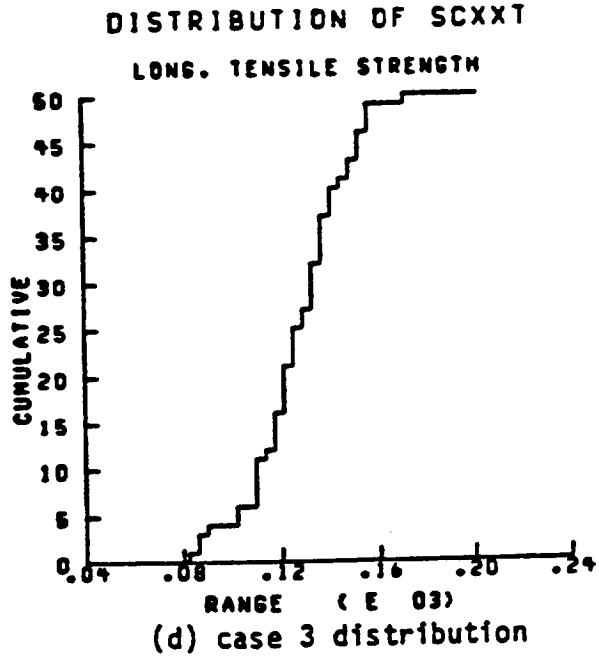

(d) case 3 distribution

Fig. 38- Sampling results for Longitudinal Tensile Strength

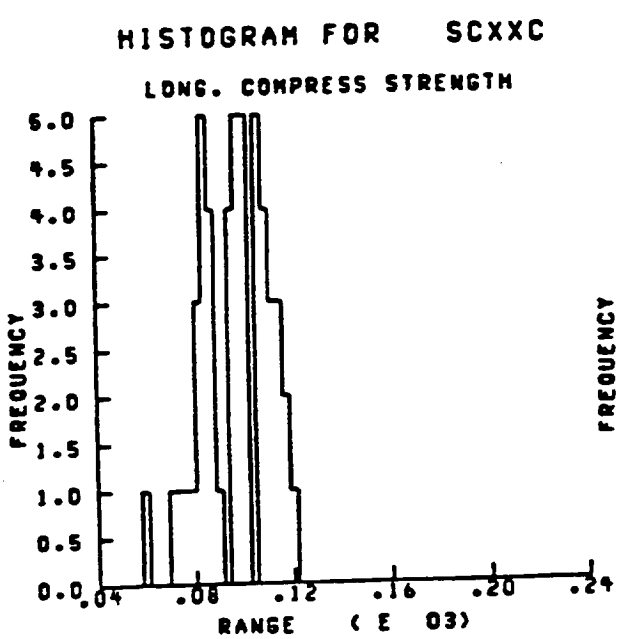

(a) case 2 histogram

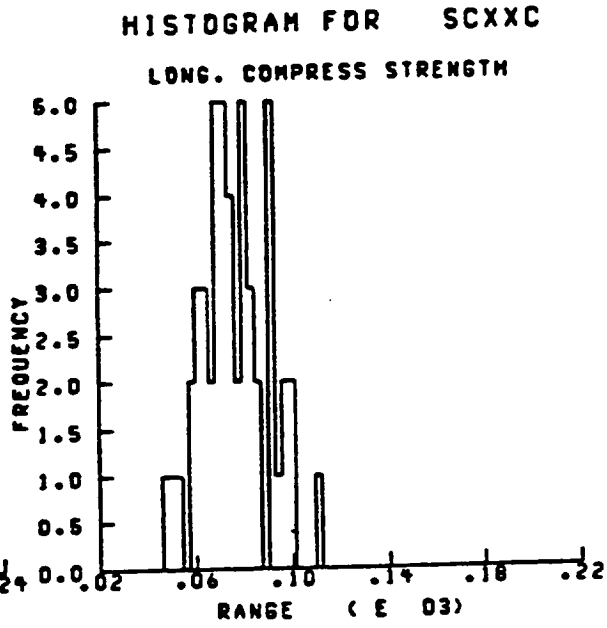

(b) case 3 histogram

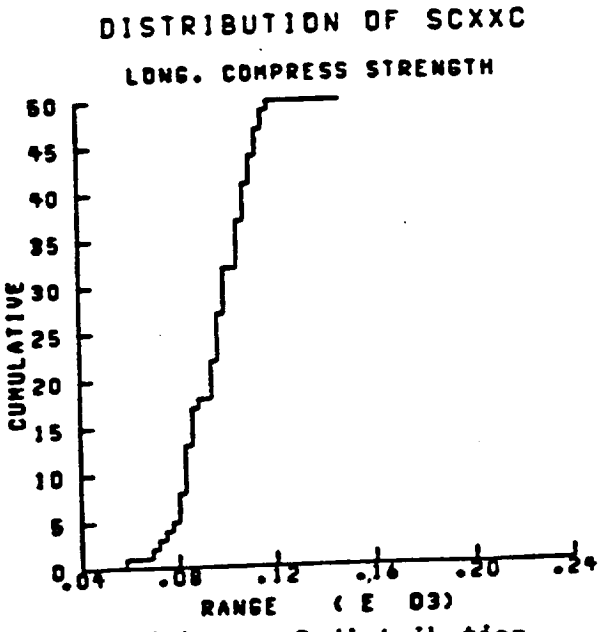

(c) case 2 distribution

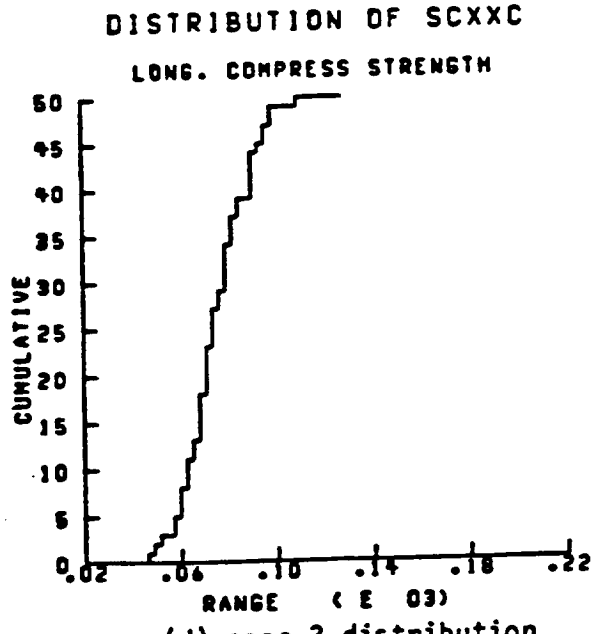

(d) case 3 distribution

Fig. 39- Sampling results for Longitudinal Compressive Strength

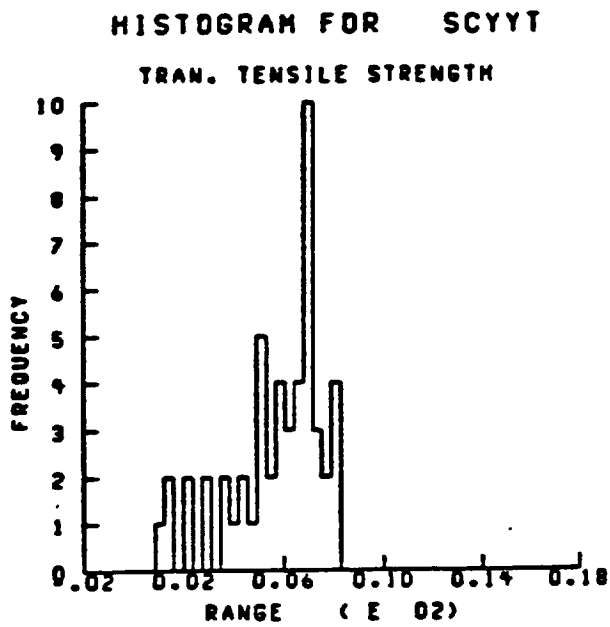

(a) case 2 histogram

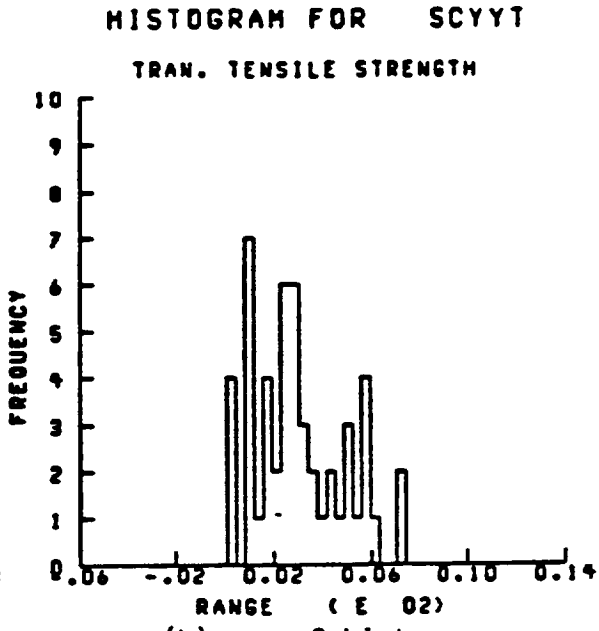

(b) case 3 histogram

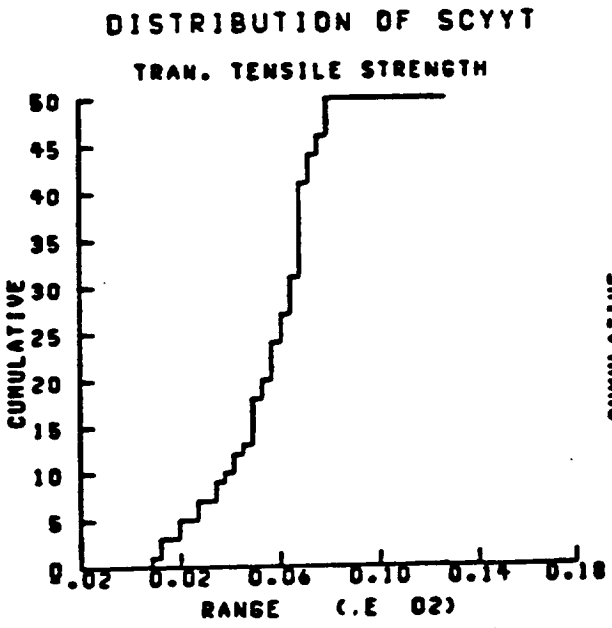

(c) case 2 distribution

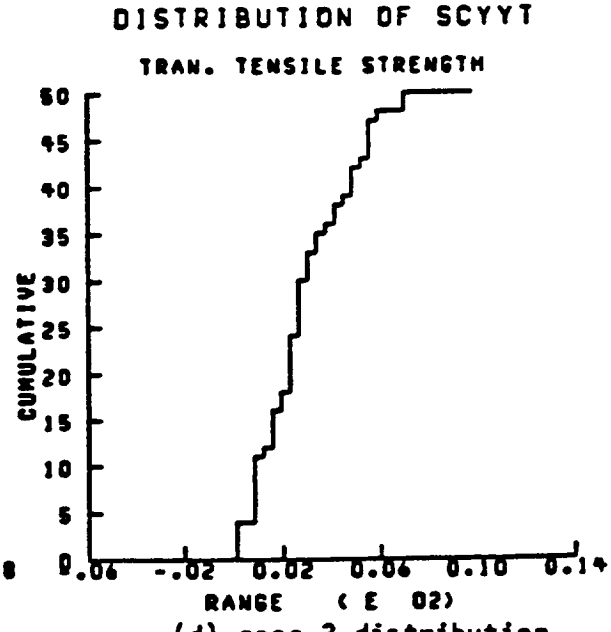

(d) case 3 distribution

Fig. 40- Sampling results for Transverse Tensile Strength

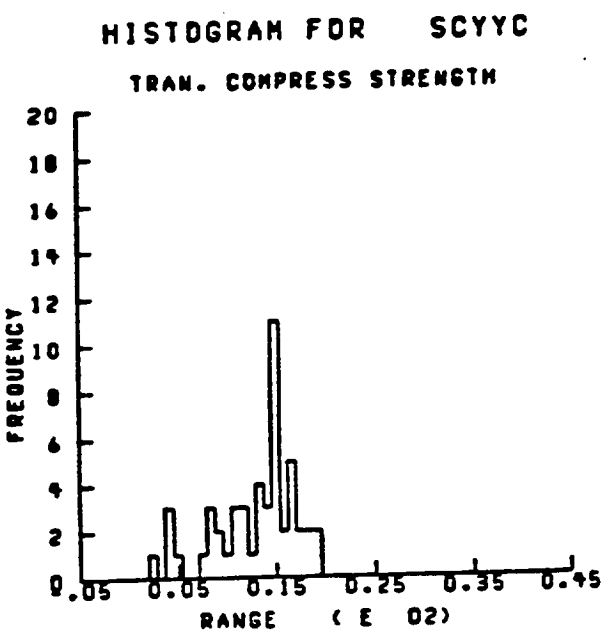

(a) case 2 histogram

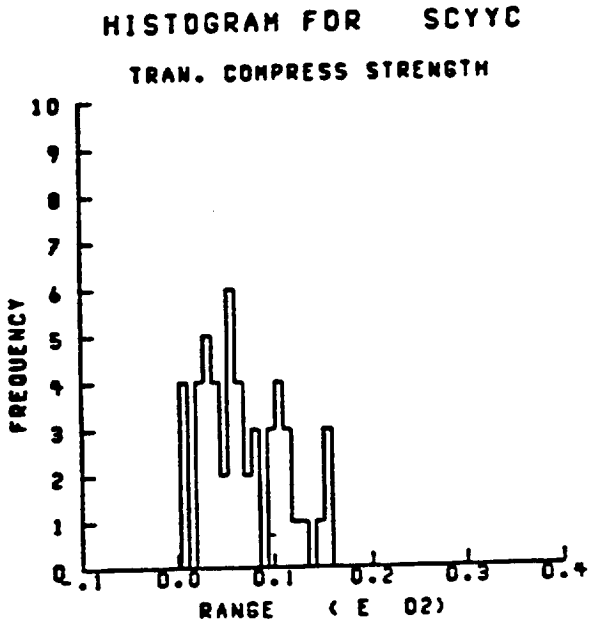

(b) case 3 histogram

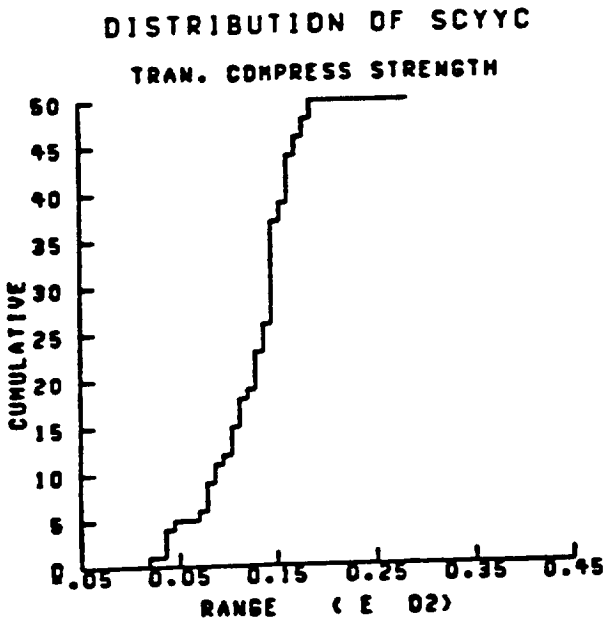

(c) case 2 distribution

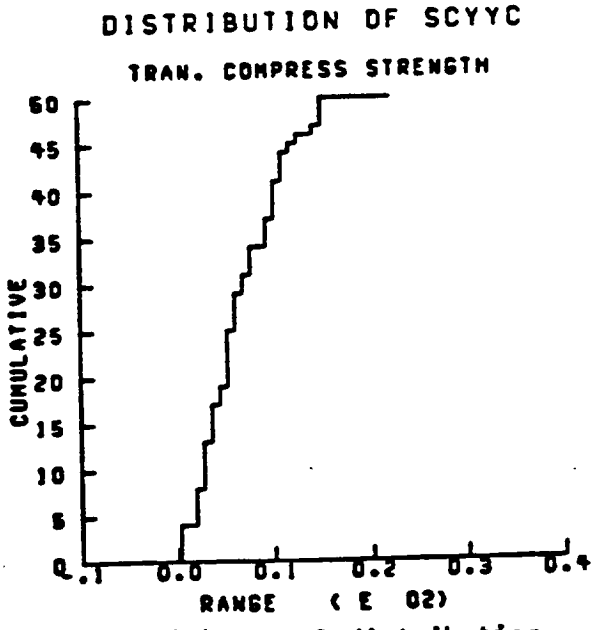

(d) case 3 distribution

Fig. 41- Sampling results for Transverse Compressive Strength

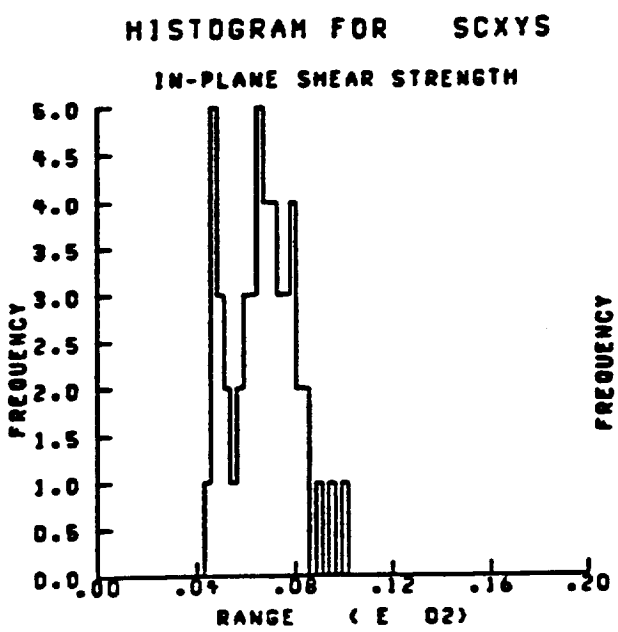

(a) case 2 histogram

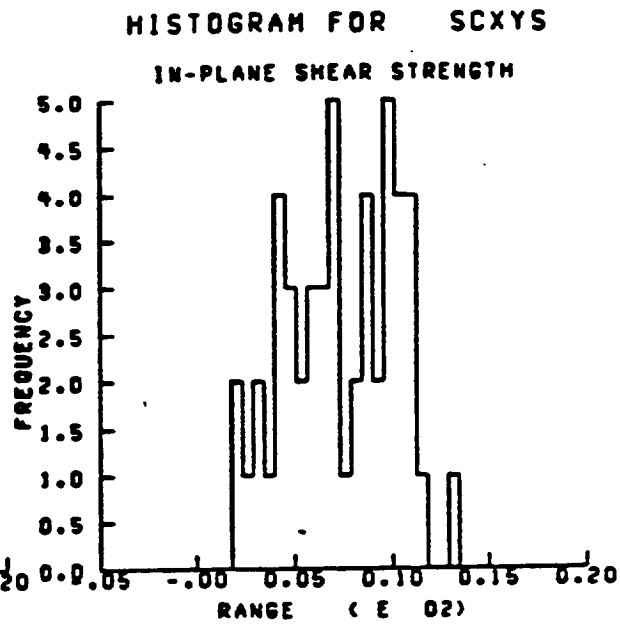

(b) case 3 histogram

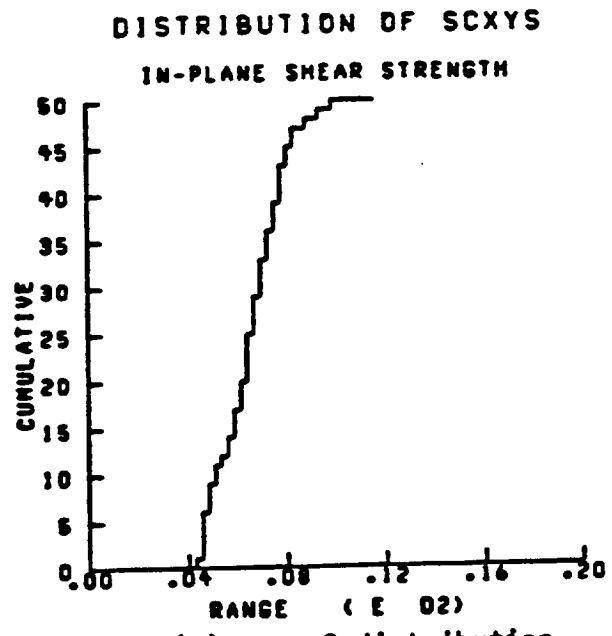

(c) case 2 distribution

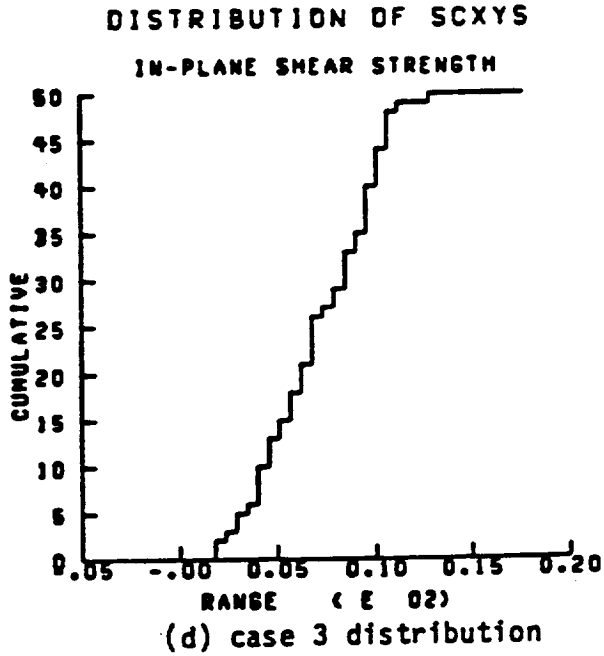

(d) case 3 distribution

Fig. 42- Sampling results for In-plane Shear Strength

B. Fiber Strength Effect

To show the effect of fiber strength changes on the longitudinal strengths of the composite, several shape parameters of the weibull distribution for fiber strength are assumed. The monte carlo procedure is then conducted at several fiber volume ratio values. All properties are varied, except fiber volume ratio. The distribution parameters of all properties except fiber strengths are held constant. The curves generated are shown in Figs. 43 and 44. In the figures the solid lines and symbols show the means of the 95% confidence interval estimates for the sample size of 50 chosen at each point. The points on both sides of each curve locate the upper and lower bounds of the confidence intervals. The convention described is intended to provide a convenient indication of the dispersion of the sample values at each point.

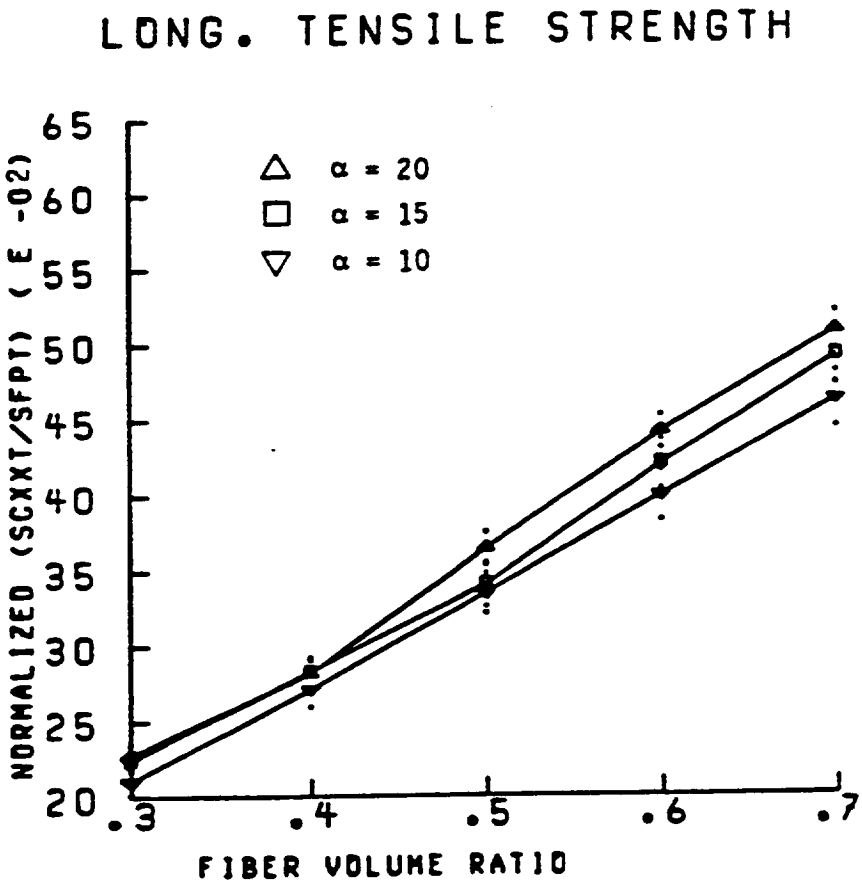

Fig. 43- Longitudinal Tensile Strength; for various shape parameters of fiber strength.

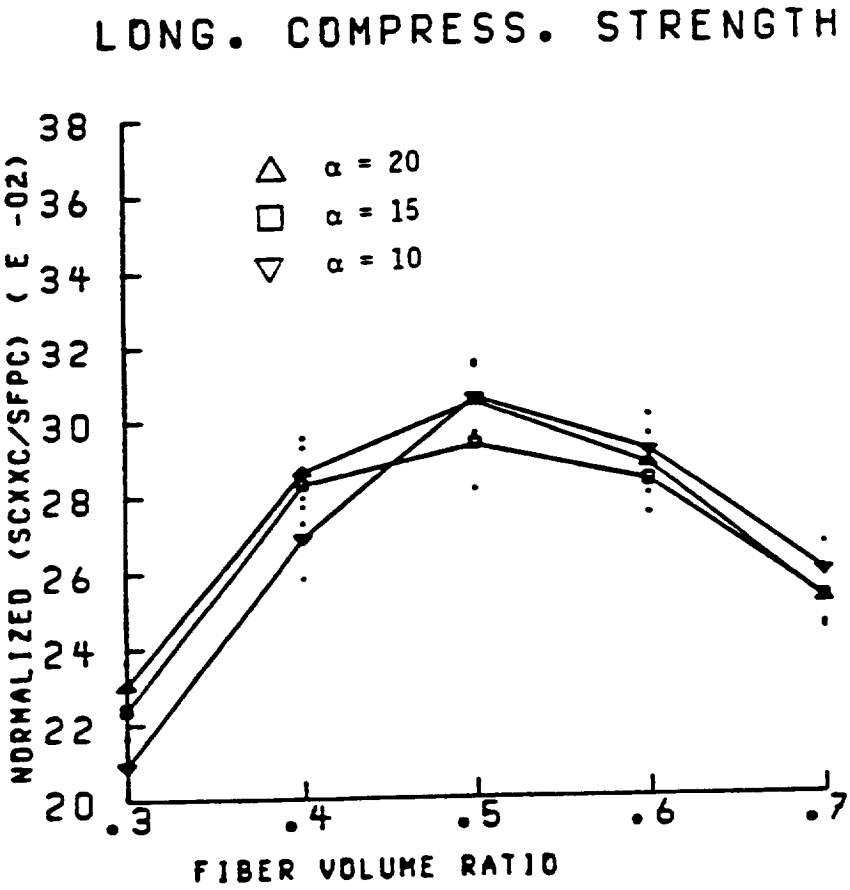

Fig. 44- Longitudinal Compressive Strength; for various shape parameters of fiber strength.

C. Matrix Strength Effect

The effects of changes in matrix strength on composite strengths are studied by suitable variation of the shape parameters governing the matrix strength distributions. Analagous to the plots given for fiber strength effects, the matrix effects are shown in Figs. 45 - 47.

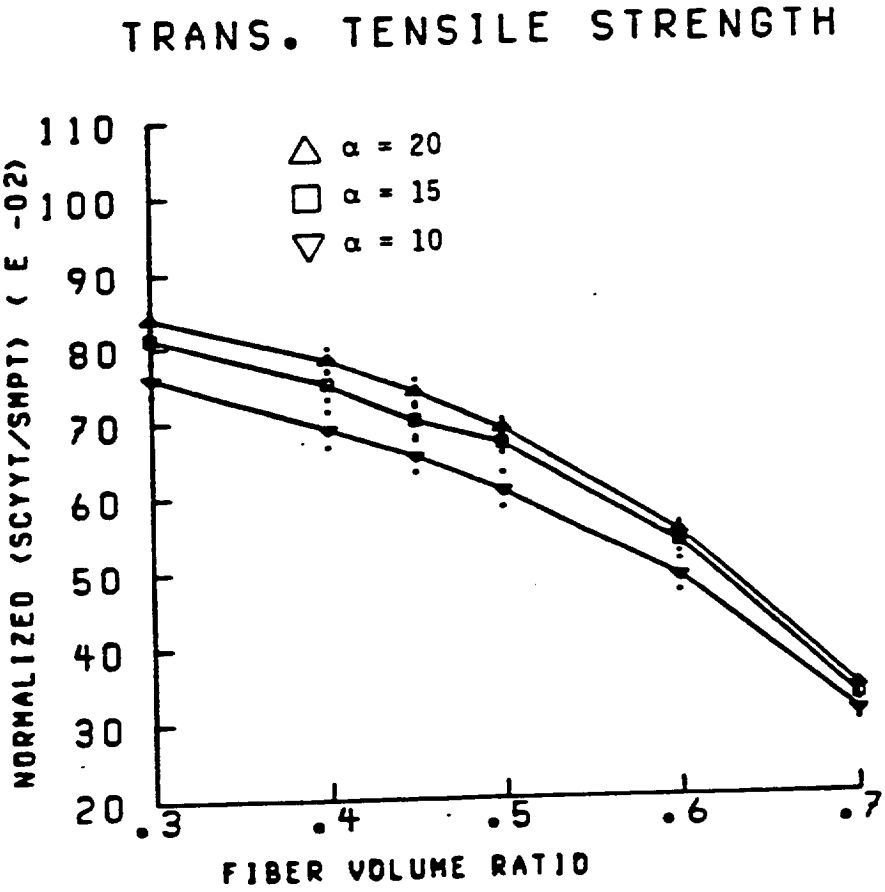

Fig. 45- Transverse Tensile Strength; for various shape parameters of matrix strengths.

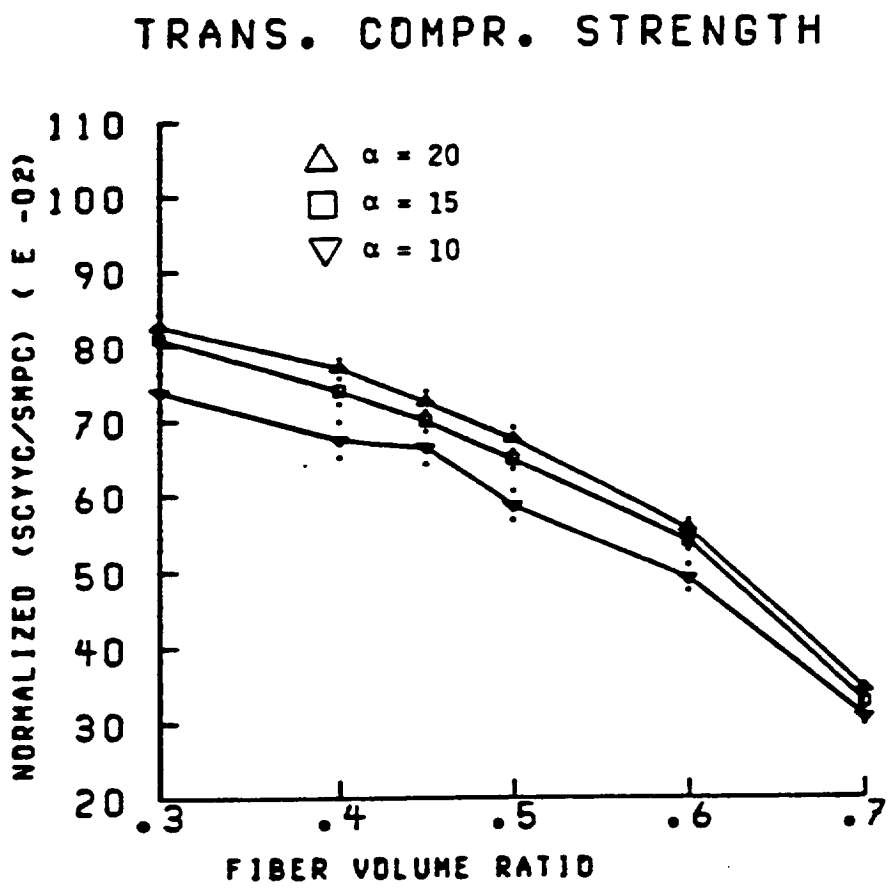

Fig. 46- Transverse Compressive Strength; for various shape parameters of matrix strengths.

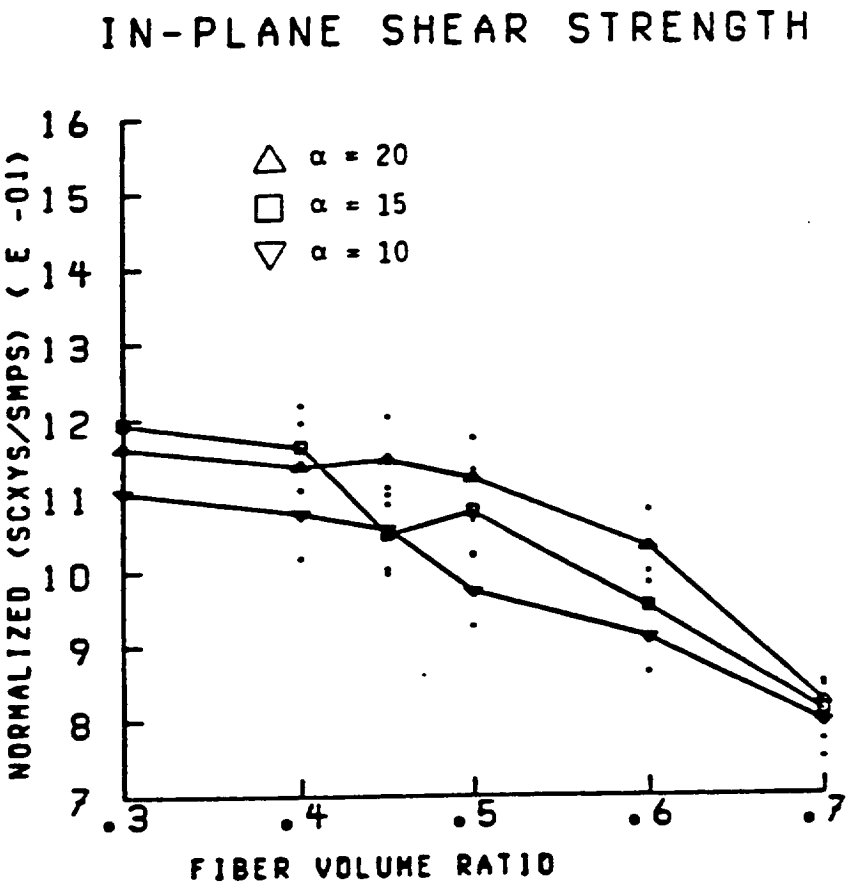

Fig. 47- In-plane Shear Strength; for various shape parameters of matrix strengths.

D. Fiber Orientation Effect

Assumed values of the fiber orientation angle distribution parameter are consecutively used in the monte carlo procedure to assess the effects on several composite properties. These plots are shown in Figs. 48 - 57.

E. Fiber Stiffness Effect

Assumed values of the fiber modulus distribution parameter are used in the simulation to similarly assess the effects on the related composite properties. The plots thus generated are shown in Figs. 58-67.

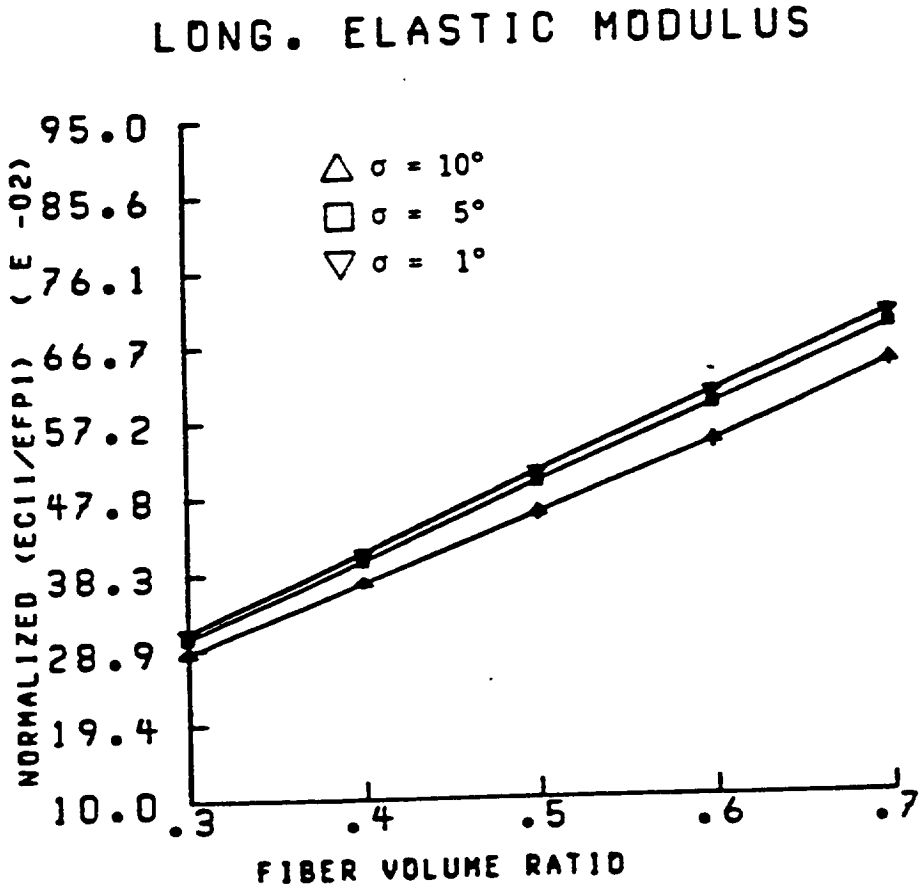

Fig. 48- Longitudinal Elastic Modulus; for various shape parameters of fiber orientation.

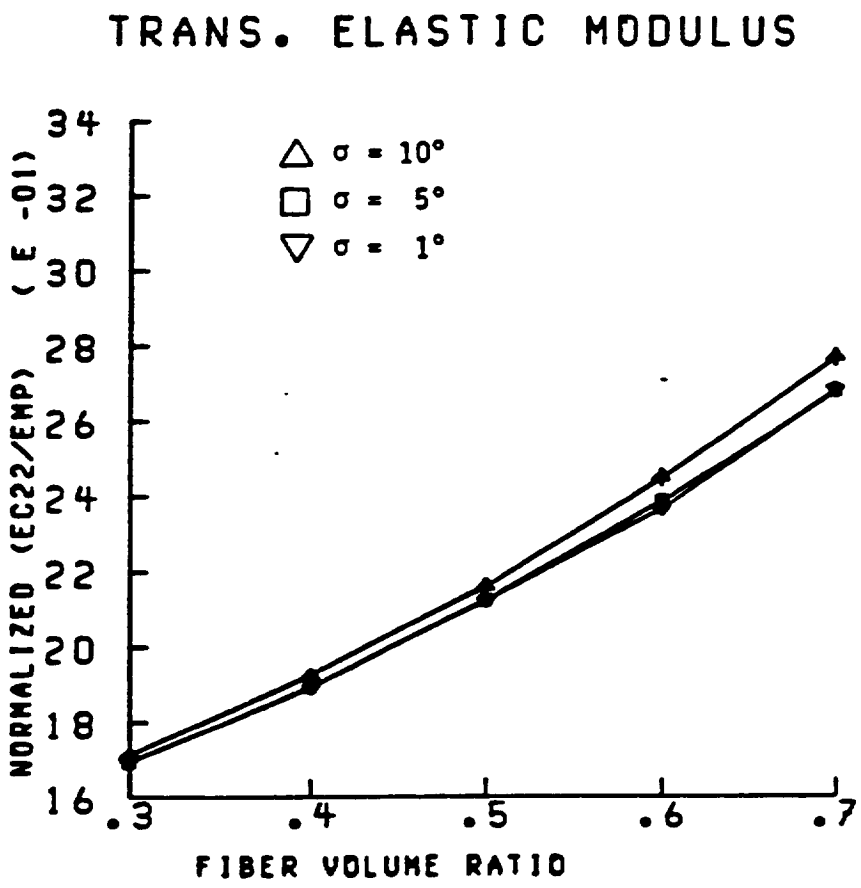

Fig. 49- Transverse Elastic Modulus; for various shape parameters of fiber orientation.

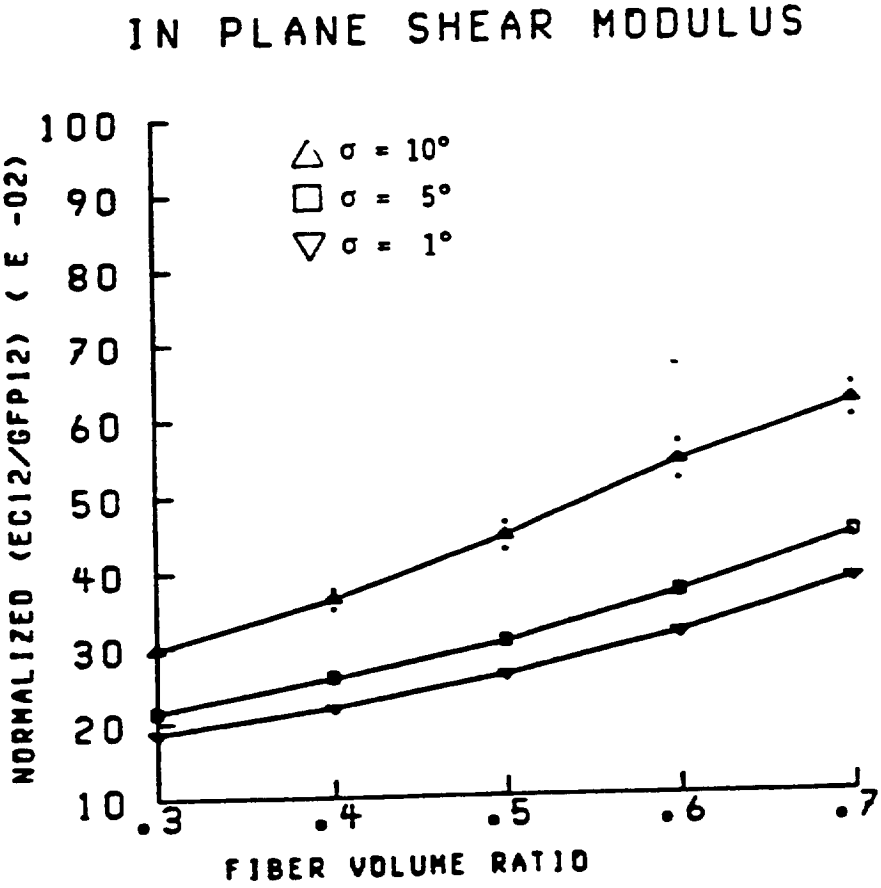

Fig. 50- In-plane Shear Modulus; for various shape parameters of fiber orientation.

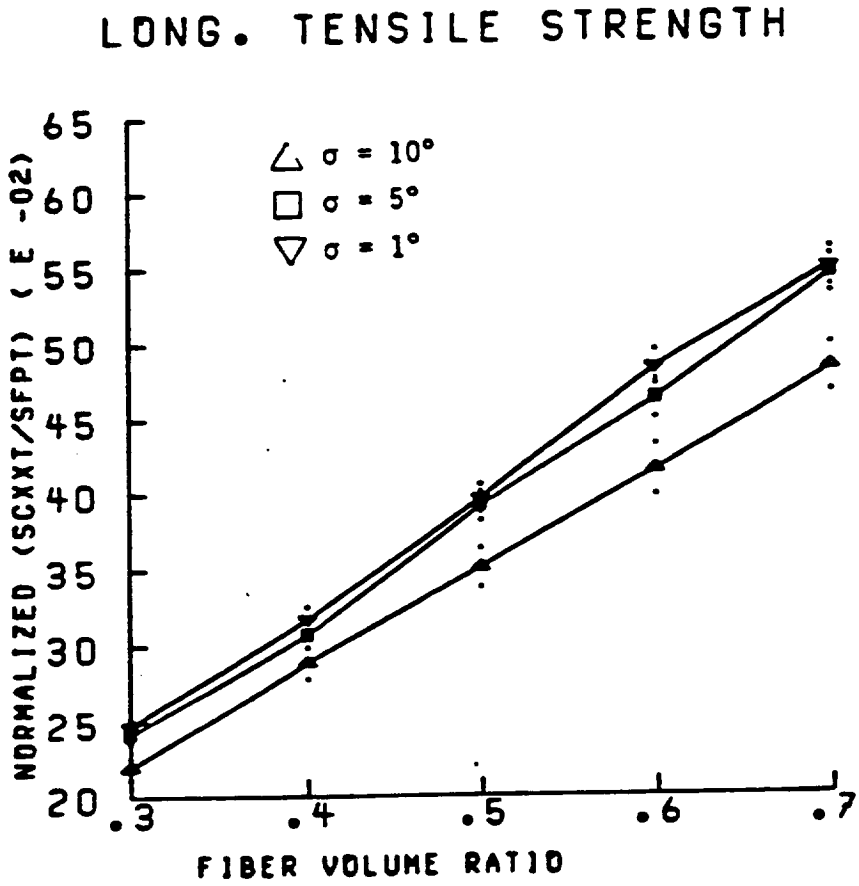

Fig. 51- Longitudinal Tensile Strength; for various shape parameters of fiber orientation.

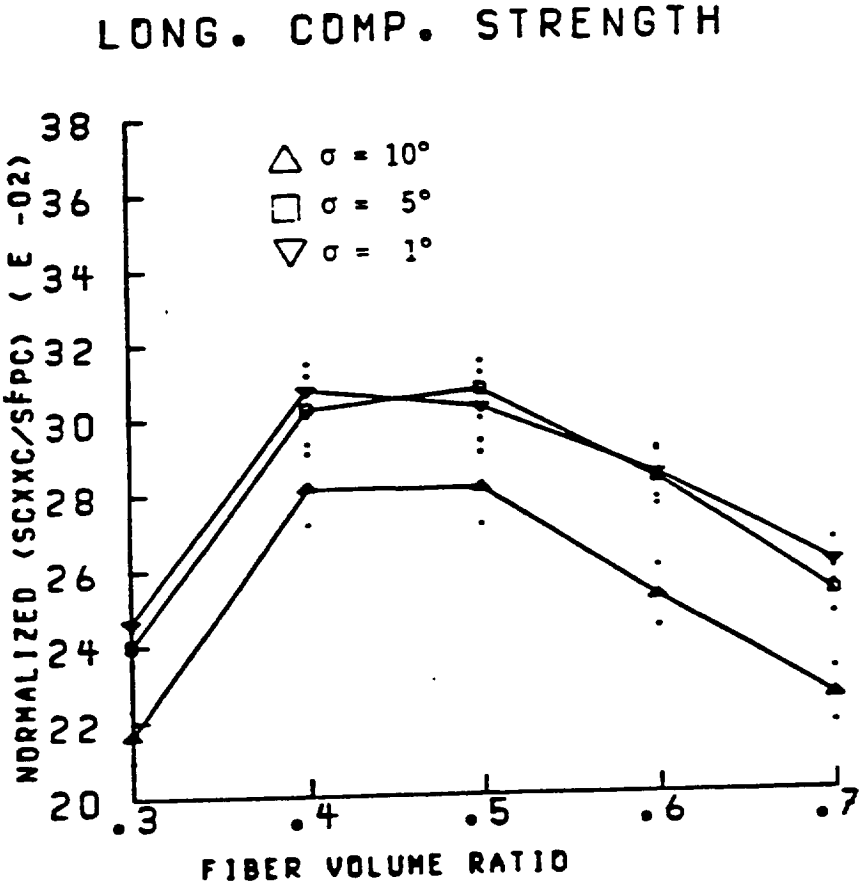

Fig. 52- Longitudinal Compressive Strength; for various shape parameters of fiber orientation.

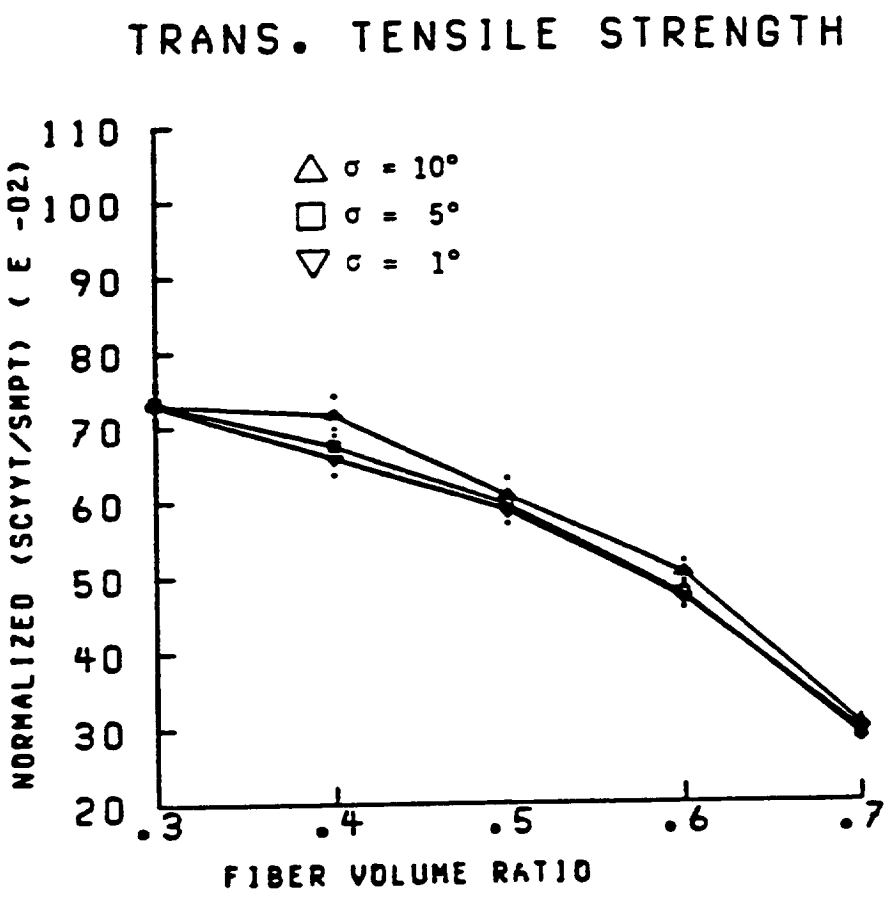

Fig. 53- Transverse Tensile Strength; for various shape parameters of fiber orientation.

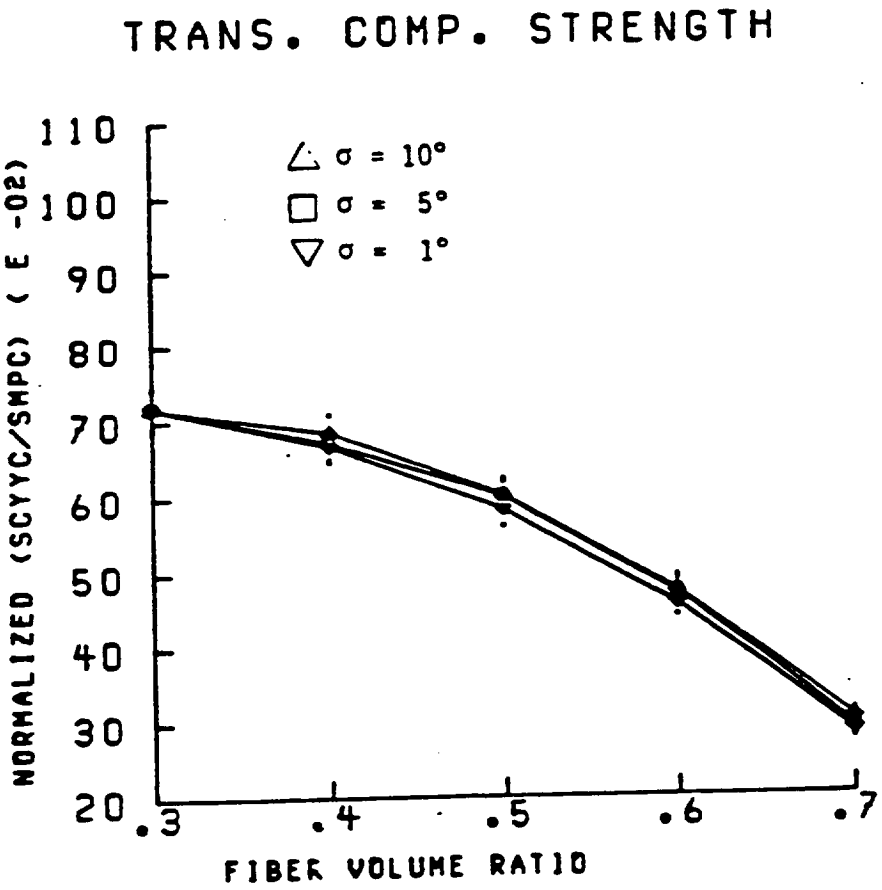

Fig. 54- Transverse Compressive Strength; for various shape parameters of fiber orientation.

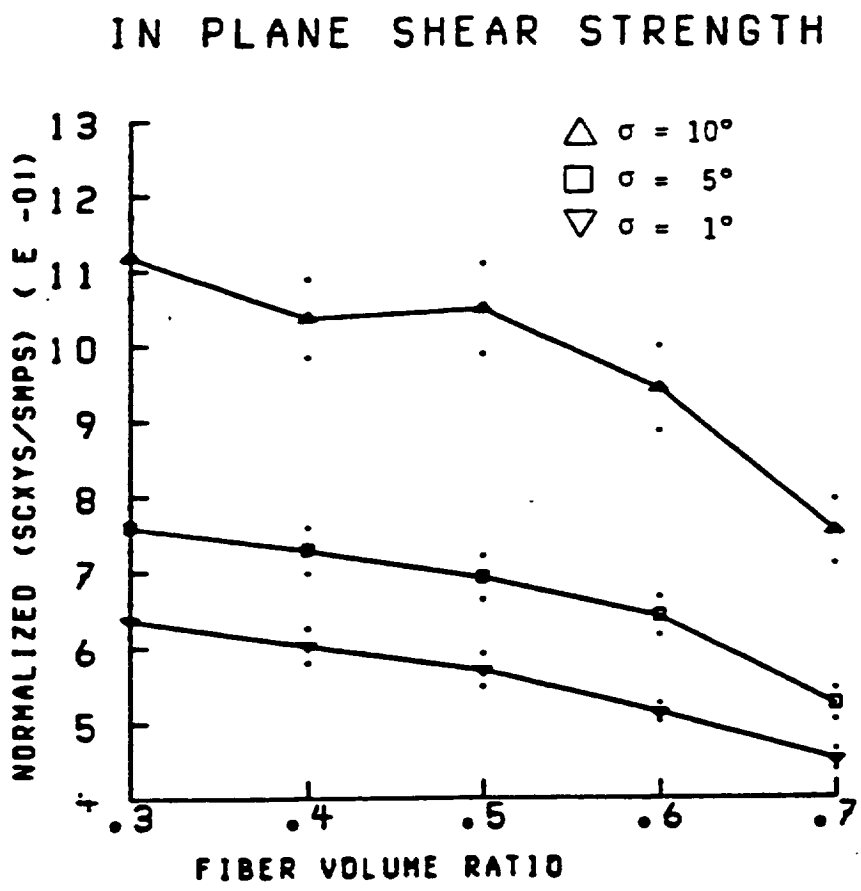

Fig. 55- In-plane Shear Strength; for various shape parameters of fiber orientation.

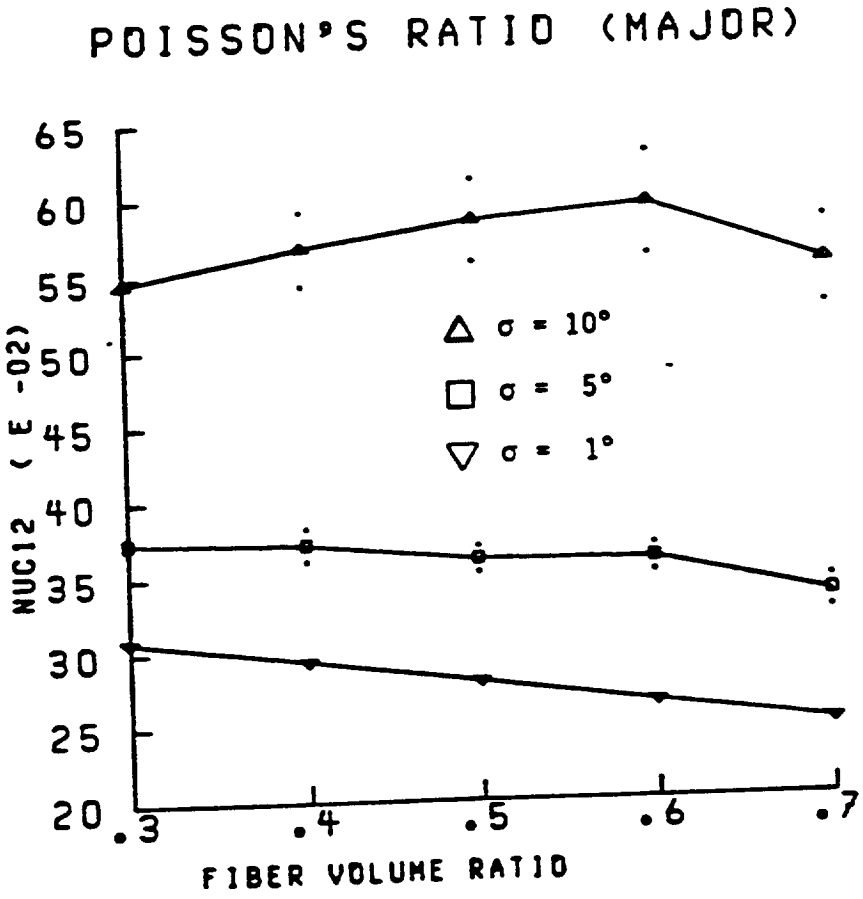

Fig. 56- Poisson's Ratio (major); for various shape parameters of fiber orientation.

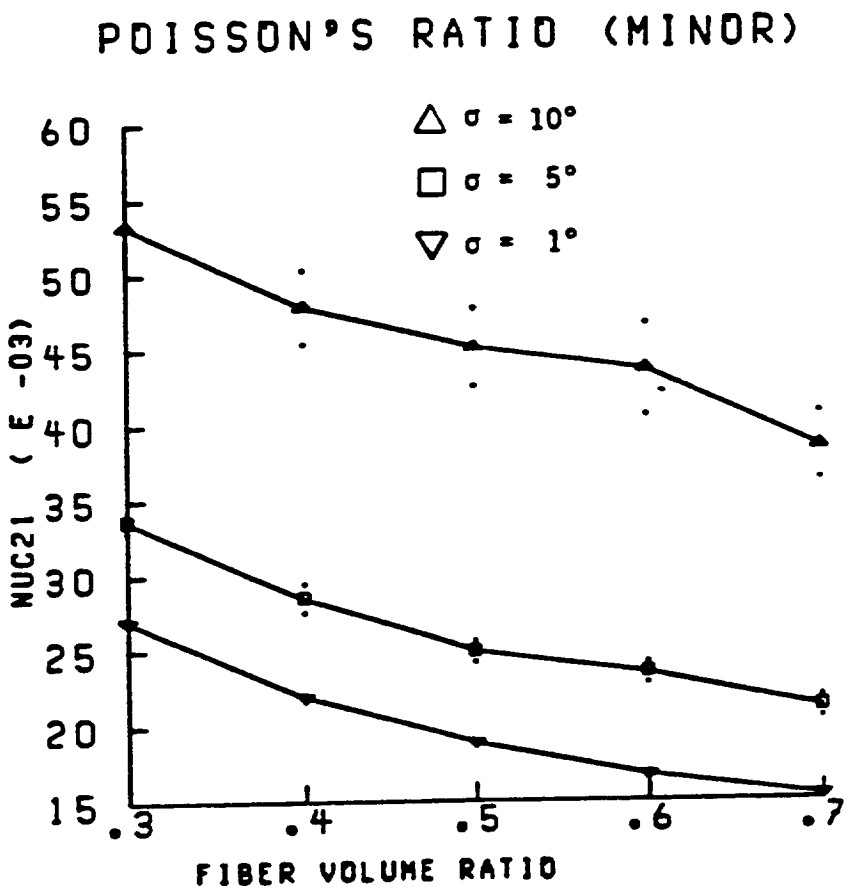

Fig. 57- Poisson's Ratio (minor); for various shape parameters of fiber orientation.

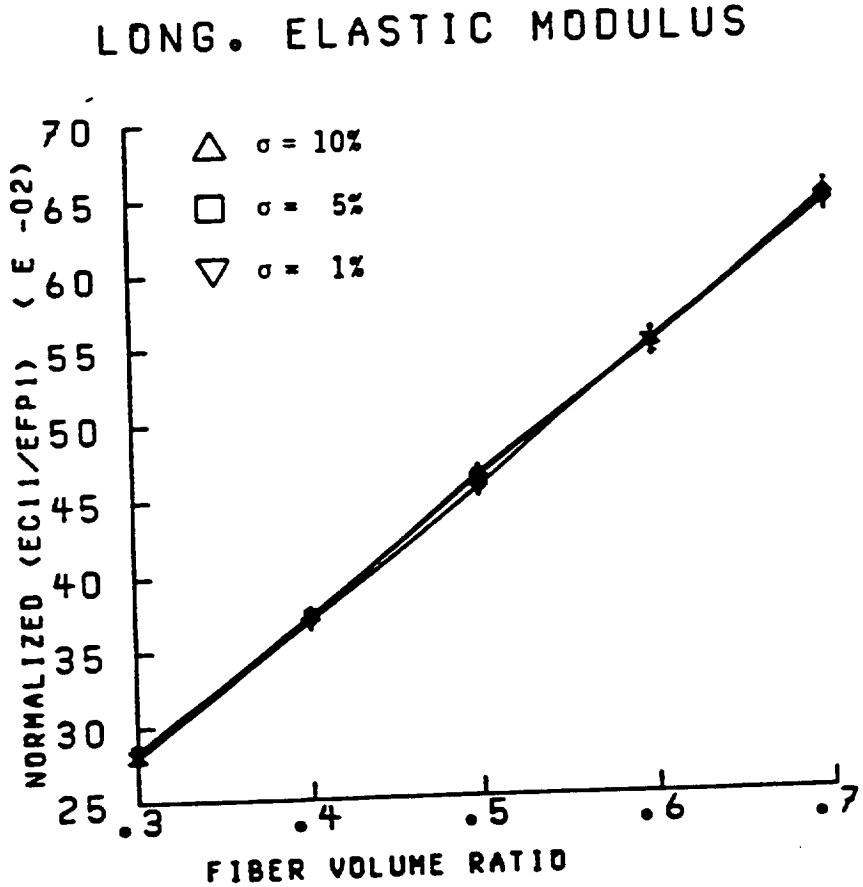

Fig. 58- Longitudinal Elastic Modulus; for various shape parameters of fiber modulus.

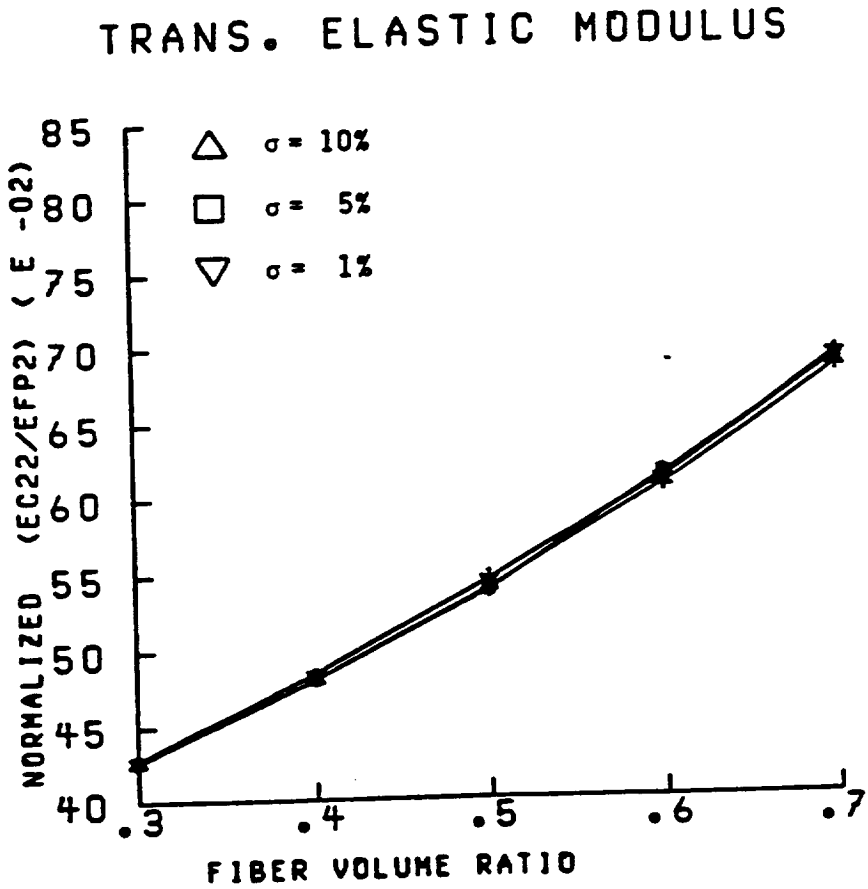

Fig. 59- Transverse Elastic Modulus; for various shape parameters of fiber modulus.

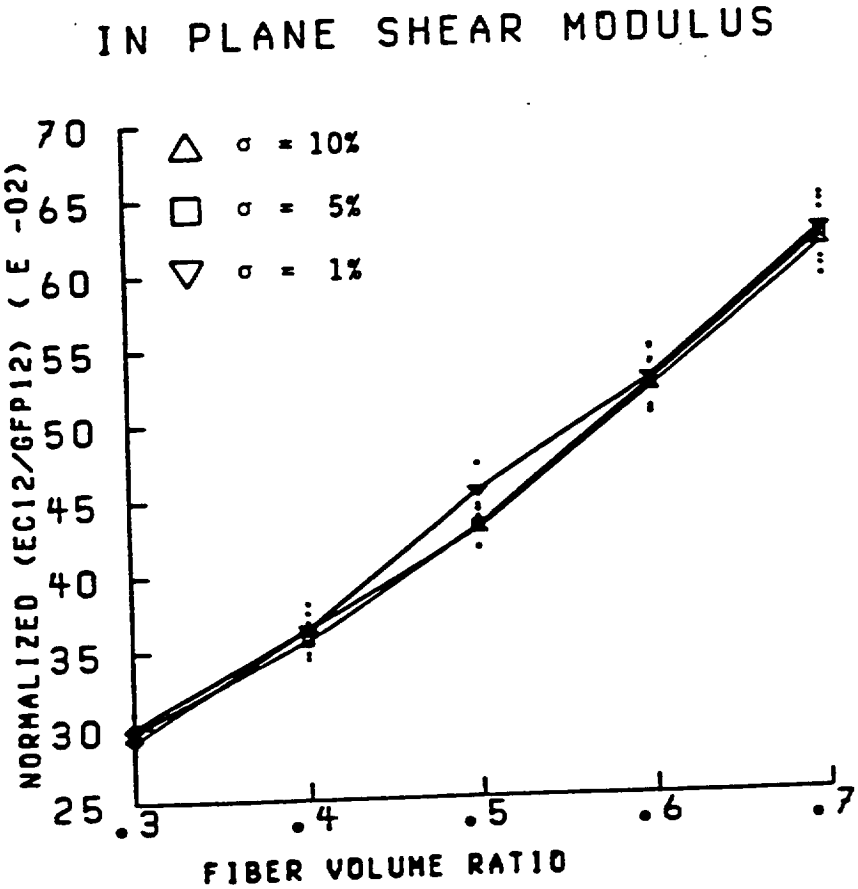

Fig. 60- In Plane Shear Modulus; for various shape parameters of fiber modulus.

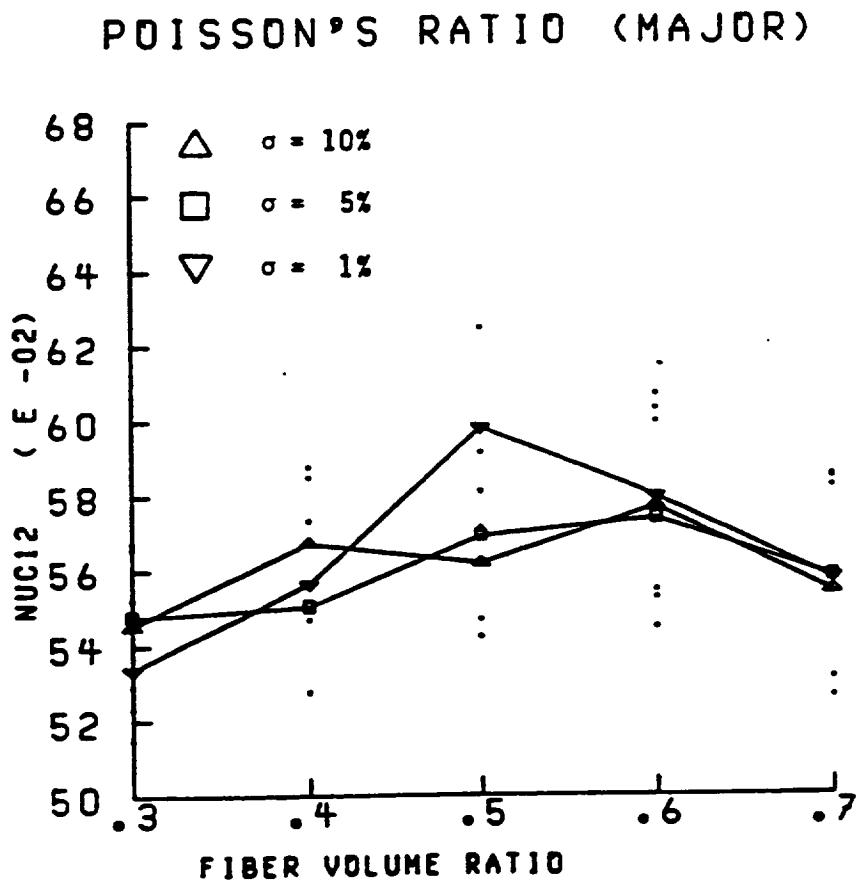

Fig. 61- Poisson's Ratio (major); for various shape parameters of fiber modulus.

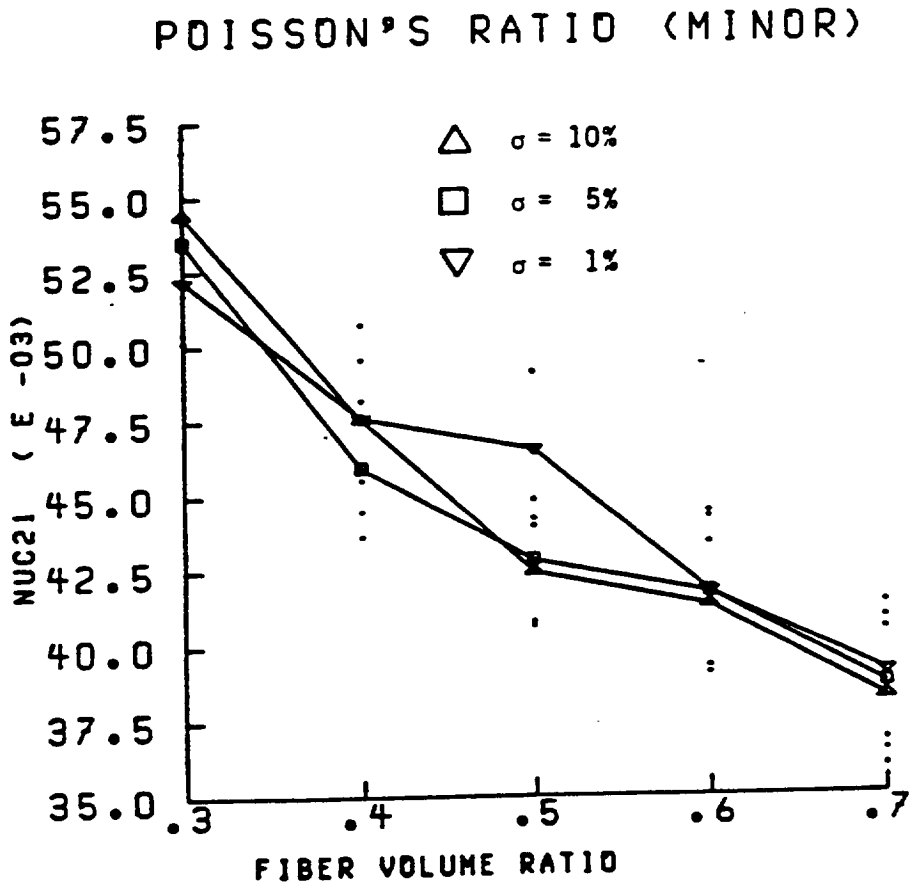

Fig. 62- Poisson's Ratio (minor) for various shape parameters of fiber modulus.

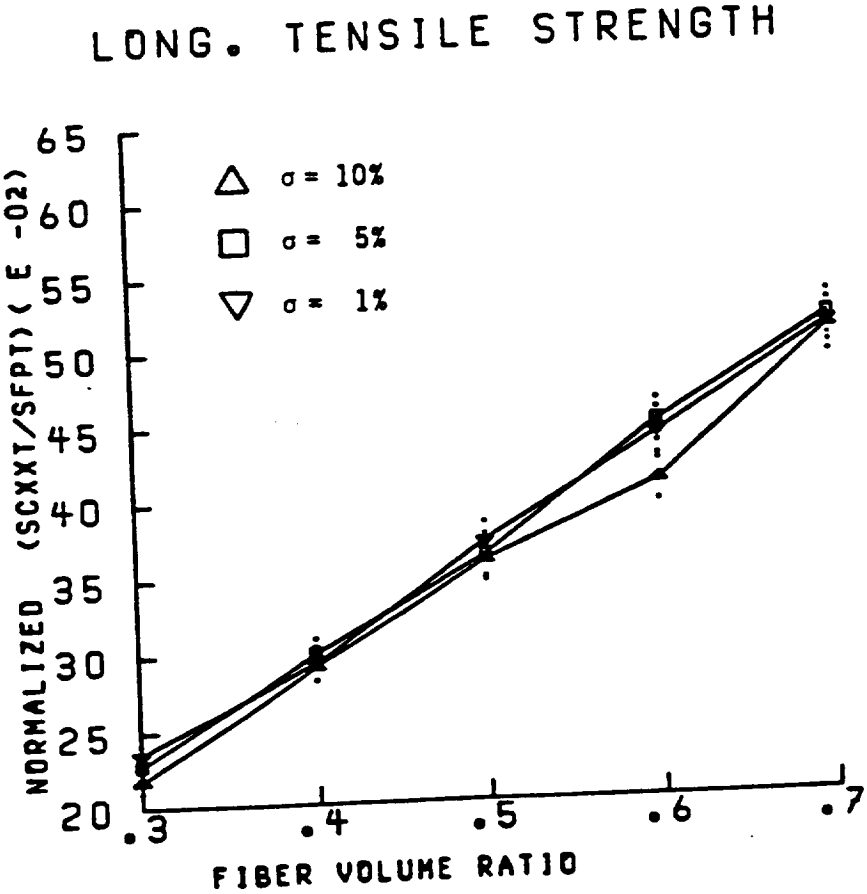

Fig. 63- Longitudinal Tensile Strength; for various shape parameters of fiber modulus.

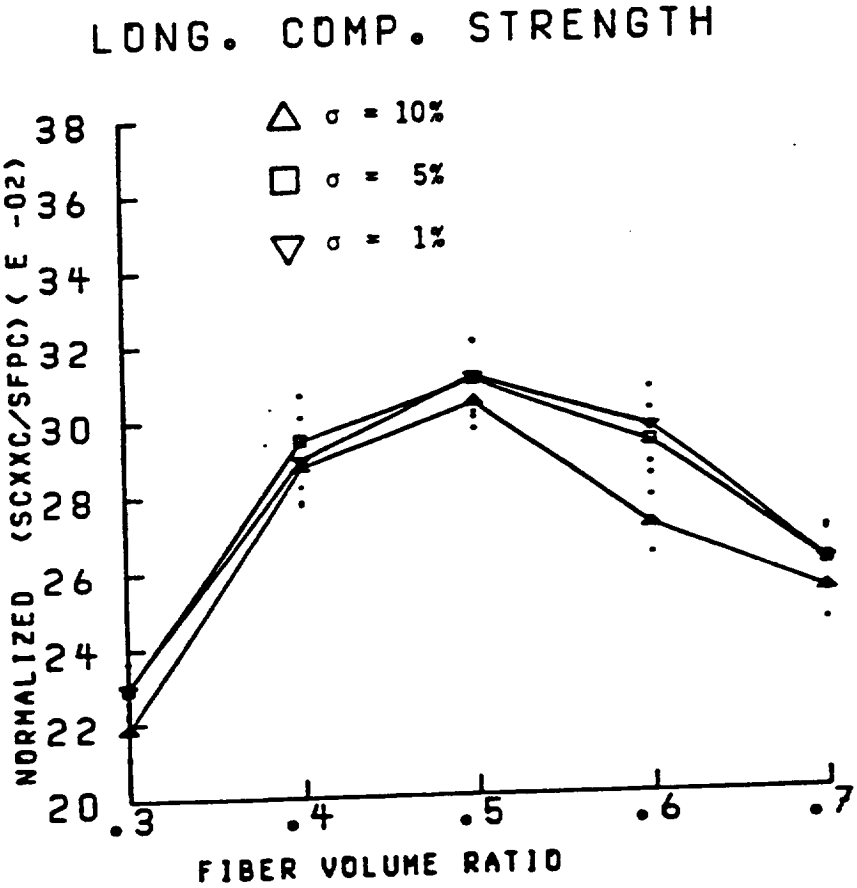

Fig. 64- Longitudinal Compressive Strength; for various shape parameters of fiber modulus.

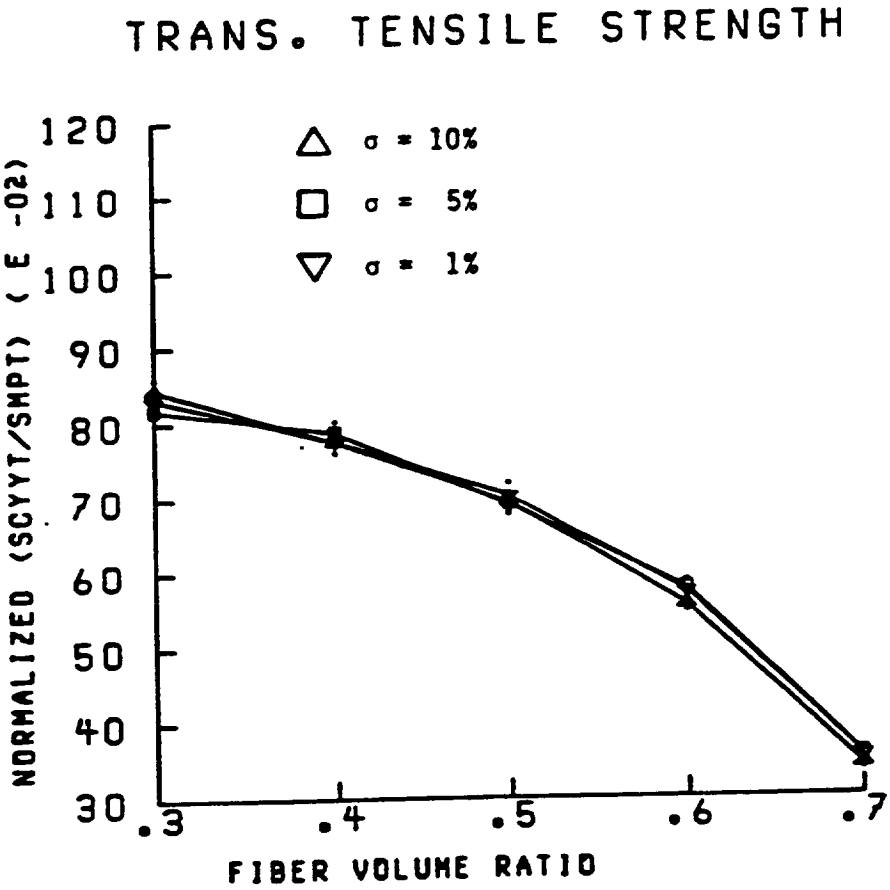

Fig. 65- Transverse Tensile Strength; for various shape parameters of fiber modulus.

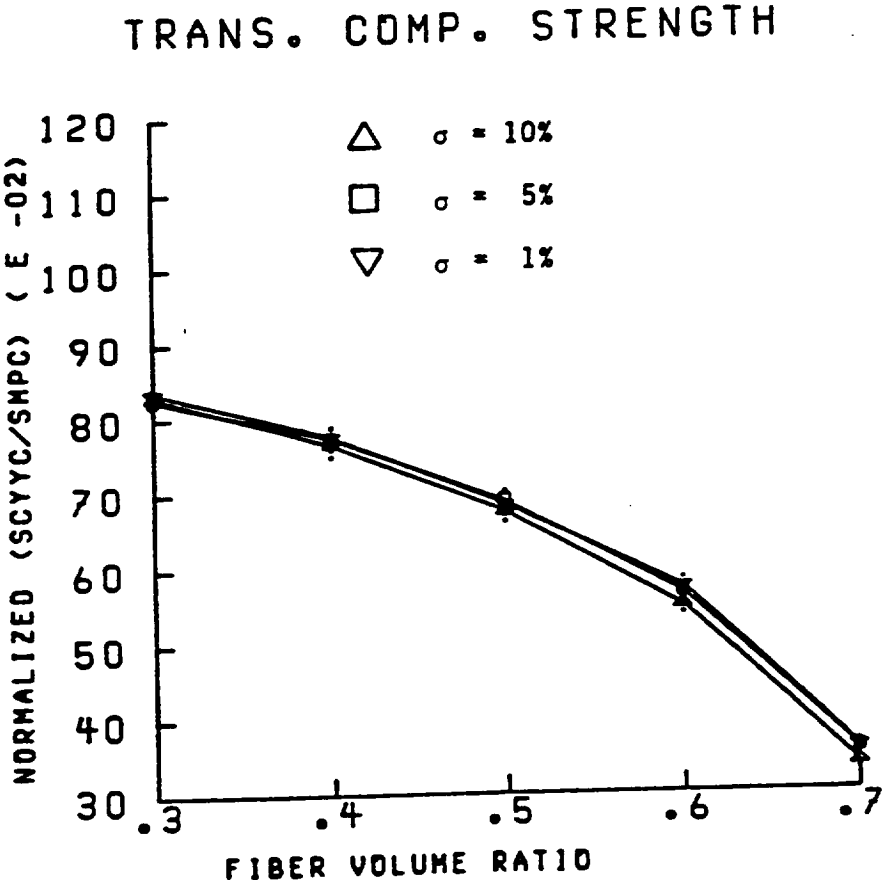

Fig. 66- Transverse Compressive Strength; for various shape parameters of fiber modulus.

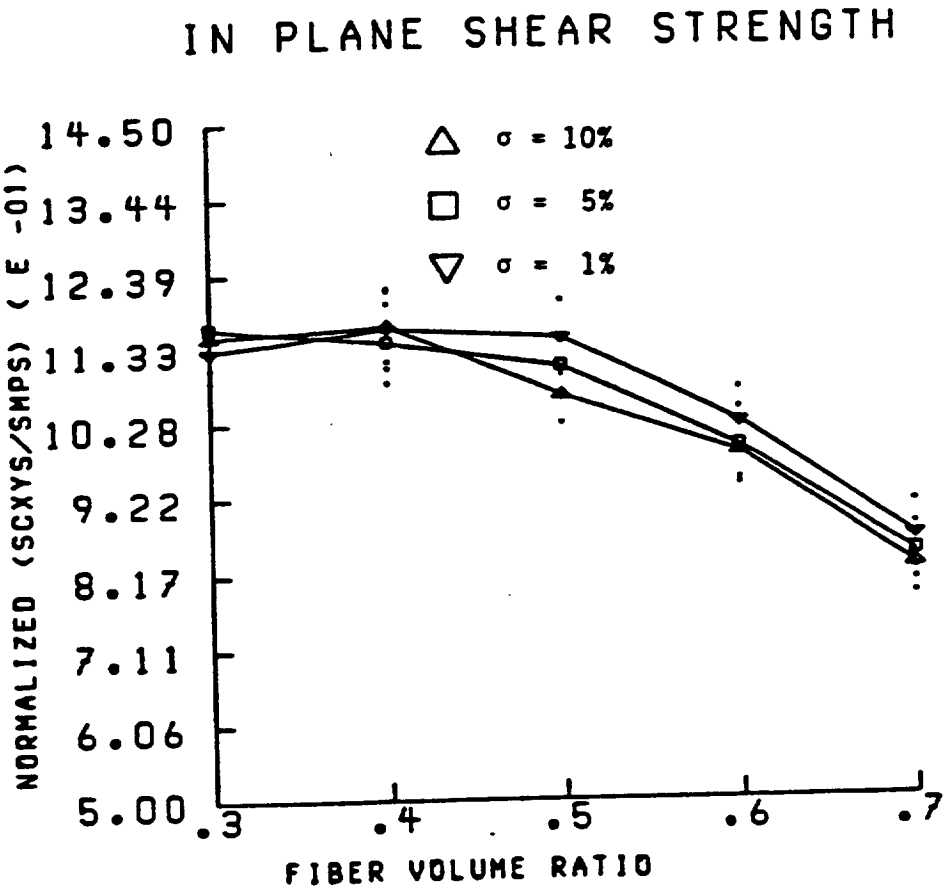

Fig. 67- In Plane Shear Strength; for various shape parameters of fiber modulus.

G. Regression Models

The output data of cases 2 through 11 are used as successive inputs to the regression scheme. The goal of stepwise regression, as used here, is to measure the degree of correlation between a dependent and a set of independent variables for a given set of data. The outputs of the regressions conducted show the independent variables accepted into the model (based on F-test criteria) in order of degree of correlation with the dependent variable of interest, along with the final R^2 statistic. (The R^2 values represent the square of the multiple correlation coefficient, a convenient measure of the fit between data values and values predicted by the regression equation.)

The ordering of predictor variables by stepwise regression has several important uses. In this study, the scheme facilitates easy investigation of the effects of material changes on composite properties. Since the monte carlo scheme permits generation of large amounts of data, the regression is easy, inexpensive, and can provide insight concerning the sensitivity of dependent variables for assumed distributions of predictor variables. A variety of material configurations and constituent distributions are examined, and a model constructed for each dependent (or response) variable. It must be noted that the relative correlations of predictor variables with response variables will be functions of the assumed distributions, the particular data sample considered, and the functional manner in which the predictor variables are incorporated into the model.

A simple regression model was assumed for each response variable.

The first set of "simple" regression models uses as predictor functions only the independent variables as individual terms. To be more precise, the predictor variables used are not simply the independent variable values, for there are 15 of these for each layup. The arithmetic mean of independent variable values is thus used as the predictor variable in the first set of regression models. The only exception to this is the use of the $\sin^2$ of the average of the fiber orientation angles as the angular dependence predictor, denoted by THETA in the tables to follow. The simpler response variables can be adequately described using the linear function forms in the regression models. The simple variables include the elastic constants, (EC11, EC22, EC12, NUC12, NUC21) and coefficients of thermal expansion (CTE11, CTE22). The results of the regressions performed in the "simple" manner are given in Tables III - XIV. In the tables the input labeled with N1 through N5 and W1 through W5 represent narrow and wide distributions of all properties. Input labeled N6 through N10 and W6 through W10 describe the same distributions, except that the composite is assumed unidirectional, i.e. no angular variation. The distinction shows the reduction in predictive capability induced by deviations of the fibers from aligned orientation.

The models assumed for the response (output) variables are of the form

$$Y = B_0 + B_1X_1 + B_2X_2 + B_3X_3 + \ldots + B_nX_n$$

where

Y = response variable (EC11, EC22, EC12, etc.)

B_n = regression parameters to be obtained

X_n = average of independent variable values through the thickness of the ply (THETA, FVR, VVR, etc.)

Each model postulated contains all independent variables that appear in the equations for the related ply property (see Appendix B).

TABLE III- LONGITUDINAL MODULUS (EC11)

SIMPLE MODEL

INPUT	FVR	TERMS ACCEPTED	R^2
N1	0.3	FVR,EFP1	83.17
N2	0.4	FVR,EFP1,THETA	92.63
N3	0.5	FVR,EFP1,THETA	94.02
N4	0.6	FVR,EFP1,THETA	94.59
N5	0.7	FVR,EFP1	84.00
W1	0.3	FVR,THETA,EFP1	64.49
W2	0.4	FVR,EFP1,THETA	89.88
W3	0.5	FVR,THETA,EFP1	72.85
W4	0.6	FVR,THETA,EFP1	65.37
W5	0.7	FVR,EFP1,THETA	57.83
N6	0.3	FVR,EFP1,EMP	99.83
N7	0.4	FVR,EFP1	99.81
N8	0.5	FVR,EFP1	99.69
N9	0.6	FVR,EFP1,EMP	99.74
N10	0.7	FVR,EFP1	99.77
W6	0.3	FVR,EFP1,VVR	99.13
W7	0.4	FVR,EFP1	98.40
W8	0.5	FVR,EFP1	98.90
W9	0.6	FVR,EFP1	99.59
W10	0.7	FVR,EFP1	99.34

TABLE IV- TRANSVERSE MODULUS (EC22)

SIMPLE MODEL

INPUT	FVR	TERMS ACCEPTED	R^2
N1	0.3	FVR,EFP2	83.50
N2	0.4	FVR	85.23
N3	0.5	FVR,EFP2	91.83
N4	0.6	FVR,EFP2	93.26
N5	0.7	FVR,EFP2,THETA	93.06
W1	0.3	FVR,THETA,EFP2	78.36
W2	0.4	FVR,THETA,EFP2	90.73
W3	0.5	FVR,THETA,EFP2	80.15
W4	0.6	FVR,THETA,EFP2	86.05
W5	0.7	FVR,THETA,EFP2	87.14
N6	0.3	FVR,EFP2	87.13
N7	0.4	FVR,EFP2	86.15
N8	0.5	FVR,EFP2	90.97
N9	0.6	FVR,EFP2	93.47
N10	0.7	FVR,EFP2	92.05
W6	0.3	FVR,EFP2	79.72
W7	0.4	FVR,EFP2	70.71
W8	0.5	FVR,EFP2	81.92
W9	0.6	FVR,EFP2	88.62
W10	0.7	FVR,EFP2	84.05

TABLE V- SHEAR MODULUS (EC12)

SIMPLE MODEL

INPUT	FVR	TERMS ACCEPTED	R^2
N1	0.3	THETA,FVR,GMP	97.01
N2	0.4	THETA,FVR,GMP,GFP23	98.85
N3	0.5	THETA,FVR,GMP,GFP12	97.50
N4	0.6	THETA,FVR,GMP	98.01
N5	0.7	THETA,FVR,GMP,GFP12	98.42
W1	0.3	THETA,FVR,GMP	94.79
W2	0.4	THETA,FVR	94.27
W3	0.5	THETA,FVR,GFP23	93.71
W4	0.6	THETA,FVR	95.62
W5	0.7	THETA,FVR,GMP,GFP23	96.67
N6	0.3	FVR,GMP	97.66
N7	0.4	FVR,GMP,GFP12	98.02
N8	0.5	FVR,GMP,GFP23	96.65
N9	0.6	FVR,GMP,GFP12	97.11
N10	0.7	FVR,GMP,GFP12	98.55
W6	0.3	FVR,GMP,GFP12	96.93
W7	0.4	FVR,GMP,GFP12	92.45
W8	0.5	FVR,GMP,GFP12	95.16
W9	0.6	FVR,GMP	97.18
W10	0.7	FVR,GMP,GFP12	96.90

TABLE VI- POISSON'S RATIO, MAJOR (NUC12)

SIMPLE MODEL

INPUT	FVR	TERMS ACCEPTED	R^2
N1	0.3	THETA,EFP1	96.39
N2	0.4	THETA,FVR	97.88
N3	0.5	THETA,FVR	96.60
N4	0.6	THETA,FVR,EFP1	98.32
N5	0.7	THETA,FVR,EFP2	96.62
W1	0.3	THETA,EFP1	88.43
W2	0.4	THETA,FVR	84.62
W3	0.5	THETA	89.48
W4	0.6	THETA,VVR	84.05
W5	0.7	THETA,FVR	92.05
N6	0.3	FVR	97.83
N7	0.4	FVR	98.48
N8	0.5	FVR	97.77
N9	0.6	FVR	98.40
N10	0.7	FVR	99.17
W6	0.3	FVR	97.32
W7	0.4	FVR,VVR	96.45
W8	0.5	FVR	96.38
W9	0.6	FVR,GFP12,EFP2	98.34
W10	0.7	FVR,EFP2	96.96

TABLE VII- POISSON'S RATIO, MINOR (NUC21)

SIMPLE MODEL

INPUT	FVR	TERMS ACCEPTED	R^2
N1	0.3	THETA,FVR	91.15
N2	0.4	THETA,FVR,EFP1	94.78
N3	0.5	THETA,FVR	94.31
N4	0.6	THETA,FVR,EFP1,EFP2	97.18
N5	0.7	THETA,FVR,EFP1	95.87
W1	0.3	THETA,FVR	90.87
W2	0.4	THETA,FVR,EFP2	89.86
W3	0.5	THETA,FVR	91.93
W4	0.6	THETA	92.57
W5	0.7	THETA,FVR,EFP1	94.78
N6	0.3	FVR,EFP1,EFP2	95.64
N7	0.4	FVR,EFP1,EFP2	94.90
N8	0.5	FVR,EFP1,EFP2	95.40
N9	0.6	FVR,EFP1,EFP2	93.12
N10	0.7	FVR,EFP1,EFP2	91.83
W6	0.3	FVR,EFP1,GFP12	87.73
W7	0.4	FVR,EFP1,EFP2	85.06
W8	0.5	FVR,EFP1,EFP2	84.29
W9	0.6	FVR,EFP1,EFP2	90.37
W10	0.7	EFP1,FVR,EFP2	91.42

TABLE VIII- LONG. THERM. EXPANSION (CTE11)

SIMPLE MODEL

INPUT	FVR	TERMS ACCEPTED	R^2
N1	0.3	FVR,THETA,EFP1	90.29
N2	0.4	THETA,FVR,EFP1,VVR	94.46
N3	0.5	FVR,THETA,EFP1,VVR	95.72
N4	0.6	FVR,THETA,EFP1,VVR	95.23
N5	0.7	THETA,FVR	87.63
W1	0.3	THETA,FVR,EFP1	80.53
W2	0.4	THETA,FVR	78.91
W3	0.5	THETA,FVR	84.77
W4	0.6	THETA,FVR,VVR	74.37
W5	0.7	THETA	80.50
N6	0.3	FVR,EFP1,VVR	97.21
N7	0.4	FVR,EFP1,VVR	96.96
N8	0.5	FVR,EFP1,VVR	96.53
N9	0.6	FVR,EFP1	96.60
N10	0.7	FVR,EFP1	96.24
W6	0.3	FVR,EFP1	91.60
W7	0.4	FVR,EFP1	90.88
W8	0.5	FVR,EFP1	91.55
W9	0.6	FVR,EFP1,VVR	96.03
W10	0.7	FVR,EFP1	94.13

TABLE IX- TRANS. THERM. EXPANSION (CTE22)

SIMPLE MODEL

INPUT	FVR	TERMS ACCEPTED	R^2
N1	0.3	FVR,THETA,VVR	99.60
N2	0.4	FVR,THETA,VVR	99.21
N3	0.5	FVR,THETA,VVR	99.46
N4	0.6	FVR,THETA	99.69
N5	0.7	FVR,THETA	99.79
W1	0.3	FVR,THETA	95.04
W2	0.4	FVR,THETA,EFP1,VVR	98.60
W3	0.5	FVR,THETA	95.19
W4	0.6	FVR,THETA	94.84
W5	0.7	FVR,THETA	97.98
N6	0.3	FVR,VVR,EFP1	99.70
N7	0.4	FVR,VVR	99.53
N8	0.5	FVR,VVR	99.65
N9	0.6	FVR	99.67
N10	0.7	FVR	99.75
W6	0.3	FVR,EFP1	99.15
W7	0.4	FVR	98.81
W8	0.5	FVR	98.88
W9	0.6	FVR	99.47
W10	0.7	FVR	99.22

TABLE X- LONG. TENSILE STRENGTH (SCXXT)

SIMPLE MODEL

INPUT	FVR	TERMS ACCEPTED	R^2
N1	0.3	FVR	12.25
N2	0.4	FVR,SFPT	43.72
N3	0.5	FVR	21.68
N4	0.6	FVR,SFPT,THETA	43.68
N5	0.7	FVR	40.97
W1	0.3	FVR,SFPT	33.37
W2	0.4	SFPT,FVR	39.02
W3	0.5	EFP1,SFPT	26.13
W4	0.6	FVR,EMP	42.27
W5	0.7	FVR,SFPT	33.55
N6	0.3	FVR,SFPT	52.12
N7	0.4	FVR,SFPT,EFP1	68.43
N8	0.5	FVR,SFPT	34.89
N9	0.6	FVR,SFPT	49.00
N10	0.7	SFPT,FVR	24.00
W6	0.3	SFPT,FVR	46.61
W7	0.4	FVR	19.33
W8	0.5	FVR,SFPT	33.13
W9	0.6	FVR,SFPT	34.40
W10	0.7	SFPT,FVR	37.65

TABLE XI- LONG. COMPRESSIVE STRENGTH (SCXXC)

SIMPLE MODEL

INPUT	FVR	TERMS ACCEPTED	R^2
N1	0.3	FVR	12.25
N2	0.4	FVR	18.23
N3	0.5	NONE	
N4	0.6	SFPC	8.52
N5	0.7	FVR	8.08
W1	0.3	VVR	8.02
W2	0.4	THETA	9.29
W3	0.5	GMP,SMPC	20.59
W4	0.6	THETA	9.18
W5	0.7	NONE	
N6	0.3	SFPC	11.30
N7	0.4	NONE	
N8	0.5	NONE	
N9	0.6	NONE	
N10	0.7	GFP12	12.01
W6	0.3	FVR	9.40
W7	0.4	VVR	10.76
W8	0.5	VVR	9.85
W9	0.6	GFP12	8.87
W10	0.7	NONE	

TABLE XII- TRANSVERSE TENSILE STRENGTH (SCYYT)

SIMPLE MODEL

INPUT	FVR	TERMS ACCEPTED	R^2
N1	0.3	FVR	27.03
N2	0.4	FVR	32.91
N3	0.5	SMPT	8.10
N4	0.6	FVR	41.92
N5	0.7	NONE	
W1	0.3	FVR,VVR,SMPT	26.89
W2	0.4	FVR	41.43
W3	0.5	FVR	14.74
W4	0.6	NONE	
W5	0.7	FVR,SMPT	31.05
N6	0.3	FVR	9.43
N7	0.4	FVR	8.19
N8	0.5	FVR,EFP2	15.58
N9	0.6	NONE	
N10	0.7	NONE	
W6	0.3	FVR	33.87
W7	0.4	FVR	13.39
W8	0.5	SMPT	8.62
W9	0.6	FVR	27.85
W10	0.7	FVR	32.77

TABLE XIII- TRANSVERSE COMPRESSIVE STRENGTH (SCYYC)

SIMPLE MODEL

INPUT	FVR	TERMS ACCEPTED	R^2
N1	0.3	FVR,SMPC	33.17
N2	0.4	FVR	30.10
N3	0.5	NONE	
N4	0.6	FVR	38.93
N5	0.7	NONE	
W1	0.3	FVR,VVR	28.19
W2	0.4	FVR	43.26
W3	0.5	FVR,SMPC	19.57
W4	0.6	NONE	
W5	0.7	FVR	15.85
N6	0.3	NONE	
N7	0.4	NONE	
N8	0.5	NONE	
N9	0.6	NONE	
N10	0.7	NONE	
W6	0.3	FVR	28.68
W7	0.4	FVR	11.64
W8	0.5	NONE	
W9	0.6	FVR	31.97
W10	0.7	FVR	33.05

TABLE XIV- IN PLANE SHEAR STRENGTH (SCXYS)

SIMPLE MODEL

INPUT	FVR	TERMS ACCEPTED	R^2
N1	0.3	FVR,THETA,GFP12	28.51
N2	0.4	FVR	8.74
N3	0.5	THETA	14.96
N4	0.6	THETA,GFP12,FVR,SMPS	31.84
N5	0.7	NONE	
W1	0.3	THETA,VVR,SMPS,FVR	48.16
W2	0.4	FVR	43.26
W3	0.5	THETA	8.40
W4	0.6	THETA	14.75
W5	0.7	NONE	
N6	0.3	NONE	
N7	0.4	NONE	
N8	0.5	NONE	
N9	0.6	SMPS	8.25
N10	0.7	VVR	8.53
W6	0.3	FVR,SMPS,GMP	29.06
W7	0.4	NONE	
W8	0.5	NONE	
W9	0.6	GFP12,FVR	22.20
W10	0.7	SMPS	17.73

Further regression models were studied, in an attempt to improve the predictive capability of the models, especially for the strengths. These models, incorporating higher order functions and combinations of predictor variables used in the simple models, show some improvement over the simple models, proving the value of including the "interaction" effects of predictor variables in the regression models. In addition, the higher order interaction models can fit response functions over a wider range of fiber volume ratio, with associated improvements in the R^2 statistics. The data cases CON1 and CON2 contain selected points from the entire range of fiber volume ratios, to supply the samples for these runs. Furthermore, since higher order models are postulated, THETA is taken to be the cosine of the average of fiber orientation angles. The variable MVR is a "dummy" variable, that is a function of other variables in the model. It is defined as

$$MVR = 1 - FVR - VVR$$

and is intended to represent an "average" matrix volume ratio over the thickness of the ply. The interaction models are shown in Tables XV - XXVI.

The general form of the postulated models now includes higher order terms, so the predictor variables are tested up to the fourth power. Symbolically,

$$\begin{aligned} Y = {} & B_0 + B_1(THETA) + B_2(FVR) + B_3(VVR) + B_4(EFP1) + B_5(EMP) + \\ & B_6(MVR) + B_7(THETA)^2 + B_8(THETA)(FVR) + B_9(THETA)(VVR) + \\ & B_{10}(THETA)(EFP1) + \ldots + B_{11}(THETA)^2(FVR)(EFP1) + \ldots \\ & B_{12}(THETA)^4 + B_{13}(FVR)^2 + \ldots \text{ etc.} \end{aligned}$$

The number of terms possible in a complete fourth power polynomial expansion becomes unwieldy for the cases studied. Considering the limitation of the size of the predictor matrix in the regression package used (100 x 100), the terms are intuitively grouped in the hope of eliminating large groups at one time. The regressions are conducted using "unlikely" candidates for admission into a particular model, and if no terms are entered, subsequent regressions are conducted without those terms. The justification for this approach is not a statistical argument, rather an interpretation of the physical principles active in any chosen model. The regressions to eliminate terms are merely used as a check on what seems intuitively reasonable.

TABLE XV- LONGITUDINAL MODULUS (EC11)

INTERACTION MODEL

INPUT	FVR	TERMS ACCEPTED	R^2
N1	0.3	$THETA^4$*FVR*EFP1	84.50
N2	0.4	$THETA^4$*FVR*EFP1	92.66
N3	0.5	$THETA^4$*FVR*EFP1	93.76
N4	0.6	$THETA^4$*FVR*EFP1	94.24
N5	0.7	$THETA^4$*FVR*EFP1	85.08
W1	0.3	$THETA^4$*FVR*EFP1	63.84
W2	0.4	$THETA^4$*FVR*EFP1	89.86
W3	0.5	$THETA^4$*FVR*EFP1	71.79
W4	0.6	$THETA^4$*FVR*EFP1	64.37
W5	0.7	$THETA^4$*FVR*EFP1	55.68
N6	0.3	FVR*EFP1, EMP^2*MVR	99.82
N7	0.4	FVR*EFP1, FVR^4	99.83
N8	0.5	FVR*EFP1	99.72
N9	0.6	FVR*EFP1, EMP^2*VVR, VVR^4	99.79
N10	0.7	FVR*EFP1, EMP*MVR	99.79
W6	0.3	FVR*EFP1, VVR	99.17
W7	0.4	FVR*EFP1, MVR^2*FVR	98.53
W8	0.5	FVR*EFP1, MVR^2*EMP	98.99
W9	0.6	FVR*EFP1	99.58
W10	0.7	FVR*EFP1, EMP*MVR	99.38
CON1	VARIES	$THETA^4$*FVR*EFP1	96.48
CON2	VARIES	FVR*EFP1, VVR^4	99.92

TABLE XVI- TRANSVERSE MODULUS (EC22)

INPUT	FVR	INTERACTION MODEL TERMS ACCEPTED	R^2
N1	0.3	FVR*EFP2*EMP, $EFP2^2$*FVR, THETA*FVR*MVR	99.19
N2	0.4	FVR*EFP2*EMP, $EFP2^2$*FVR, THETA	99.55
N3	0.5	FVR*EFP2*EMP, $THETA^2$*EFP2, MVR^4	98.92
N4	0.6	FVR*EFP2*EMP, $THETA^2$*EFP2, $EFP2^2$*FVR	99.22
N5	0.7	*** NEARLY SINGULAR	
W1	0.3	$THETA^2$*MVR, EMP^2*EFP2, MVR^2	93.26
W2	0.4	FVR*EMP, THETA, $EFP2^2$*FVR	96.79
W3	0.5	FVR*EFP2*EMP, THETA, FVR*EFP2*MVR	93.49
W4	0.6	$THETA^2$*MVR, MVR^2*EFP2, EMP*MVR	88.35
W5	0.7	*** NEARLY SINGULAR	
N6	0.3	FVR*EFP2*EMP, $EFP2^2$*FVR, EMP*MVR	99.22
N7	0.4	FVR*EFP2*EMP, EMP^2FVR	99.07
N8	0.5	FVR*EFP2*EMP, FVR*EFP2*MVR	98.89
N9	0.6	FVR*EFP2*EMP, FVR^2*EMP	99.14
N10	0.7	FVR^4, EFP2*EMP	99.23
W6	0.3	FVR*EFP2*EMP, EFP2, $EFP2^2$*EMP, FVR*EFP2	98.62
W7	0.4	FVR*EFP2*EMP, FVR*EFP2*MVR, FVR*VVR	98.28
W8	0.5	FVR*EFP2*EMP, FVR*EFP2*MVR	97.93
W9	0.6	FVR*EFP2*EMP, $EFP2^2$*MVR	98.44
W10	0.7	FVR*EFP2*EMP, MVR^2*FVR	97.86
CON1	VARIES	*** NEARLY SINGULAR	
CON2	VARIES	FVR*EFP2*EMP, FVR*EFP2*MVR	99.79

TABLE XVII- IN PLANE SHEAR MODULUS (EC12)

INPUT	FVR	INTERACTION MODEL TERMS ACCEPTED	R^2
N1	0.3	THETA, FVR*GMP, $THETA^4$*FVR*GMP	97.86
N2	0.4	*** NEARLY SINGULAR	
N3	0.5	$THETA^2$, FVR^2*GMP, GFP12*GMP	97.75
N4	0.6	THETA, FVR^2*MVR	98.01
N5	0.7	THETA, FVR^2*GMP, GFP12	98.46
W1	0.3	$THETA^4$, FVR^4*GMP, FVR^2	95.49
W2	0.4	*** NEARLY SINGULAR	
W3	0.5	$THETA^4$*FVR*MVR, $THETA^4$*VVR, VVR*GMP	91.04
W4	0.6	$THETA^4$, FVR^3*GMP, THETA	96.70
W5	0.7	*** NEARLY SINGULAR	
N6	0.3	FVR*GMP, MVR^2*GFP12	97.73
N7	0.4	FVR*GMP, GFP12	97.97
N8	0.5	FVR*GMP, FVR*GFP12	96.52
N9	0.6	FVR*GMP, FVR^2*GFP12	97.10
N10	0.7	FVR^4*GMP, FVR*GFP12*GMP, MVR^2*GMP	98.90
W6	0.3	FVR*GMP, FVR*GFP12	96.91
W7	0.4	FVR*GMP, FVR*GFP12	92.37
W8	0.5	FVR*GMP, FVR*GFP12	95.08
W9	0.6	FVR*GMP, FVR^2*GFP12	97.42
W10	0.7	FVR^4*GMP, FVR*GFP12*GMP, MVR^2*GMP	96.85
CON1	VARIES	FVR^2*VVR, VVR*MVR, FVR*GMP, $THETA^4$*FVR*GMP	99.09
CON2	VARIES	FVR^2*GMP, VVR*GMP, GFP12*GMP	99.54

TABLE XVIII- LONG. THERMAL EXPANSION (CTE11)

INPUT	FVR	INTERACTION MODEL TERMS ACCEPTED	R^2
N1	0.3	$THETA^2*MVR, MVR^2, FVR*EFP1*MVR, EMP^2*EFP1$	92.51
N2	0.4	$THETA^2*MVR, THETA^4, EFP1^4, EMP^2*FVR, MVR^2*EFP1$	96.38
N3	0.5	$THETA^2*MVR, MVR, EMP^2*MVR, EMP^2*EFP1$	97.26
N4	0.6	$FVR*EFP1, THETA*FVR*EFP1, EMP^2*MVR$	96.32
N5	0.7	$THETA, EMP*MVR$	90.66
W1	0.3	*** NEARLY SINGULAR	
W2	0.4	$THETA^4, MVR^2*EMP$	80.81
W3	0.5	$THETA^4, EMP^2*MVR,$	87.98
W4	0.6	$THETA^4, MVR^2*VVR$	75.20
W5	0.7	$THETA^4, FVR^2*MVR$	82.97
N6	0.3	$MVR^2*EMP, EFP1^2*EMP, FVR^4$	99.29
N7	0.4	$MVR^2*EMP, FVR*EFP1*MVR, MVR^2*VVR$	99.17
N8	0.5	$MVR^2*EMP, EFP1, FVR^4$	98.94
N9	0.6	$MVR^2*EMP, EFP1^2*MVR$	98.94
N10	0.7	$MVR^2*EMP, EFP1*MVR.$	99.33
W6	0.3	$MVR^2*EMP, FVR*EFP1*MVR$	98.35
W7	0.4	$MVR^2*EMP, FVR*EFP1*MVR$	98.55
W8	0.5	$MVR^2*EMP, EFP1^2*MVR$	98.56
W9	0.6	$MVR^2*EMP, EFP1^2*MVR$	99.00
W10	0.7	MVR^2*EFP1, EMP^2*MVR	98.20
CON1	VARIES	$THETA, MVR^3, EFP1^2*VVR, FVR*VVR*EFP1$	96.82
CON2	VARIES	$MVR^2*EMP, FVR*EFP1*MVR, FVR^4, FVR^2*VVR...$	99.84

TABLE XIX- TRANS. THERMAL EXPANSION (CTE22)

INPUT	FVR	INTERACTION MODEL TERMS ACCEPTED	R^2
N1	0.3	$THETA^2*MVR$, VVR	99.60
N2	0.4	$THETA^2*MVR$, MVR^2*FVR, FVR*EFP1*EMP	99.38
N3	0.5	$THETA^2*MVR$, MVR^2*FVR, FVR^4	99.48
N4	0.6	$THETA^2*MVR$, MVR^2*FVR, EMP^2*VVR, MVR^2*VVR	99.73
N5	0.7	FVR^2, THETA, $THETA^2*FVR$	99.81
W1	0.3	$THETA^2*MVR$, MVR, $EFP1^2*VVR$	95.16
W2	0.4	$THETA^2*MVR$, MVR, FVR*EFP1*MVR	98.71
W3	0.5	$THETA^2*MVR$, MVR^2*FVR, $EFP1^2*VVR$	95.91
W4	0.6	$THETA^2*MVR$, THETA, $THETA^4$	95.69
W5	0.7	*** NEARLY SINGULAR	
N6	0.3	FVR, MVR^3	99.70
N7	0.4	FVR, MVR^4	99.59
N8	0.5	FVR, MVR^2	99.67
N9	0.6	FVR, EMP^2*EFP1	99.70
N10	0.7	FVR, MVR^4	99.82
W6	0.3	FVR, FVR*EFP1*EMP	99.26
W7	0.4	FVR, MVR^4	98.97
W8	0.5	FVR	98.88
W9	0.6	FVR, MVR^4	99.57
W10	0.7	FVR, EMP^2*FVR	99.29
CON1	VARIES	$THETA^2*MVR$	99.32
CON2	VARIES	FVR, FVR^3, MVR^2*EMP	99.95

TABLE XX- POISSON RATIO; MAJOR (NUC12)

INPUT	FVR	INTERACTION MODEL TERMS ACCEPTED	R^2
N1	0.3	*** NEARLY SINGULAR	
N2	0.4	THETA,EFP2*MVR	97.96
N3	0.5	THETA,GFP112*MVR	96.71
N4	0.6	THETA,EFP1*MVR	98.17
N5	0.7	THETA,FVR*EFP2	96.48
W1	0.3	*** NEARLY SINGULAR	
W2	0.4	THETA,THETA^4*FVR*GFP12	84.73
W3	0.5	THETA	89.43
W4	0.6	THETA,VVR*GFP12	84.27
W5	0.7	THETA,FVR*MVR	92.10
N6	0.3	FVR	97.83
N7	0.4	FVR	98.48
N8	0.5	FVR	97.77
N9	0.6	FVR,FVR*MVR	98.52
N10	0.7	FVR	99.17
W6	0.3	FVR	97.32
W7	0.4	FVR,VVR*EFP2	96.50
W8	0.5	FVR	96.38
W9	0.6	FVR,EFP1*EFP2,GFP12*MVR	98.41
W10	0.7	FVR,FVR*EFP2	96.97
CON1	VARIES	*** SINGULAR	
CON2	VARIES	MVR,FVR*MVR,EFP1*MVR	99.77

TABLE XXI- POISSON RATIO; MINOR (NUC21)

INTERACTION MODEL

INPUT	FVR	TERMS ACCEPTED	R^2
N1	0.3	THETA,THETA^4*FVR*EFP1	91.69
N2	0.4	THETA,FVR*EFP1	94.66
N3	0.5	THETA,FVR*EFP1,EFP2*GFP12	95.10
N4	0.6	THETA,THETA^4*FVR*EFP1,EFP2	97.15
N5	0.7	THETA,THETA^4*FVR*EFP1	95.82
W1	0.3	THETA,FVR*GFP12	91.16
W2	0.4	THETA,EFP2*MVR	89.52
W3	0.5	THETA,FVR*EFP1	92.06
W4	0.6	THETA	92.53
W5	0.7	THETA,FVR*EFP1,THETA^4*FVR*MVR,EFP2*MVR	95.60
N6	0.3	FVR*EFP1,FVR*EFP2	95.48
N7	0.4	FVR*EFP1,FVR*EFP2	94.69
N8	0.5	FVR*EFP1,FVR*EFP2,FVR*GFP12	95.52
N9	0.6	FVR*EFP1,FVR*EFP2	92.85
N10	0.7	FVR*EFP1,FVR*EFP2	91.77
W6	0.3	FVR*EFP1,GFP12*MVR	87.83
W7	0.4	FVR*EFP1,FVR*EFP2,FVR*MVR	86.48
W8	0.5	FVR*EFP1,EFP2	84.36
W9	0.6	FVR*EFP1,FVR*EFP2	89.84
W10	0.7	FVR*EFP1,FVR*EFP2	91.55
CON1	VARIES	THETA,FRV*GFP12,EFP2,THETA^4*FVR*MVR,...	98.70
CON2	VARIES	FVR*EFP1,FVR*MVR,EFP2,VVR*GFP12	98.35

TABLE XXII- LONGITUDINAL TENSILE STRENGTH (SCXXT)

INTERACTION MODEL

INPUT	FVR	TERMS ACCEPTED	R^2
N1	0.3	$THETA^4$*FVR*SFPT	17.72
N2	0.4	$THETA^4$*FVR*SFPT, MVR^4	47.65
N3	0.5	$THETA^4$*FVR*SFPT	27.65
N4	0.6	$THETA^4$*FVR*SFPT, FVR^2*EMP	44.67
N5	0.7	$THETA^4$*FVR*SFPT	45.35
W1	0.3	FVR*SFPT, FVR*EFP1*MVR	39.18
W2	0.4	FVR*SFPT, FVR^2*MVR	42.87
W3	0.5	EFP1*SFPT, EMP*MVR	33.97
W4	0.6	EMP^2*MVR, $THETA^2$*SFPT*MVR	45.09
W5	0.7	$THETA^2$*FVR*SFPT	32.56
N6	0.3	FVR*SFPT, FVR^2*EMP	52.95
N7	0.4	FVR*SFPT, FVR*EFP1	64.41
N8	0.5	FVR*SFPT, MVR^2*FVR	39.12
N9	0.6	FVR*SFPT	47.13
N10	0.7	FVR*SFPT, FVR*EMP	27.43
W6	0.3	FVR*SFPT, MVR^2*EFP1	49.71
W7	0.4	FVR*SFPT	25.19
W8	0.5	FVR*SFPT	32.16
W9	0.6	FVR*SFPT	34.06
W10	0.7	FVR*SFPT	35.09
CON1	VARIES	$THETA^4$*FVR*SFPT, FVR*VVR*MVR, FVR*EFP1*MVR	81.20
CON2	VARIES	FVR*SFPT, FVR*VVR, MVR^2*SFPT	84.79

TABLE XXIII- LONGITUDINAL COMPRESSIVE STRENGTH (SCXXC)

INPUT	FVR	INTERACTION MODEL TERMS ACCEPTED	R^2
N1	0.3	SFPC*SMPC	12.53
N2	0.4	FVR*MVR	19.45
N3	0.5	NONE	
N4	0.6	SFPC*GMP	9.81
N5	0.7	FVR*GFP12	10.20
W1	0.3	VVR^4	10.40
W2	0.4	$THETA^4$	9.32
W3	0.5	EMP*SMPC, $THETA^2$*EMP	23.32
W4	0.6	$THETA^4$	9.20
W5	0.7	NONE	
N6	0.3	SFPC, GFP12*SMPC	20.04
N7	0.4	NONE	
N8	0.5	NONE	
N9	0.6	NONE	
N10	0.7	GFP12*EMP	14.96
W6	0.3	FVR*MVR	11.91
W7	0.4	VVR	10.76
W8	0.5	VVR	9.85
W9	0.6	$GFP12^4$	9.10
W10	0.7	NONE	
CON1	VARIES	FVR*VVR	46.48
CON2	VARIES	FVR*VVR, SFPC	44.44

TABLE XXIV- TRANSVERSE TENSILE STRENGTH (SCYYT)

INTERACTION MODEL

INPUT	FVR	TERMS ACCEPTED	R^2
N1	0.3	MVR^2*SMPT	31.60
N2	0.4	MVR^2*SMPT	37.23
N3	0.5	EMP*SMPT	9.61
N4	0.6	FVR^2*MVR	47.59
N5	0.7	NONE	
W1	0.3	FVR^2*VVR,SMPT	25.39
W2	0.4	SMPT*MVR	43.94
W3	0.5	MVR^2*FVR	16.32
W4	0.6	FVR*VVR*EFP2,EMP	24.10
W5	0.7	FVR*SMPT	30.29
N6	0.3	FVR*MVR	10.47
N7	0.4	MVR^2*FVR	8.94
N8	0.5	FVR*EFP2*SMPT	13.54
N9	0.6	$SMPT^2$*MVR	9.40
N10	0.7	FVR*EMP	9.13
W6	0.3	MFR^2*EMP	35.13
W7	0.4	MVR^2*VVR	19.34
W8	0.5	$SMPT^2$*MVR	12.89
W9	0.6	FVR^2*EFP2	29.27
W10	0.7	MVR^2*SMPT	36.77
CON1	VARIES	$THETA^{\dagger}$*SMPT*MVR,FVR*EFP2*MVR,*$SMPT^2$*MVR	73.42
CON2	VARIES	$SMPT^2$*MVR,FVR*VVR*MVR	76.40

TABLE XXV- TRANSVERSE COMPRESSIVE STRENGTH (SCYYC)

INPUT	FVR	INTERACTION MODEL TERMS ACCEPTED	R^2
N1	0.3	SMPC*MVR	33.39
N2	0.4	FVR^2*EMP	32.99
N3	0.5	NONE	
N4	0.6	FVR^2*MVR	42.31
N5	0.7	NONE	
W1	0.3	FVR^2*VVR	26.24
W2	0.4	FVR^2*EMP	43.86
W3	0.5	$SMPC^2$*MVR	21.13
W4	0.6	FVR*VVR*EFP2,EMP	25.75
W5	0.7	SMPC*MVR	18.63
N6	0.3	$SMPC^2$*MVR	11.57
N7	0.4	EFP2*MVR	9.03
N8	0.5	FVR*EFP2	9.87
N9	0.6	NONE	
N10	0.7	$SMPC^2$*MVR,FVR^2*MVR	19.07
W6	0.3	MVR^2*EMP	32.50
W7	0.4	EFP2*MVR	14.58
W8	0.5	NONE	
W9	0.6	MVR^2*SMPC	32.85
W10	0.7	MVR^4	35.79
CON1	VARIES	$THETA^4$*SMPC*MVR,FVR^4	76.43
CON2	VARIES	MVR^4,FVR^2*MVR,MVR^2*SMPC	75.59

TABLE XXVI- IN PLANE SHEAR STENGTH (SCXYS)

INTERACTION MODEL

INPUT	FVR	TERMS ACCEPTED	R^2
N1	0.3	FVR*GFP12*GMP, THETA^4	27.64
N2	0.4	FVR*GFP12*EMP	13.51
N3	0.5	THETA	14.97
N4	0.6	THETA^4*GFP12, SMPS*MVR	30.84
N5	0.7	NONE	
W1	0.3	THETA, FVR*VVR*EMP, THETA^4*SMPS, FVR*MVR	52.20
W2	0.4	THETA^4*FVR, THETA^4*GFP12	26.58
W3	0.5	THETA^4	12.89
W4	0.6	THETA, FVR*VVR	22.33
W5	0.7	THETA^4*FVR	10.72
N6	0.3	NONE	
N7	0.4	SMPS*MVR	11.24
N8	0.5	NONE	
N9	0.6	SMPS, SMPS^4	16.14
N10	0.7	FVR^2*MVR	11.40
W6	0.3	SMPS*MVR, GMP^4	28.58
W7	0.4	FVR*GFP12*MVR	8.28
W8	0.5	NONE	
W9	0.6	FVR*GFP12*MVR	19.20
W10	0.7	SMPS	17.73
CON1	VARIES	THETA^4*FVR, FVR^2*SMPS	36.74
CON2	VARIES	FVR*VVR, MVR^4, FVR^2*VVR	61.46

CHAPTER IV

DISCUSSION

A. Overview

The numerical simulations conducted show that certain assumptions about the statistical distribution of local nonuniformities in fiber composites lead directly to quantifiable variations in material properties. The advantages inherent in the stochastic characterization are numerous. The development of quality control and reliabilty measures for composites is crucial to their acceptance in aircraft designs. The reduction in needed experimental data achievable through judicious simulation of the wide variety of available composite material systems could significantly lower the costs of material selection and acceptance testing. In the results of this study, the confidence intervals calculated can be interpreted as the product of an experimental program, specifically designed as an analog of the physical processes which occur in real materials.

B. Histograms and Distributions

Data cases 1, 2, and 3 demonstrate the differences between a deterministic base case and random cases with narrow and wide dispersion of input data about the base case.

In Fig. 30, it is apparent that the deterministic case 1 value of 15750 ksi. for longitudinal modulus falls near the mean of the case 2 data. However, the case 3 sample appears to have a mean slightly lower (approximately 15000 ksi.). It should be noted that the size of the interval over which the sample occurs is noticeably larger in the widely distributed case 3 run.

Transverse modulus, (Fig. 31) demonstrates a higher mean value for the wide distribution than for the narrow, which is greater than the deterministic value of 1065 ksi. reported in Table II. The increased transverse modulus is related to the added stiffness available in fibers with high misalignment relative to longitudinal direction.

Shear modulus, (Fig. 32) is measurably changed by nonuniformities. The deterministic value of 516 ksi is exceeded by the case 2 value of approximately 620 ksi, which is further exceeded by the case 3 value near 900 ksi. Fiber misaligment has a significant effect in shear modulus variation.

Poisson's ratios (Fig. 33, 34) show similar trends in location of sample means and relative dispersion of the sample for the data studied. Poisson's ratios generally increase with fiber misaligment and volume fraction changes.

The coefficients of thermal expansion (Figs. 35, 36) for the sample studied reflect the longitudinal contraction of graphite fibers when heated. The longitudinal coefficient of thermal expansion for AS-graphite fiber is -0.550×10^{-6}/ F, while the transverse coefficient is 0.560×10^{-5}/ F. The offset orientation of crystal lattice planes in graphite fibers can explain this behavior. These values, the fiber misalignment, and fiber volume ratio near 0.5 all contribute to the occurrence of a negative longitudinal coefficient of thermal expansion for the composite. At higher fiber volume ratios, the values calculated would be less than in the present case, because of the contolling fiber behavior for high fiber volume ratio.

The longitudinal strengths (Fig. 38, 39) are significantly reduced when nonuniformities are present. The deterministic case 1 value of 203 ksi. for tensile strength is compared to a mean near 160 ksi for case 2 and a mean near 130 for case 3. In compression, the deterministic value of 165 ksi. compares to means near 100 ksi. and 80 ksi. for the narrow and wide distributions, respectively. The failure mode in compression varies in the random samples.

Transverse strengths (Fig. 40, 41) show sensitivity to the variations assumed. Misalignments, volume fraction nonuniformities, and constituent strength variations all contibute to reduction in the strength values. Sub-ply shear failures occur, which undermine the already low transverse composite strengths.

In plane shear strength (Fig. 42) values decline from 10.01 ksi. for case 1 to a mean near 8.0 ksi. for case 2. However, case 3 shows a

value of a mean near 8.0 also. It appears that the added shear strength due to fiber misalignment is balanced by the reduced strength due to variable fiber volume fraction.

C. Confidence Curves

The effects of various shape parameters of fiber strength are shown in Figs. 43 and 44. The higher weibull distribution shape parameter of 20 produces a narrow distribution of fiber strength values. The composite that has few weaker fibers is expected to be stronger, and Fig. 43 demonstrates this for lonitudinal tensile strength. However, compressive failure (Fig. 44) is a more complex phenomenon. In the region of low fiber volume ratio, the 'rule of mixtures' failure criteria for a subply can control the failure mode. At higher fiber volume ratio, however, compressive failure can be initiated by delamination, or by a shear failure in a sub-ply. The mixture of failure modes in compressive failure is not well understood, but can explain the seeming inconsistency of the intersection of the curves in Fig. 44. At a fiber volume of 0.7, the weakest fibers (α = 10) are in the strongest composite, when strength is normalized with respect to fiber compressive strength.

The effects of various shape parameters for matrix strengths are studied in Figs. 45, 46, and 47. Transverse tensile and compressive strengths show expected reductions for lower matrix strengths. In-plane shear strength shows lower dispersion at a large fiber volume of 0.7, and also declines in general for higher fiber volume.

The fiber misalignment effects are studied in Figs. 48-57. Longitudinal modulus (Fig. 48) shows narrow intervals and slight reductions for greater misalignment. Transverse modulus (Fig. 49) and in plane shear modulus (Fig. 50) are enhanced by fiber misalignment. Longitudinal tensile and compressive strengths are degraded by misalignment (Figs. 51, 52). Transverse tensile and compressive strengths are enhanced (Figs. 53, 54). In-plane shear strength shows total separation of confidence intervals between curves with different degrees of misalignment. Poisson's ratios (Figs. 56, 57) increase for high fiber misalignment values.

The fiber stiffness effects (Figs. 58-67) are very small for the distribution parameters studied.

D. Examination of Regression Models

The regression models for thermoelastic properties demonstrate resonably high predictive capability in the simple models assumed. Marginal improvements are achieved in expanding the models to include higher order interaction terms. Further improvement is gained by using sample data from the wide range of volume percent values. The higher multiple correlation coefficients of these models may be due to the additional information available in the sample size of 100 that was used. The nearly singular predictor matrices which occur in the higher order models indicate that terms must by selectively removed to eliminate linearity between assumed predictor terms. The regression results support the use of the simple models for thermoelastic

properties, because improvements in predictive capability in the higher order models for the same data are small.

Strengths are not modeled well by the simple or the interaction models. The predictors chosen are average properties, whereas the strengths are based on the weakest points in the material. Even the unidirectional cases (N6-N10, W6-W10) present data that the interaction models have considerable difficulty in accomodating. Somewhat greater predictive value is gained by using the expanded data for strength model prediction. Using fourth order algebraic functions, values of the multiple correlation coefficient square approach 85% for longitudinal tensile strength. The other strengths generally have poorer results.

CHAPTER V

CONCLUSIONS

A tractable, constituent based, probabilistic analysis procedure for fiber composites has been developed using the ICAN program as a basis. Within the limitations of the mechanics of material model, properties and strengths of a variety of composite material configurations can be simulated.

This study quantifies the thermoelastic and strength properties of a graphite/epoxy ply subject to assumed uncertainties for fiber misalignment, constituent volume fractions, and constituent properties. The results show several advantages of probabilistic characterization of this material. These include the identification of unforseen variations in composite material properties, and the mechanical effects of local nonuniformities. The relative importance of the various fabrication and material variables on composite properties is identified, and the resulting behavior quantified.

The advantages of a probabilistic formulation of composite material

properties over a deterministic one are numerous. Comparison of the results of this study with test data could reveal some sources of previously unaccounted scatter in the data. Expected value ranges could be predicted for experimental results. Since the simulations provide data that is analagous to experimental data at lower cost, laboratory classification, material selection, and acceptance testing of composites can be guided by the information made available by these methods.

Although the method presented provides results for only the basic ply, extension of the simulation to include lamination angle variations in a general layup is feasible. Since finite element material property cards are generated, structural analysis of components with randomly varied properties defined at a number of points in the body can supply a more realistic description of the random nature of structural response due to material inhomogeneity.

The stochastic formulation of material properties is generally recognized as one requirement of failure theories for materials. Although the failure criteria in the models used in this study are conservative, progressive failure of fiber composites could be modeled by incorporating load redistribution and material property recalculation in the vicinity of failed material.

REFERENCES

1. Harter, H. Leon: A Survey on the Literature on the Size Effect on Material Strength. AFFDL-TR-77-11, Wright Patterson AFB, April, 1977.
2. Griffith, A. A.: The Phenomena of Rupture and Flow in Solids. Philosophical Transactions of the Royal Society of London A, Vol. 221, pp. 163-198.
3. Murthy, P. L. N. and Chamis, C. C.: Integrated Composites Analyzer (ICAN) User's and Programmer's Maunual. NASA TP 2515, March 1986.
4. Flaggs, D. L.: ADVLAM- An Advanced Composite Laminate Analysis Code. Lockheed Missles and Space Company, Inc., 1983.
5. Chamis, C. C. and Sinclair, J. H.: Micromechanics of Intraply Hybrid Composites: Elastic and Thermal Properties. NASA TM 79253.
6. Kural, M. H. and Min, B. K.: The Effects of Matrix Plasticity on the Thermal Deformation of Continuous Fiber Graphite/Metal Composites. J. Comp. Mater., v.18, Nov. 1984, pp.519-535.
7. Bolotin, V. V.: Statistical Methods in Structural Mechanics (trans. S. Aroni). San Francisco, Holden Day, Inc. 1969
8. Sobol, I. M.(USSR Academy of Sciences): The Monte Carlo Method. Chicago, The University of Chicago, 1974.
9. Nance, R. E. and Overstreet, C.: A Bibliography of Random Number Generation. Computing Reviews, Oct. 1972, pp. 495-508.
10. Lehmer, D. H.: Mathematical Methods in Large-Scale Computing Units, Proceedings of the 2nd Symposium on Large-Scale Digital Computing Machinery, Cambridge, Harvard University Press, 1951 pp. 141-146.
11. Hammersly, J. M. and Handscomb, D. C.: Monte Carlo Methods. London, Menthuen & Co. Ltd., 1964, pp. 28-31.
12. Oh, Kong P.: A Monte Carlo Study of the Strength of Unidirectional Fiber-Reinforced Composite Materials. Journal of Composite Materials, Vol. 13, p. 311.
13. Box, G. E. P., and Mueller, M. E.: A Note on the Generation of Random Normal Deviates. Annals of Mathematical Statistics, Vol. 29(2), 1958, pp. 610-611.

14. Howell, L. W. and Rheinfurth, M. H.: Generation of Pseudo-Random Numbers. NASA TP 2105, 1982, pp. 7-8.
15. Weibull, W.: Statistical Theory of Strength of Materials. (In English) Ingenoirs Vetenskaps Akademien Handlinger, Vol. 151, p. 45.
16. Chamis, C. C.: Simplified Composite Micromechanics Equations for Strength, Fracture Toughness, Impact Resistance, and Environmental Effects. NASA TM 83696, 1984.
17. Ryan, Thomas A., Jr.: MINITAB. The Pennsylvania State University Computation Center, Jan 15, 1981.
18. Draper, N.R. and Smith, H.: Applied Regression Analysis. New York, John Wiley & Sons, Inc., 1981.
19. Ginty, C. A.: unpublished data.

APPENDIX A

```
C ##################################################################
C ##################################################################
C      PROBABILISTIC INTEGRATED COMPOSITES ANALYZER ( P I C A N )
C      ---------------------------------------------------------
C A COMPUTER CODE FOR ANALYSIS OF PROBABILISTIC VARIATIONS IN
C COMPOSITE PROPERTIES USING THE INTEGRATED COMPOSITES ANALYZER
C (ICAN).  THE ANALYSIS SAMPLES FROM INPUT DISTRIBUTIONS TO OBTAIN
C COMPOSITE PROPERTIES AND GEOMETRY, WHICH ARE THEN INPUT TO ICAN,
C AS MANY TIMES AS THE USER REQUESTS.
C FINAL OUTPUT INCLUDES OUTPUT DATASETS OF ICAN WHICH ARE NAMED
C "ICANOUT", AND CAN BE REPEATEDLY USED BY ANALYSIS ROUTINE.
C ##################################################################
C ##################################################################
C
C
C---  THIS IS A MASTER PROGRAM FOR "ICAN" WHICH ALLOCATES      ---
C---  DYNAMICALLY SUFFICIENT STORAGE FOR THE ARRAY VARIABLES   ---
C---  IN "ICAN" AND "PICAN" CODES.
C
      COMMON A(9000)
      COMMON /PSIZE/ MAXLEN,M(100)
      MAXLEN = 9000
      CALL SPIMIT
      STOP
      END
```

```
      SUBROUTINE SPINIT
C READ INPUT DATASET TO DETERMINE IF PROBABILISTIC ANALYSIS IS DESIRED
      COMMON A(1)
      COMMON /ILAB14/ INHYDI,OUTF,INF,INPF,INDS,IDBK
      DIMENSION L(8)
      LOGICAL BSTAT,ANGLEV,VORATV,FIRATV
      CHARACTER*4 CDUM
      INTEGER PIN,RUNS,RUNNO,OUTF
      DATA PIN/5I/
      READ (PIN,1003) CDUM
      READ (PIN,1002) NL,NUMS,BSTAT
      IF (.NOT. BSTAT) GO TO 500
C
      READ (PIN,1001) RUNS
C SET UP POINTERS FOR MASTER ARRAY
      L(1) = 1
      L(2) = L(1) + NUMS
      L(3) = L(2) + NUMS
      L(4) = L(3) + NUMS
      L(5) = L(4) + NUMS
      L(6) = L(5) + NUMS
      L(7) = L(6) + NL
      L(8) = L(7) + NL
      L1 = L(1)
      L2 = L(2)
      L3 = L(3)
      L4 = L(4)
      L5 = L(5)
      L6 = L(6)
      L7 = L(7)
      L8 = L(8)
C  LOOP 'RUNS' TIMES THROUGH DATA CREATION AND ICAN ROUTINE
      DO 100 RUNNO = 1,RUNS
         CALL UPDAT(A,A(L2),A(L3),A(L4),A(L5),A(L6),A(L7),A(L8),NL,NUMS)
         REWIND IDBK
         CALL ICANMN
         ENDFILE OUTF
  100 CONTINUE
      REWIND OUTF
      GO TO 6000
  500 CONTINUE
      CALL COPY
      CALL ICANMN
 1001 FORMAT (6X,I6)
 1002 FORMAT (8X,I8,8X,I8,2X,L6)
 1003 FORMAT(A4)
 6000 CONTINUE
      RETURN
      END
```

```
      SUBROUTINE UPDAT(VFS,VSC,VVS,VFP,VVP,THETA,THMU,THSIG,NL,NUMS)
C ***************************************************************
C  ROUTINE UPDAT READS INPUT AND GENERATES STATISTICALLY VARYING INPUT *
C  FILE TO ICAM USING VARIOUS RANDOM NUMBER GENERATION SCHEMES         *
C ***************************************************************
      DIMENSION DECK(20),PL(75,1),CODES(2,2,1),VFS(1),VSC(1),VVS(1),
     1THETA(1),NBS(33,1),DBS(4,1),MBS(3,1),VFP(1),VVP(1),IDENT(5)
      LOGICAL CSAMB,COMSAT,BIDE,RINDV,NONUDF,ANGLEV,VORATV,FIRATV,CONV
      INTEGER NL,NLC,NMS,INT,IR,INPF
      INTEGER PIN,ISEEDF,ISEED
      CHARACTER*8 PLY,IDENT
      COMMON /SEED/ ISEED
      COMMON /COMST/ CONV
      DATA PIN,INPF,ISEEDF/51,5,55/
      REAL TU,TCU,NBS,MBS
      DATA PLY/'      PLY'/
C
C   READ IN UNIFORM RANDOM NUMBER GENERATOR SEED
      REWIND ISEEDF
      READ(ISEEDF,6) ISEED
C
      REWIND INPF
      REWIND PIN
      READ(PIN,7) (DECK(I),I=1,20)
      WRITE (INPF,7) (DECK(I),I=1,20)
C
      READ(PIN,9) IDENT(1),NL,NLC,NMS
      IF(NL.EQ.NMS) GO TO 30
      WRITE (INPF,24)
      STOP
C
   30 WRITE (INPF,10) IDENT(1),NL,NLC,NMS
C
      READ(PIN,12) COMSAT,ANGLEV,FIRATV,VORATV,CONV
      WRITE (INPF,11) COMSAT
      READ(PIN,13) CSAMB,THMU,THSIG,VFPMU,VFPSIG,VVPLAM,KVVP
      WRITE (INPF,11) CSAMB
      READ (PIN,11) BIDE
      WRITE (INPF,11) BIDE
      READ (PIN,11) RINDV
      WRITE(INPF,11) RINDV
      READ(PIN,11) NONUDF
      WRITE (INPF,11) NONUDF
C     READ LAYER DATA
      READ (PIN,14) IDENT(2),TU,TCU,PL(72,1),PL(7,1)
      IF (IDENT(2).EQ.PLY) GO TO 80
      WRITE (INPF,8)
      WRITE (INPF,2) IDENT(2)
      STOP
C
   80 IF (ANGLEV) GO TO 84
         DO 82 IR = 1,NL
      THETA(IR) = THMU
   82 CONTINUE
```

```
      GO TO 101
   84 DO 100 IR = 1,NL
      CALL URAND(X1)
      CALL URAND(X2)
      CALL NORM(X1,X2,THMU,THSIG,Y)
      THETA(IR) = Y
  100 CONTINUE
  101 DO 105 IR = 1,NL
       WRITE(INPF,15) IDENT(2),IR,IR,TU,TCU,PL(72,1),THETA(IR),PL(7,1)
  105 CONTINUE
C
C   READ MATERIAL DATA
      READ(PIN,16) IDENT(4),(CODES(1,J,1),J=1,2),
     1(CODES(2,J,1),J=1,2),VSC(1),VFS(1),VVS(1)
C
         IF (FIRATV) GO TO 114
       DO 110 IR = 1,NMS
         VFP(IR) = VFPMU
  110 CONTINUE
      GO TO 128
  114 DO 125 IR = 1,NMS
  115 CALL URAND(X1)
      CALL URAND(X2)
      CALL NORM(X1,X2,VFPMU,VFPSIG,Y)
         IF (Y .GT. 0.78) GO TO 115
         IF (Y .LT. 0.30) GO TO 115
        VFP(IR) = Y
  125 CONTINUE
C
  128 IF (VORATV) GO TO 140
         DO 130 IR = 1,NMS
         VVP(IR) = VVPLAM
  130 CONTINUE
      GO TO 200
C
  140 DO 190 IR = 1,NMS
      CALL GAM(VVPLAM,KVVP,VVP(IR))
      VVP(IR) = VVP(IR)/100.
  190 CONTINUE
C
  200 DO 203 IR = 1,NMS
      WRITE (INPF,17) IDENT(4),(CODES(1,J,1),J=1,2),VFP(IR),VVP(IR),
     1(CODES(2,J,1),J=1,2),VSC(1),VFS(1),VVS(1)
  203 CONTINUE
C
C   READ LOADING CONDITIONS
C
       DO 300 IR = 1,NLC
         READ (PIN,18) IDENT(3),MBS(1,IR),MBS(2,IR),MBS(3,IR),THCS
         WRITE(INPF,19) IDENT(3),MBS(1,IR),MBS(2,IR),MBS(3,IR),THCS
         READ (PIN,18) IDENT(3),MBS(1,IR),MBS(2,IR),MBS(3,IR)
         WRITE (INPF,19) IDENT(3),MBS(1,IR),MBS(2,IR),MBS(3,IR)
         READ(PIN,18) IDENT(3),(DBS(I,IR),I=1,4)
         WRITE (INPF,19) IDENT(3),(DBS(I,IR),I=1,4)
```

```
  300 CONTINUE
C
C  READ OUTPUT OPTIONS
C
      READ(PIN,20) IDENT(5),IOUT
      WRITE (INPF,21) IDENT(5),IOUT

C
C     INCREMENT AND REFILE SEED FOR FUTURE RUNS
      ISEED = ISEED + 100
      REWIND ISEEDF
      WRITE (ISEEDF,6) ISEED

C
    2 FORMAT (1X,10HIDENT(2) =,A8)
    6 FORMAT (I6)
    7 FORMAT (20A4)
    8 FORMAT (' THERE IS A MIX UP IN THE LAYER PROPERTIES CARD')
    9 FORMAT (A8,3I8)
   10 FORMAT (A8,3I8)
   11 FORMAT (L6)
   12 FORMAT (L6,6X,4L6)
   13 FORMAT (L6,6X,2(2X,F5.1),2(2X,F5.3),2X,F5.2,2X,I4)
   14 FORMAT (A8,16X,3F8.3,8X,F8.3)
   15 FORMAT (A8,2I8,5F8.3)
   16 FORMAT (A8,2A4,16X,2A4,3F8.2)
   17 FORMAT (A8,2A4,2F8.2,2A4,3F8.2)
   18 FORMAT (A8,7F8.4)
   19 FORMAT (A8,7F8.4)
   20 FORMAT (A8,I8)
   21 FORMAT (A8,I8)
   22 FORMAT (I5)
   23 FORMAT (4E10.3)
   24 FORMAT (' INPUT ERROR...  MMS MUST BE SET EQUAL TO NL.')
      RETURN
      END
```

```
      SUBROUTINE URAND(Z)
C ##################################################################
C       SUBROUTINE FOR GENERATING RANDOM NUMBERS HAVING A UNIFORM
C       DISTRIBUTION. BY THE MIXED MULTIPLICATIVE CONGRUENTIAL METHOD.
C ##################################################################
      DATA I/1/
      INTEGER A, X
      COMMON /SEED/ ISEED
      IF (I .EQ. 0) GO TO 1
         I = 0
         M = 2**20
         FM = M
         X = ISEED
         A = 2**10 + 3
C
    1 X = MOD(A*X, M)
      FX = X
      Z = FX/FM
      RETURN
      END
```

```
      SUBROUTINE NORM(X1,X2,MU,SIGMA,Y)
C ##################################################################
C
C       SUBROUTINE FOR GENERATING RANDOM VARIABLE Y ACCORDING
C       TO THE NORMAL DISTRIBUTION N(MU,SIGMA), USING THE
C       UNIFORM RANDOM VARIABLES X1 AND X2.
C
C ##################################################################
      REAL PI,MU,SIGMA,X1,X2,Y
      PI = ATAN(1.)*4
      Y = (SIGMA*((-2*ALOG(X1))**0.5)*(COS(2*PI*X2)))+MU
      RETURN
      END
```

```
      SUBROUTINE GAM(RLAMDA,K,X)
C ##################################################################
C     SUBROUTINE FOR GENERATING GAMMA VARIATES WITH PARAMETERS
C           RLAMDA AND K.
C ##################################################################
      DIMENSION U(100)
      DIMENSION P(100)
      COMMON /SEED/ ISEED
      DO 50 I = 1,K
   50 CALL URAND(U(I))
      P(1) = U(1)
      DO 100 I = 2,K
  100      P(I) = U(I) * P(I-1)
      X = (-1.0/RLAMDA) * ALOG(P(K))
      RETURN
      END
```

```
      SUBROUTINE WEIB(X1,ALPHA,BETA,Y)
C ***********************************************************************
C     THIS ROUTINE GENERATES THE DESIRED WEIBULL DISTRIBUTED RANDOM
C     VARIABLES PRESCRIBED BY INPUT OF SHAPE AND SCALE PARAMETERS.
C ***********************************************************************
C       VARIABLE DISCRIPTIONS
C        ALPHA = SHAPE PARAMETER
C        BETA  = SCALE PARAMETER
C          X1  = UNIFORMLY DISTRIBUTED RANDOM VARIABLE ON (0,1)
C           Y  = WEIBULL DISTRIBUTED RANDOM VARIABLE
C
C       USE IS MADE OF THE WEIBULL DISTRIBUTION FUNCTION
C
C         F(X) = 1 - EXP( - (X/BETA) ** ALPHA)      FOR X .GE. ZERO
C
        OMX1 = 1 - X1
        Y = BETA * ( -ALOG(OMX1)) ** (1/ALPHA)
        RETURN
        END
```

```
      SUBROUTINE COPY
C ##################################################################
C   THIS ROUTINE SIMPLY COPIES THE INPUT DATA INTO THE FILE TO BE READ
C   BY ICAN.
C ##################################################################
      DIMENSION DECK(20),PL(79,20),IP(20),INP(20),CODES(2,2,20),VFS(8), -
     1VSC(8),VVS(8),THETA(15),MBS(33,1),DBS(4,1),MBS(3,1),VFP(8),VVP(8)
      DIMENSION IDENT(5)
      CHARACTER*8 IDENT,PLY
      LOGICAL CSAMB,COMSAT,BIDE,RINDV,NONUDF
      INTEGER NL,NLC,NMS,INT,IR
      INTEGER PIN,POUT
      DATA PIN/5I/,POUT/6/
      REAL TU,TCU,MBS,MBS
      DATA PLY/'     PLY'/
C
      READ(PIN,6) (DECK(I),I=1,20)
      WRITE (POUT,7) (DECK(I),I=1,20)
C
      READ(PIN,9) IDENT(1),NL,NLC,NMS
      WRITE (POUT,10) IDENT(1),NL,NLC,NMS
C
      READ(PIN,12) COMSAT
      WRITE (POUT,13) COMSAT
      READ(PIN,12) CSAMB
      WRITE (POUT,13) CSAMB
      READ (PIN,12) BIDE
      WRITE (POUT,13) BIDE
      READ (PIN,12) RINDV
      WRITE(POUT,13)RINDV
      READ(PIN,12) NONUDF
      WRITE (POUT,13) NONUDF
C
C     READ LAYER DATA
      IR=1
  100 READ (PIN,14) IDENT(2),INP(IR),IP(IR),TU,TCU,PL(72,IR),THETA(IR), -
     1PL(7,IR)
      IF (IDENT(2).NE.PLY) GO TO 105
      GO TO 106
  105 WRITE (POUT,8)
      WRITE (POUT,2) IDENT(2)
      STOP
  106 WRITE (POUT,15) IDENT(2),INP(IR),IP(IR),TU,TCU,PL(72,IR),
     1THETA(IR),PL(7,IR)
      IF (IR.EQ.NL) GO TO 109
      IR=IR+1
      GO TO 100
C
C     READ MATERIAL DATA
C
  109 IR=0
  110 IR=IR+1
      READ(PIN,16) IDENT(4),(CODES(1,J,IR),J=1,2),VFP(IR),VVP(IR),
     1(CODES(2,J,IR),J=1,2),VSC(IR),VFS(IR),VVS(IR)
```

```
      WRITE (POUT,17) IDENT(4),(CODES(1,J,IR),J=1,2),VFP(IR),VVP(IR),
     1(CODES(2,J,IR),J=1,2),VSC(IR),VFS(IR),VVS(IR)
      IF (IR.EQ.NMS) GO TO 120
      GO TO 110
C
C     READ LOADING CONDITIONS
C
  120 IR=0
  130 IR=IR+1
      READ (PIN,18) IDENT(3),MBS(1,IR),MBS(2,IR),MBS(3,IR),THCS
      WRITE(POUT,19) IDENT(3),MBS(1,IR),MBS(2,IR),MBS(3,IR),THCS
      READ (PIN,18) IDENT(3),MBS(1,IR),MBS(2,IR),MBS(3,IR)
      WRITE (POUT,19) IDENT(3),MBS(1,IR),MBS(2,IR),MBS(3,IR)
      READ(PIN,18) IDENT(3),(DBS(I,IR),I=1,4)
      WRITE (POUT,19) IDENT(3),(DBS(I,IR),I=1,4)
      IF (IR.EQ.NLC) GO TO 140
      GO TO 130
C
  140 CONTINUE
C
C     READ OUTPUT OPTIONS
C
      READ(PIN,19) IDENT(5),IOUT
      WRITE (POUT,20) IDENT(5),IOUT
    2 FORMAT (1X,10HIDENT(2) =,A8)
    6 FORMAT (20A4)
    7 FORMAT (20A4)
    8 FORMAT (' THERE IS A MIX UP IN THE LAYER PROPERTIES CARD')
    9 FORMAT (A8,5I8)
   10 FORMAT (A8,5I8)
   12 FORMAT (L6)
   13 FORMAT (L6)
   14 FORMAT (A8,2I8,5F8.3)
   15 FORMAT (A8,2I8,5F8.3)
   16 FORMAT (A8,2A4,2F8.2,2A4,3F8.2)
   17 FORMAT (A8,2A4,2F8.2,2A4,3F8.2)
   18 FORMAT (A8,7F8.4)
   19 FORMAT (A8,7F8.4)
   20 FORMAT (A8,I8)
   21 FORMAT (A8,I8)
   22 FORMAT (I5)
   23 FORMAT (4E10.3)
      RETURN
      END
```

```
      SUBROUTINE VARCON(PFP,PFS,PMP,PMS,CODES,NMS)
C ##################################################################
C  SUBROUTINE TO SUPPLY VARIATIONS IN CONSTITUENT PROPERTIES
C    AS DESIRED BY THE USER ON INPUT PROMPT BOOLEANS.
C ##################################################################
      INTEGER PIN
      DATA PIN/52/
      LOGICAL BOOL
      DIMENSION DUM1(19),PFP(21,1),PFS(21,1),PMP(16,1),PMS(16,1),
     1 CODES(2,2,1)
C VARY EACH PROPERTY WHICH CORRESPONDS TO A BOOLEAN WITH VALUE 'TRUE'
C
      DO 50 J = 1,NMS
C
C  GENERATE FIBER PROPERTIES
C
      READ(PIN,1001) BOOL,SMEAN,STDEV
      IF(.NOT. BOOL) GO TO 5
         CALL URAND(X1)
         CALL URAND(X2)
         CALL NORM(X1,X2,SMEAN,STDEV,EFP11)
         PFP(3,J) = EFP11
C
    5 READ(PIN,1001) BOOL,SMEAN,STDEV
      IF(.NOT. BOOL) GO TO 6
         CALL URAND(X1)
         CALL URAND(X2)
         CALL NORM(X1,X2,SMEAN,STDEV,EFP22)
         PFP(4,J) = EFP22
C
    6 READ(PIN,1001) BOOL,SMEAN,STDEV
      IF(.NOT.BOOL) GO TO 7
         CALL URAND(X1)
         CALL URAND(X2)
         CALL NORM(X1,X2,SMEAN,STDEV,GFP12)
         PFP(7,J) = GFP12
C
    7 READ(PIN,1001) BOOL,SMEAN,STDEV
      IF(.NOT.BOOL) GO TO 8
         CALL URAND(X1)
         CALL URAND(X2)
         CALL NORM(X1,X2,SMEAN,STDEV,GFP23)
         PFP(8,J) = GFP23
C
    8 READ(PIN,1001) BOOL,BETA,ALPHA
      IF(.NOT. BOOL) GO TO 9
         CALL URAND(X1)
         CALL WEIB(X1,ALPHA,BETA,SFPT)
         PFP(14,J) = SFPT
C
    9 READ(PIN,1001) BOOL,BETA,ALPHA
      IF(.NOT. BOOL ) GO TO 10
         CALL URAND(X1)
         CALL WEIB(X1,ALPHA,BETA,SFPC)
```

```
            PFP(15,J) = SFPC
C
   10 CONTINUE
C
C  GENERATE MATRIX PROPERTIES
C
   20 READ(PIN,1001) BOOL,SMEAN,STDEV
      IF(.NOT. BOOL) GO TO 21
         CALL URAND(X1)
         CALL URAND(X2)
         CALL NORM(X1,X2,SMEAN,STDEV,EMNP)
         PMP(3,J) = EMNP
C
   21 READ(PIN,1001) BOOL,BETA,ALPHA
      IF(.NOT. BOOL) GO TO 22
         CALL URAND(X1)
         CALL WEIB(X1,ALPHA,BETA,SMTP)
         PMP(9,J) = SMTP
C
   22 READ(PIN,1001) BOOL,BETA,ALPHA
      IF(.NOT. BOOL) GO TO 23
         CALL URAND(X1)
         CALL WEIB(X1,ALPHA,BETA,SMCP)
         PMP(10,J) = SMCP
C
   23 READ(PIN,1001) BOOL,BETA,ALPHA
      IF(.NOT. BOOL) GO TO 24
         CALL URAND(X1)
         CALL WEIB(X1,ALPHA,BETA,SMSP)
         PMP(11,J) = SMSP
C
   24 CONTINUE
C
      REWIND PIN
   50 CONTINUE
 1001 FORMAT(14X,L6,2E20.10)
      RETURN
      END
```

APPENDIX B

This appendix outlines the theories and equations in the ICAN program that are used in this project. In the first section on composite micromechanics, the elastic and thermal properties of a composite ply are defined with respect to its principal material axes. The next section, devoted to laminate theory, contains the transformations and summations of ply properties used to arrive at laminate properties. The last section contains a brief discussion of the failure criteria.

1. Composite micromechanics

The theory for calculation of the properties of a unidirectional fiber composite ply based on the properties, volume fractions, and orientation of its constituents is known as composite micromechanics. In this section, the subscripts f, m, v, and l represent fiber, matrix, void, and laminate, respectively. The symbolic notation and the equations used are summarized below:

Volume fractions:

$$k_f + k_m + k_v = 1$$

Longitudinal Modulus:

$$E_{l11} = k_f E_{f11} + k_m E_m$$

Transverse Modulus:

$$E_{l22} = E_{l33} = \frac{E_m}{1 - \sqrt{k_f}\,(1 - E_m/E_{f22})}$$

Shear Moduli:

$$G_{l12} = \frac{G_m}{1 - \sqrt{k_f}\,(1 - G_m/G_{f12})}$$

$$G_{l23} = \frac{G_m}{1 - \sqrt{k_f}\,(1 - G_m/G_{f23})}$$

Poisson's Ratios:

$$\nu_{l12} = \nu_{l13} = \nu_m + k_f(\nu_{f12} - \nu_m)$$

$$\nu_{l23} = k_f\,\nu_{f23} + k_m\left[2\nu_m - \frac{\nu_{l12}}{E_{l11}}E_{l22}\right]$$

Coefficients of thermal expansion

$$\alpha_{l11} = \frac{\alpha_{f11} + k_m[(\alpha_m E_m/E_{f11}) - \alpha_{f11}]}{1 + k_m(E_m/E_{f11} - 1)}$$

$$\alpha_{l22} = \alpha_m(1 - \sqrt{k_f}\,)\left[\frac{1 + k_f\nu_m E_{f11}}{E_{f11} + k_m(E_m - E_{f11})}\right] + \alpha_{f22}k_f$$

$$\alpha_{33} = \alpha_{l22}$$

2. Laminate Theory

This section describes the methods which are used to calculate the elastic properties of laminates from the properties, orientation, and distribution of individual laminae. The elastic properties are then used to predict the response of the laminate to external loads. The methods used to predict stresses in the laminae under application of external loads are also described. Failure loads can be predicted by using these methods; as described in a following section.

a. Generalized Hooke's Law

The stresses acting at a point in a solid can be represented by the stresses acting on the planes normal to the coordinate directions, or equivalently, on the surfaces of an infinitesimal cube as shown in Fig. B-1. The stresses (σ_{ij}) on each face are resolved into three components: one normal stress and two shearing stresses. The first subscript refers to the direction normal to the plane in which the stress acts and the second subscript to the direction in which the stress acts. The stress components shown on the faces of the cube are taken as positive and can be taken as the forces (per unit area) exerted by the material outside the cube upon the material inside. A stress component is positive if it acts in the positive direction on a positive face of the cube. Thus normal tensile stresses are positive, and normal compressive stresses are negative. Nine stress components must be used to define the state of stress at a point, namely σ_{11}, σ_{22}, σ_{33}, σ_{23}, σ_{31}, σ_{12}, σ_{32}, σ_{13}, and σ_{21}. There are nine corresponding strain

components, following the same subscript convention.

For bodies in which each strain component is a linear function of all six stress components, the generalized Hooke's Law can be expressed

$$\sigma_{ij} = E_{ijkl}\,\varepsilon_{kl}$$

where E_{ijkl} is a fourth order tensor of elastic constants. For nine stress components and nine strain components, there must be 81 elastic constants defining E_{ijkl}. Certain reductions in the number of independent constants for an anisotropic body are due to symmetry properties of the tensor E_{ijkl}. By considering moment equilibrium about the center of the cube, it can be shown that at any point $\sigma_{23} = \sigma_{32}$, $\sigma_{31} = \sigma_{13}$, and $\sigma_{12} = \sigma_{21}$. Thus, E_{ijkl} is symmetric with respect to the first two indices. Second, because the strains are symmetric (that is, $\varepsilon_{ij} = \varepsilon_{ji}$), E_{ijkl} must be symmetric with respect to the second two indices. This reduces the number of elastic constants to 36. Further reduction to the final 21 elastic constants for a general anisotropic material is accomplished by assuming the existence of a strain energy density function, such that

$$U = U(\varepsilon_{ij})$$

with the property

$$\frac{\partial U}{\partial \varepsilon_{ij}} = \sigma_{ij}$$

From the generalized Hooke's Law,

$$\frac{\partial U}{\partial \varepsilon_{ij}} = E_{ijkl}\varepsilon_{kl}$$

Partial differentiation with respect to ε_{kl} yields

$$\frac{\partial}{\partial \varepsilon_{kl}} \left[\frac{\partial U}{\partial \varepsilon_{ij}}\right] = E_{ijkl}$$

Since the order of partial differentiation is immaterial,

$$\frac{\partial}{\partial \varepsilon_{kl}} \left[\frac{\partial U}{\partial \varepsilon_{ij}}\right] = \frac{\partial}{\partial \varepsilon_{ij}} \left[\frac{\partial U}{\partial \varepsilon_{kl}}\right]$$

and the subscripts can be interchanged to yield

$$\frac{\partial}{\partial \varepsilon_{kl}} \left[\frac{\partial U}{\partial \varepsilon_{ij}}\right] = E_{klij}$$

so that

$$E_{ijkl} = E_{klij}$$

Thus the first pair of subscripts in E_{ijkl} can be interchanged with the second pair without any change in the values. The number of elastic constants is thus reduced to 21.

b. Lamina Constitutive Relation

Several simplifications to the generalized Hooke's Law can be made for the special case of a thin orthotropic material, which approximates a unidirectional fiber composite lamina. By considering the invariance of elastic properties under coordinate transformation for planes of symmetry, the tensor E_{ijkl} can be reduced to the following nine constants:

$$E_{ijkl} = \begin{bmatrix} E_{1111} & E_{1122} & E_{1133} & & & \\ E_{1122} & E_{2222} & E_{2233} & & & \\ E_{1133} & E_{2233} & E_{3333} & & & \\ & & & 0 & & \\ & & & & 0 & \\ & & & & & 0 \end{bmatrix}$$

It is now convenient to make the following notation changes:

$$\sigma_{11} = \sigma_1 \qquad e_{11} = \varepsilon_1$$

$$\sigma_{22} = \sigma_2 \qquad e_{22} = \varepsilon_2$$

$$\sigma_{33} = \sigma_3 \qquad e_{33} = \varepsilon_3$$

$$\sigma_{23} = \tau_{23} = \sigma_4 \qquad 2e_{23} = \gamma_{23} = \varepsilon_4$$

$$\sigma_{13} = \tau_{13} = \sigma_5 \qquad 2e_{13} = \gamma_{13} = \varepsilon_5$$

$$\sigma_{12} = \tau_{12} = \sigma_6 \qquad 2e_{12} = \gamma_{12} = \varepsilon_6$$

The generalized form of Hooke's Law can now be written

$$\sigma_i = \sum_{j=1}^{6} C_{ij}\varepsilon_j \quad \text{for} \quad i,j = 1,\ldots,6$$

The matrix C_{ij} is known as the stiffness matrix, and ε_j are the engineering strain components. In matrix form Hooke's Law is written

$$\begin{bmatrix} \sigma_1 \\ \sigma_2 \\ \sigma_3 \\ \tau_{23} \\ \tau_{31} \\ \tau_{12} \end{bmatrix} = \begin{bmatrix} C_{11} & C_{12} & C_{13} & 0 & 0 & 0 \\ C_{12} & C_{22} & C_{23} & 0 & 0 & 0 \\ C_{13} & C_{23} & C_{33} & 0 & 0 & 0 \\ 0 & 0 & 0 & C_{44} & 0 & 0 \\ 0 & 0 & 0 & 0 & C_{55} & 0 \\ 0 & 0 & 0 & 0 & 0 & C_{66} \end{bmatrix} \begin{bmatrix} \varepsilon_1 \\ \varepsilon_2 \\ \varepsilon_3 \\ \gamma_{23} \\ \gamma_{31} \\ \gamma_{12} \end{bmatrix}$$

where the coordinate axes coincide with the symmetry axis of the material. For laminae that are assumed sufficiently thin, the through the thickness stresses are zero. Thus $\sigma_3 = \sigma_4 = \sigma_5 = 0$, for plane stress. It is apparent that $\varepsilon_4 = \varepsilon_5 = 0$

The stress strain relations for a thin unidirectional lamina are written

$$\begin{bmatrix} \sigma_1 \\ \sigma_2 \\ \tau_{12} \end{bmatrix} = \begin{bmatrix} Q_{11} & Q_{12} & 0 \\ Q_{12} & Q_{22} & 0 \\ 0 & 0 & 2Q_{66} \end{bmatrix} \begin{bmatrix} \epsilon_1 \\ \epsilon_2 \\ \frac{1}{2}\gamma_{12} \end{bmatrix}$$

using the tensorial strain $\frac{1}{2}\gamma_{12}$ instead of the engineering strain γ_{12}. The Q terms are known as reduced stiffnesses, i.e.

$$Q_{11} = C_{11} = \frac{E_1}{1 - \nu_{12}\nu_{21}}$$

$$Q_{12} = C_{12} = \frac{\nu_{12}E_2}{1 - \nu_{12}\nu_{21}} = \frac{\nu_{21}E_1}{1 - \nu_{12}\nu_{21}}$$

$$Q_{22} = C_{22} = \frac{E_2}{1 - \nu_{12}\nu_{21}}$$

$$Q_{66} = \frac{1}{2}(C_{11} - C_{12}) = G_{12}$$

where E_1, E_2, ν_{12}, ν_{21}, and G_{12} are the ply elastic constants, measured with respect to the natural material system. It may be noted that only four of these constants are independent.

The stress- strain relation above shows that there is no coupling between tensile and shear strains, as long as the applied stresses are coincident with the principal material directions. However, coupling appears when a lamina is tested at arbitrary angles with respect to the principal material directions. The general form of the stress-strain relation for any angular orientation of a lamina is considered next.

c. Stiffness matrix transformations

A lamina is loaded along a coordinate system x-y oriented at some

angle θ with respect to the principal material directions as shown in Fig. B-2. Since stress and strain are second order tensors, they are transformed by

$$\begin{bmatrix} \sigma_1 \\ \sigma_2 \\ \tau_{12} \end{bmatrix} = [T] \begin{bmatrix} \sigma_x \\ \sigma_y \\ \tau_{xy} \end{bmatrix}$$

and

$$\begin{bmatrix} \varepsilon_1 \\ \varepsilon_2 \\ \frac{1}{2}\gamma_{12} \end{bmatrix} = [T] \begin{bmatrix} \varepsilon_x \\ \varepsilon_y \\ \frac{1}{2}\gamma_{xy} \end{bmatrix} .$$

where [T] is the transformation matrix for plane stress and plane strain transformed by clockwise rotation about the (3,z) axes, given by

$$[T] = \begin{bmatrix} \cos^2\theta & \sin^2\theta & 2\sin\theta\cos\theta \\ \sin^2\theta & \cos^2\theta & -2\sin\theta\cos\theta \\ -\sin\theta\cos\theta & \sin\theta\cos\theta & \cos^2\theta - \sin^2\theta \end{bmatrix}$$

Inversion and substitution yields

$$\begin{bmatrix} \sigma_x \\ \sigma_y \\ \tau_{xy} \end{bmatrix} = [T]^{-1}[Q][T] \begin{bmatrix} \varepsilon_x \\ \varepsilon_y \\ \frac{1}{2}\gamma_{xy} \end{bmatrix}$$

which is the stress strain relation for a lamina referred to arbitrary axes. For simplicity, the notation [$\bar{Q}$] is introduced

$$[\bar{Q}] = [T]^{-1}[Q][T]$$

where $[\bar{Q}]$ is called the transformed reduced stiffness matrix.

Using the approach outlined above, it is possible to obtain

expressions for the elastic properties referred to the x-y coordinate system.

d. Elastic properties of laminates

A number of assumptions are made in laminate theory to obtain theoretical predictions. These are:

1. the lamina are perfectly bonded and do not slip relative to each other
2. the bond between the laminae is infinitesimally thin
3. the laminate has the properties of a thin sheet

These assumptions allow the laminate to be treated as a thin elastic plate. The classical hypothesis of Kirchhoff is applied to derive the strain distribution throughout the plate under external forces. Because the laminate is composed of laminae oriented in different directions with respect to each other, the stress-strain equation for each layer (k) is defined as

$$\begin{bmatrix} \sigma_x \\ \sigma_y \\ \tau_{xy} \end{bmatrix}_k = \begin{bmatrix} \bar{Q}_{11} & \bar{Q}_{12} & \bar{Q}_{16} \\ \bar{Q}_{12} & \bar{Q}_{22} & \bar{Q}_{26} \\ \bar{Q}_{16} & \bar{Q}_{26} & \bar{Q}_{66} \end{bmatrix}_k \begin{bmatrix} \varepsilon_x \\ \varepsilon_y \\ \frac{1}{2}\gamma_{xy} \end{bmatrix}$$

Thus for a given strain distribution, the stress in each layer can be determined. The strain at any point in a laminate undergoing deformation must be related to the displacements and curvatures of its midplane. The discussion which follows assumes that the laminate is thin. Kirchhoff plate theory is used in this formulation.

The deformation of an arbitrary section of a laminate is shown in Fig. B-3. It is assumed that lines straight and perpendicular to the

midplane before deformation remain so after deformation. This is equivalent to neglecting transverse shearing deformations. Comparing Fig. B-4(b) with Fig. B-4(a), in which the normals to the midplane remain perpendicular after deformation, it is seen that the upper and lower surfaces of the plate must not shift their relative positions. It is obvious that the resistance of a thin plate to such deformation is large, much larger than its resistance to deformations perpendicular to the midplane.

It is assumed that the point B at the midplane undergoes displacements u_0, v_0, and w_0 along the x, y, and z axes, respectively. The displacement u in the x direction of a point C located on the normal ABCD at a distance z from the midplane is given by

$$u = u_0 - z\alpha$$

where α is the slope of the midplane in the x direction,

$$\alpha = \frac{\partial w_0}{\partial x}$$

The last two equations can be used to obtain the displacement u of an arbitrary point at a distance z from the midplane as

$$u = u_0 - z \frac{\partial w_0}{\partial x}$$

Similarly,

$$v = v_0 - z \frac{\partial w_0}{\partial y}$$

Since the strains normal to the midplane are neglected (plane strain), the displacement w at any point is taken equal to the displacement w_0 at the midplane. The strains in terms of displacement u and v are

$$\varepsilon_x = \frac{\partial u}{\partial x} = \frac{\partial u_0}{\partial x} - z\frac{\partial^2 w_0}{\partial x^2}$$

$$\varepsilon_y = \frac{\partial v}{\partial y} = \frac{\partial v_0}{\partial y} - z\frac{\partial^2 w_0}{\partial y^2}$$

$$\gamma_{xy} = \frac{\partial u}{\partial y} + \frac{\partial v}{\partial x} = \frac{\partial u_0}{\partial y} + \frac{\partial v_0}{\partial x} - 2z\frac{\partial^2 w_0}{\partial x \partial y}$$

In terms of midplane strains and plate curvatures, the strains in a laminate vary linearly through the thickness,

$$\begin{bmatrix} \varepsilon_x \\ \varepsilon_y \\ \gamma_{xy} \end{bmatrix} = \begin{bmatrix} \varepsilon_x^0 \\ \varepsilon_y^0 \\ \gamma_{xy}^0 \end{bmatrix} + z \begin{bmatrix} k_x \\ k_y \\ k_{xy} \end{bmatrix}$$

where midplane strains are given by

$$\begin{bmatrix} \varepsilon_x^0 \\ \varepsilon_y^0 \\ \gamma_{xy}^0 \end{bmatrix} = \begin{bmatrix} \dfrac{\partial u_0}{\partial x} \\ \dfrac{\partial v_0}{\partial y} \\ \dfrac{\partial u_0}{\partial y} + \dfrac{\partial v_0}{\partial x} \end{bmatrix}$$

and the plate curvatures by

$$\begin{bmatrix} k_x \\ k_y \\ k_{xy} \end{bmatrix} = - \begin{bmatrix} \dfrac{\partial^2 u_0}{\partial x^2} \\ \dfrac{\partial^2 w_0}{\partial y^2} \\ \dfrac{\partial^2 w_0}{\partial x \partial y} \end{bmatrix}$$

The stresses in any (k) lamina can be obtained by substituting the previous equation into the stress strain equation

$$\begin{bmatrix} \sigma_x \\ \sigma_y \\ \tau_{xy} \end{bmatrix}_k = \begin{bmatrix} \bar{Q}_{11} & \bar{Q}_{12} & \bar{Q}_{16} \\ \bar{Q}_{12} & \bar{Q}_{22} & \bar{Q}_{26} \\ \bar{Q}_{16} & \bar{Q}_{26} & \bar{Q}_{66} \end{bmatrix}_k \left[\begin{bmatrix} \varepsilon_x^0 \\ \varepsilon_y^0 \\ \gamma_{xy}^0 \end{bmatrix} + z \begin{bmatrix} k_x \\ k_y \\ k_{xy} \end{bmatrix} \right]$$

e. Laminate Stiffness Matrix

Classical laminate theory provides a method of calculating the resultant forces and moments per unit length acting on the laminate by integrating the stresses acting in each lamina through the thickness (h) of the laminate. Resultant forces are obtained by

$$N_x = \int_{-h/2}^{h/2} \sigma_x \, dz$$

$$N_y = \int_{-h/2}^{h/2} \sigma_y \, dz$$

$$N_{xy} = \int_{-h/2}^{h/2} \tau_{xy} \, dz$$

The moment resultants are obtained by integration through the thickness of the corresponding moments of stresses about the midplane:

$$M_x = \int_{-h/2}^{h/2} \sigma_x \, z \, dz$$

$$M_y = \int_{-h/2}^{h/2} \sigma_y \, z \, dz$$

$$M_{xy} = \int_{-h/2}^{h/2} \tau_{xy} \, z \, dz$$

The units of N_x, N_y, N_{xy} are force per unit length and M_x, M_y, M_{xy} are moment per unit length. The sign conventions are shown in Fig. B-5.

Using the resultant force and moment relations, a system is defined that is statically equivalent to the laminate stress system, but applied

at the midplane. Thus, the external loading has been reduced to a system that does not contain the laminate thickness or z coordinate explicitly.

For a laminate consisting of n laminae (Fig. B-6), the resultant force-moment system acting at the midplane can be obtained by adding integrals representing the contribution of each layer by

$$\begin{bmatrix} N_x \\ N_y \\ N_{xy} \end{bmatrix} = \int_{-h/2}^{h/2} \begin{bmatrix} \sigma_x \\ \sigma_y \\ \tau_{xy} \end{bmatrix} dz = \sum_{k=1}^{n} \int_{h_{k-1}}^{h_k} \begin{bmatrix} \sigma_x \\ \sigma_y \\ \tau_{xy} \end{bmatrix}_k dz$$

$$\begin{bmatrix} M_x \\ M_y \\ M_{xy} \end{bmatrix} = \int_{-h/2}^{h/2} \begin{bmatrix} \sigma_x \\ \sigma_y \\ \tau_{xy} \end{bmatrix} z\, dz = \sum_{k=1}^{n} \int_{h_{k-1}}^{h_k} \begin{bmatrix} \sigma_x \\ \sigma_y \\ \tau_{xy} \end{bmatrix}_k z\, dz$$

Using the expressions for the stresses in the k-th lamina derived earlier, and noting that the midplane strains and plate curvatures are constant not only within the lamina, but for all laminae, it is apparent that they can be taken outside the integral sign. The stiffness matrix $[\bar{Q}]$ is constant within a lamina so it also can be taken outside the integration to give

$$\begin{bmatrix} N_x \\ N_y \\ N_{xy} \end{bmatrix} = \left[\sum_{k=1}^{n} \begin{bmatrix} \bar{Q}_{11} & \bar{Q}_{12} & \bar{Q}_{16} \\ \bar{Q}_{12} & \bar{Q}_{22} & \bar{Q}_{26} \\ \bar{Q}_{16} & \bar{Q}_{26} & \bar{Q}_{66} \end{bmatrix}_k \int_{h_{k-1}}^{h_k} dz \right] \begin{bmatrix} \varepsilon_x^0 \\ \varepsilon_y^0 \\ \gamma_{xy}^0 \end{bmatrix}$$

$$+ \left[\sum_{k=1}^{n} \begin{bmatrix} \bar{Q}_{11} & \bar{Q}_{12} & \bar{Q}_{16} \\ \bar{Q}_{12} & \bar{Q}_{22} & \bar{Q}_{26} \\ \bar{Q}_{16} & \bar{Q}_{26} & \bar{Q}_{66} \end{bmatrix}_k \int_{h_{k-1}}^{h_k} z\, dz \right] \begin{bmatrix} k_x \\ k_y \\ k_{xy} \end{bmatrix}$$

$$\begin{bmatrix} M_x \\ M_y \\ M_{xy} \end{bmatrix} = \left[\sum_{k=1}^{n} \begin{bmatrix} \bar{Q}_{11} & \bar{Q}_{12} & \bar{Q}_{16} \\ \bar{Q}_{12} & \bar{Q}_{22} & \bar{Q}_{26} \\ \bar{Q}_{16} & \bar{Q}_{26} & \bar{Q}_{66} \end{bmatrix}_k \int_{h_{k-1}}^{h_k} z\, dz \right] \begin{bmatrix} \varepsilon_x^0 \\ \varepsilon_y^0 \\ \gamma_{xy}^0 \end{bmatrix}$$

$$+ \left[\sum_{k=1}^{n} \begin{bmatrix} \bar{Q}_{11} & \bar{Q}_{12} & \bar{Q}_{16} \\ \bar{Q}_{12} & \bar{Q}_{22} & \bar{Q}_{26} \\ \bar{Q}_{16} & \bar{Q}_{26} & \bar{Q}_{66} \end{bmatrix}_k \int_{h_{k-1}}^{h_k} z^2 dz \right] \begin{bmatrix} k_x \\ k_y \\ k_{xy} \end{bmatrix}$$

Three new matrices, A_{ij}, B_{ij}, and D_{ij}, are defined, where

$$A_{ij} = \sum_{k=1}^{n} (\bar{Q}_{ij})_k (h_k - h_{k-1})$$

$$B_{ij} = \frac{1}{2} \sum_{k=1}^{n} (\bar{Q}_{ij})_k (h_k^2 - h_{k-1}^2)$$

$$D_{ij} = \frac{1}{3} \sum_{k=1}^{n} (\bar{Q}_{ij})_k (h_k^3 - h_{k-1}^3)$$

These new matrices, A, B, and D, simplify the resultant force and moment relations, and are known as the extensional, coupling, and bending stiffness matrices, respectively. The total plate constitutive equation is then

$$\begin{bmatrix} N \\ M \end{bmatrix} = \begin{bmatrix} A & B \\ B & D \end{bmatrix} \begin{bmatrix} \varepsilon^0 \\ k \end{bmatrix}$$

It may be recalled that in an orthotropic lamina with arbitrary orientation the shear stress is coupled with the normal strain and the normal stresses are coupled with the shear strain. In general, a resultant shearing force on a laminated plate produces midplane normal strains in addition to the expected shearing strain. Similarly, a

resultant normal force will induce shear strains in addition to midplane normal strains.

The nonzero coupling matrix B in the plate constitutive equation explains the coupling between bending and extension of the laminated plate. Thus, normal and shear forces at the midplane induce not only midplane deformations, (and hence, midplane strains) but also twisting and bending, producing plate curvatures. Similarly, resultant bending and twisting moments induce midplane strains.

f. Lamina stresses and strains

The aim of the analysis of a laminated composite is to determine the stresses and strains in each of the laminae forming the laminate. These stresses and strains are used with failure criteria to predict the loads for failure initiation for a laminate. The failure criteria are discussed in the section devoted specifically to that purpose.

The strains in a lamina caused by external loading are a function of laminate midplane strains and plate curvatures, as previously discussed. Once the lamina strains are known, lamina stresses can be found using the lamina stress-strain law. Thus, the starting point for calculating lamina stresses is the determination of laminate midplane strains and plate curvatures in terms of the applied loading. The plate constitutive equation given previously can be inverted to give the midplane strains and plate curvatures explicitly in terms of the resultant external forces and moments. The result of the inversion process is

$$\begin{bmatrix} \varepsilon^0 \\ k \end{bmatrix} = \begin{bmatrix} A' & B' \\ C' & D' \end{bmatrix} \begin{bmatrix} N \\ M \end{bmatrix} = \begin{bmatrix} A' & B' \\ B' & D' \end{bmatrix} \begin{bmatrix} N \\ M \end{bmatrix}$$

where A', B', and D' are simplified forms of the inversion process results, and are functions of the A, B, and D matrices of the original form of the plate constitutive equation.

It is now apparent that with these equations, an analysis of a laminate subjected to external forces and moments can be conducted:

1. calculate midplane strains and plate curvatures

$$\begin{bmatrix} \varepsilon^0 \\ k \end{bmatrix} = \begin{bmatrix} A' & B' \\ B' & D' \end{bmatrix} \begin{bmatrix} N \\ M \end{bmatrix} .$$

2. calculate lamina stresses in global (x-y) system

$$\begin{bmatrix} \sigma_x \\ \sigma_y \\ \tau_{xy} \end{bmatrix}_k = \begin{bmatrix} \bar{Q}_{11} & \bar{Q}_{12} & \bar{Q}_{16} \\ \bar{Q}_{12} & \bar{Q}_{22} & \bar{Q}_{26} \\ \bar{Q}_{16} & \bar{Q}_{26} & \bar{Q}_{66} \end{bmatrix}_k \left[\begin{bmatrix} \varepsilon^0_x \\ \varepsilon^0_y \\ \gamma^0_{xy} \end{bmatrix} + z \begin{bmatrix} k_x \\ k_y \\ k_{xy} \end{bmatrix} \right]$$

3. calculate lamina stresses in natural (longitudinal and transverse to fiber) system.

$$\begin{bmatrix} \sigma_1 \\ \sigma_2 \\ \tau_{12} \end{bmatrix} = [T] \begin{bmatrix} \sigma_x \\ \sigma_y \\ \tau_{xy} \end{bmatrix}$$

The strain variations in a lamina are calculated in an analagous manner. The stress-strain variation is compared with the allowable stresses and strains in each lamina. Thus the load at which failure is initiated in one of the lamina can be calculated, as long as a strength criteria exists in terms of the lamina natural axis system. The formulation of lamina failure criteria is discussed in the next section.

3. Strength Theories

It is assumed that the strength of a laminate must be related to the strengths of the individual laminae. A simple failure criteria consists of evaluating the lamina strengths in their principal material directions subject to induced stresses or strains at the boundaries of the lamina. In this context, it is assumed that the lamina and its constituents behave in a linear elastic manner to failure. The strength analysis described here assumes that the behavior of each lamina in an arbitrary laminate is the same as the behavior observed in the natural axis system when the lamina is part of any other laminate under the same stresses or strains. In other words, it is assumed that the strength criteria for a lamina in plane stress is valid for any orientation of the lamina in a laminate. In the ICAN program, the lamina strengths are calculated using the expressions given below.

Longitudinal tension

$$S_{l11T} = S_{fT} \left(k_f + k_m E_m / E_{f11}\right)$$

Longitudinal compression:

The longitudinal compressive strength must be computed on the basis of three different criteria:

a. rule of mixtures

$$S_{l11C} = S_{fC} \left(k_f + k_m E_m / E_{f11}\right)$$

b. delamination

$$S_{l11C} = \left(13\, S_{l12} + S_{mC}\right)$$

c. fiber microbuckling

$$S_{l11C} = \frac{F_2 G_m}{1 - k_f(1 - G_m/G_{f12})}$$

Transverse tension

$$S_{l22T} = S_{mT}(FACT/DENOM)$$

Transverse compression

$$S_{l22C} = S_{mC} / DENOM$$

Transverse shear

$$S_{l12} = \frac{[(F_1 - 1 + G_m/G_{f12})F_2 G_{l12} S_{mS}]}{G_m F_1} FACT$$

where F_1 and F_2 are given by

$$F_1 = \sqrt{\frac{n}{4k_f}}$$

$$F_2 = 1 - \sqrt{\frac{4k_v}{nk_m}}$$

The variable DENOM is introduced for convenience:

$$DENOM = [1 - \sqrt{k_f}(1 - E_m/E_{f22})] \sqrt{1 + \varphi(\varphi - 1) + 1/3(\varphi - 1)^2}$$

where φ is given by

$$\varphi = \frac{F_1 - \frac{E_m}{E_{f22}[1 - \sqrt{k_f}(1 - E_m/E_{f22})]}}{F_1 - 1}$$

The variable FACT is used to correlate the strengths of HMS and Kevlar fiber composites with the experimentally observed values. Since neither of these fibers is used in this work, FACT takes the value unity.

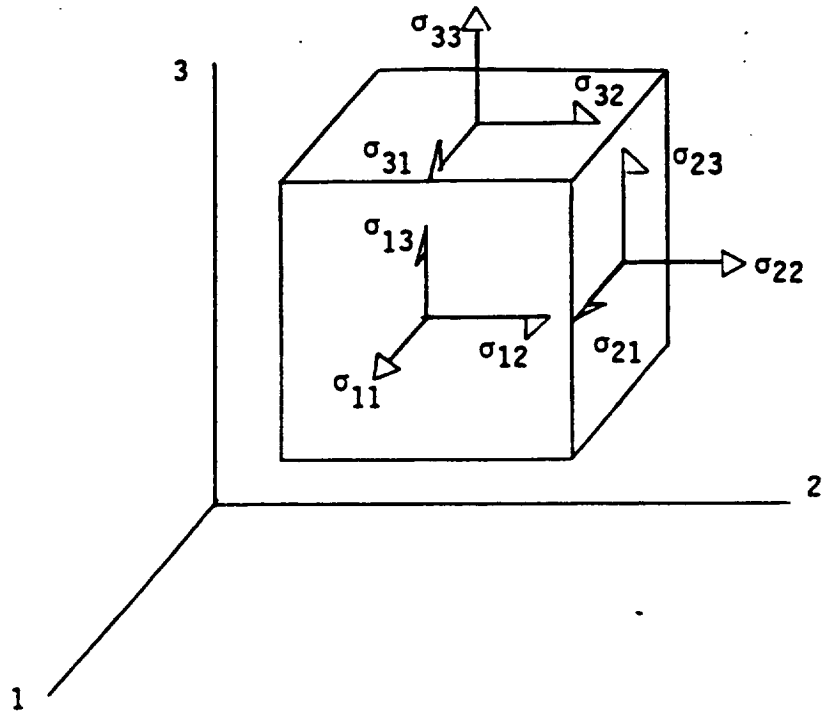

Fig. B.1- Components of Stress acting on elemental unit cube.

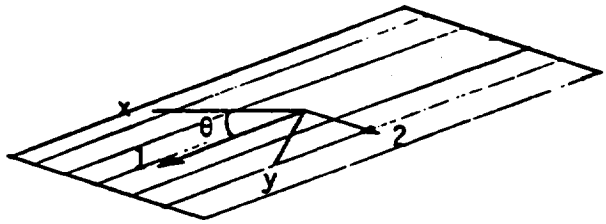

Fig. B.2- Rotation of coordinates from 1-2 to x-y.

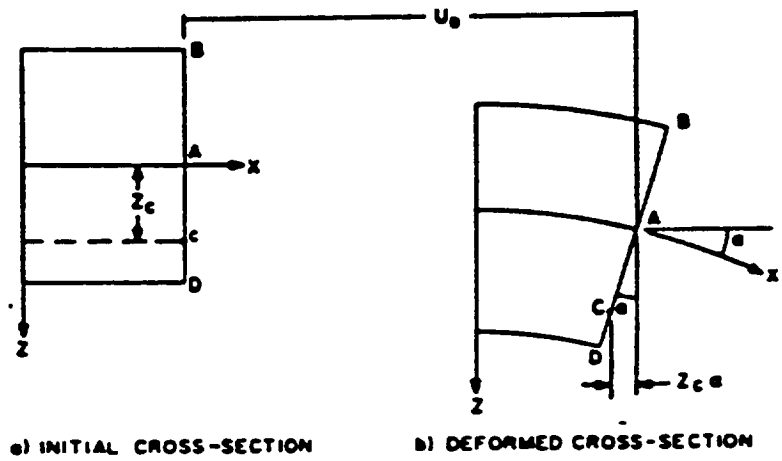

Fig. B.3- Bending geometry in the x-z plane.

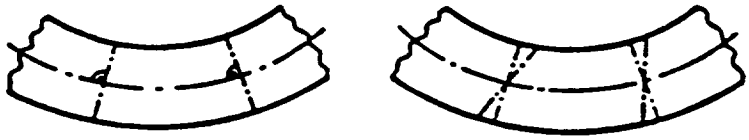

a. *Deflected bar without shear deformations*

b. *Deflected bar with shear deformations*

Fig. B.4-Shearing force deformations on straight cross section.

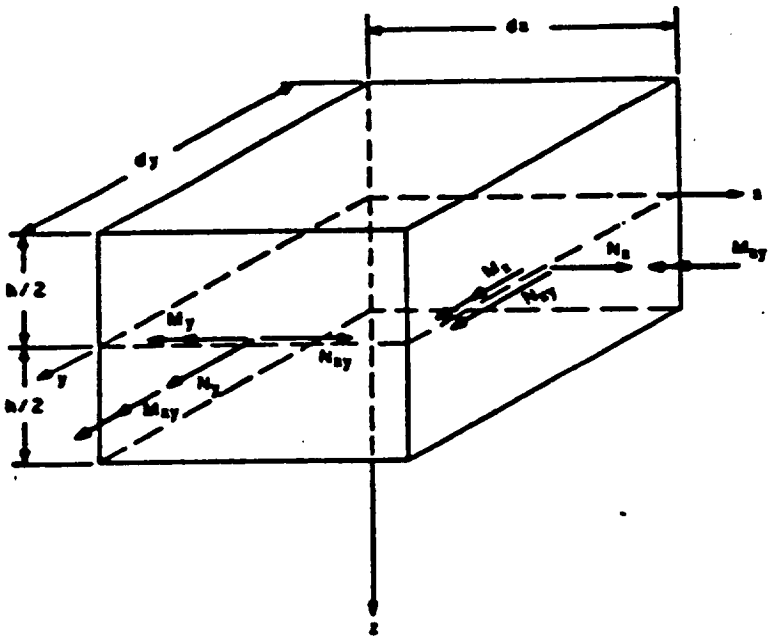

Fig. B.5- Plate stress and moment resultants

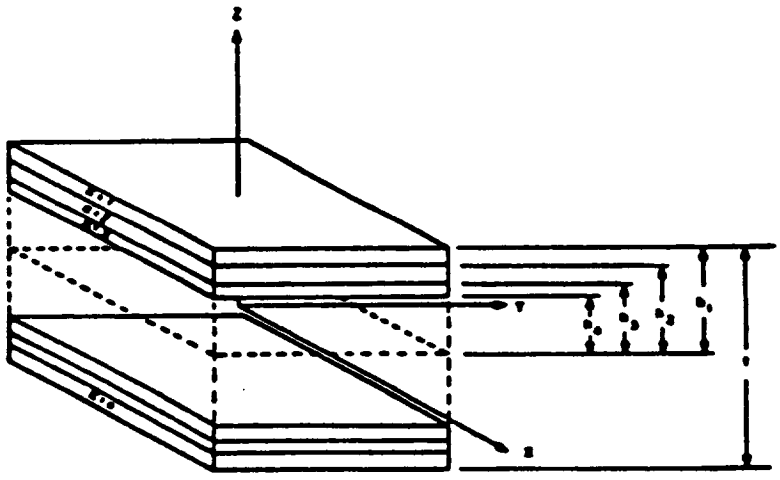

Fig. B.6- Laminate index notation convention.

REPORT DOCUMENTATION PAGE

Form Approved
OMB No. 0704-0188

1. AGENCY USE ONLY (*Leave blank*)	2. REPORT DATE	3. REPORT TYPE AND DATES COVERED
	January 1996	Final Contractor Report

4. TITLE AND SUBTITLE

Probabilistic Fiber Composite Micromechanics

5. FUNDING NUMBERS

WU-505-63-5B
G-NAG3-550

6. AUTHOR(S)

Thomas A. Stock

7. PERFORMING ORGANIZATION NAME(S) AND ADDRESS(ES)

Cleveland State University
Fenn Tower 1010
1983 E. 24th St.
Cleveland, Ohio 44115

8. PERFORMING ORGANIZATION REPORT NUMBER

E-10082

9. SPONSORING/MONITORING AGENCY NAME(S) AND ADDRESS(ES)

National Aeronautics and Space Administration
Lewis Research Center
Cleveland, Ohio 44135-3191

10. SPONSORING/MONITORING AGENCY REPORT NUMBER

NASA CR-198443

11. SUPPLEMENTARY NOTES

This report was submitted as a thesis in partial fulfillment of the requirements for the degree Master of Science in Civil Engineering to Cleveland State University, Cleveland, Ohio 44115. Project Manager, Christos C. Chamis, Structures Division, NASA Lewis Research Center, organization code 5200, (216) 433-3252.

12a. DISTRIBUTION/AVAILABILITY STATEMENT

Unclassified - Unlimited
Subject Category 05

This publication is available from the NASA Center for Aerospace Information, (301) 621-0390.

12b. DISTRIBUTION CODE

13. ABSTRACT (*Maximum 200 words*)

Probabilistic composite micromechanics methods are developed that simulate expected uncertainties in unidirectional fiber composite properties. These methods are in the form of computational procedures using Monte Carlo simulation. The variables in which uncertainties are accounted for include constituent and void volume ratios, constituent elastic properties and strengths, and fiber misalignment. A graphite/epoxy unidirectional composite (ply) is studied to demonstrate fiber composite material property variations induced by random changes expected at the material micro level. Regression results are presented to show the relative correlation between predictor and response variables in the study. These computational procedures make possible a formal description of anticipated random processes at the intraply level, and the related effects of these on composite properties.

14. SUBJECT TERMS

Computational simulation; Uncertainties; Probabilistic distribution; Monte Carlo; Fiber content; Void content; Misalignment; Graphite fibers; Epoxy matrix; Micro level; Unidirectional; Random processes

15. NUMBER OF PAGES

192

16. PRICE CODE

A09

17. SECURITY CLASSIFICATION OF REPORT	18. SECURITY CLASSIFICATION OF THIS PAGE	19. SECURITY CLASSIFICATION OF ABSTRACT	20. LIMITATION OF ABSTRACT
Unclassified	Unclassified	Unclassified	

National Aeronautics and
Space Administration
Lewis Research Center
21000 Brookpark Rd.
Cleveland, OH 44135-3191